B. I. G.
166990

Romanian Journal of PETROLOGY

continuation of

DĂRI DE SEAMĂ ALE ŞEDINŢELOR INSTITUTULUI DE GEOLOGIE ŞI GEOFIZICĂ
COMPTES RENDUS DES SÉANCES DE L'INSTITUT DE GÉOLOGIE ET GÉOPHYSIQUE
(1. Mineralogie-Petrologie)

Founded 1906 by the Geological Institute of Romania

CENTENNIAL VOLUME

ISSN 1220-563X

Vol. 78

CONTENTS

166990

Institutul Geologic al României
Bucureşti – 2006

Institutul Geologic al României

GEOLOGICAL INSTITUTE OF ROMANIA
Director General Dr. Ştefan Marincea

The **Geological Institute of Romania** is now publishing the following periodicals:

Romanian Journal of Mineralogy
Romanian Journal of Petrology
Romanian Journal of Mineral Deposits
Romanian Journal of Paleontology
Romanian Journal of Stratigraphy
Romanian Journal of Tectonics and Regional Geology
Romanian Journal of Geophysics
Anuarul Institutului Geologic al României
Memoriile Institutului Geologic al României

Romanian Journals supersede "Dări de Seamă ale Şedinţelor" and "Studii Tehnice şi Economice", whose first issues go back to 1910. Besides regular volumes, each series may occasionally contain Supplements (for abstracts and excursion guides to congresses and symposia held in Romania) and Special Issues (for larger papers of special interest). "Anuarul Institutului Geologic al României" appears also in a new form, containing both the annual activity report and review papers.

Editorial Board: Gheorghe Udubaşa (chairman), Şerban Veliciu (vice-chairman), Emilian Roşu, Tudor Berza, Mircea Săndulescu

Editorial Office:
Geological Institute of Romania
Str. Caransebeş Nr. 1
RO-012271 Bucureşti 32
Tel. (+40) -21-3181328
Fax (+40)-21-3181326
e-mail: GEOL@IGR.RO

The editor has changed the name as follows: Institutul Geologic al României (1906-1952), Comitetul Geologic (1953-1966), Comitetul de Stat al Geologiei (1967-1969), Institutul Geologic (1970-1974), Institutul de Geologie şi Geofizică (1975-1993), Institutul Geologic al României (since 1994).

ROMANIAN JOURNAL OF PETROLOGY supersedes "Dări de Seamă ale Şedinţelor, Series 1/Mineralogie-Petrologie – the last volume with this title being No. 74.

Scientific Editor: Tudor Berza

The manuscripts should be sent to the scientific editor and/or executive secretary. Correspondence concerning advertisements, announcements and subscriptions should be sent to the Editorial Office.

©GIR 2006
ISSN-563X
Classification index for libraries 55(058)

Printed by the Geological Institute of Romania
Bucharest

Institutul Geologic al României

THE NORTHERN APOPHYSIS OF THE DITRĂU ALKALINE MASSIF - A PETROGRAPHIC APPROACH

Lucian IONESCU

GEOLEX S. A., str. Körösi Cs. 7, 4100 Miercurea Ciuc

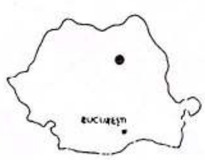

Key words: Alkaline pluton. East Carpathians, Romania. Contact metamorphism.

Abstract: In the northern part of the Ditrău Massif, a 7.5 km long apophysis has been intruded in the Cambrian schists of the Tulgheş Group. Its sharp eastern limit is due to a directional fault. The apophysis is built up by alkalifeldspathic granitoids, alkaline granitoids, alkalifeldspathic syenites and foid syenites. Its up to 2.5 km - large thermal aureole comprises a great variety of newly- formed minerals, from biotite zone to andalusite - cordierite - sillimanite - corundum - K-feldspar contact assemblages. Mo and RE mineralizations are related to the apophysis.

Introduction

The studied apophysis is rooted in the middle of the northern border of the Ditrău Alkaline Massif, representing its singular structural element of this kind. At its root it has a maximum width of 1.2 km and it gradually thins out along a distance of 7.5 km. The apophysis has been intruded in the Cambrian low-grade metamorphic formations of the Tulgheş Group, represented in the area by the Sandominic sequence. Only Tg3 and Tg4 formations of the Sandominic sequence crop out. These formations are folded, the fold hinges being parallel to the apophysis. The Tg3 Formation is represented by acidic metavolcanics that crop out across a restricted area on Paraul Lung creek. The Tg 4 Formation crops out on a large territory, being built up by quartzitic- sericitic schists ± chlorite ± graphite with intercalated blastodetrital rocks, acidic metavolcanics, greenschists and black quartzites, which occur only westwards as thin and discontinuous lithons. At its upper part (eastwards from the apophysis), the terminal sequence of the Tg4 Formation is represented by Mândra Porphyroids, bordered by blastodetrital rocks.

In the studied region the contact phenomena generated by the Ditrău Alkaline Massif occur in the Tulgheş Group westwards from the apophysis and in its northern extension up to a distance of 2.5 km. Inside the termally affected zone, small granitic intrusions (westwards) and syenitic intrusions (south - westwards) occur. The Ditrău Massif and its apophysis contain enclaves and intercalations of hornfelsed regionally metamorphosed rocks (Fig.).

Genesis, structure and petrography of the apophysis

The intrusion of the apophysis is probably contemporaneous with the emplacement of the Ditrău Massif because it is built up by the same rocks that occur on the northern border of the massif. The intrusion seems to have tectonically been controlled by an important directional fault with respect to the metamorphic structures. This fault is NNE - SSW directed and it limits the apophysis to the east. This old tectonic fracture, now healed, is still recognizable by the well-developed cataclastic features. The mylonites are obvious only along the apophysis, northwards this major tectonic rupture behaving as a simple slip strike-fault. Because of this fault, the shape of the eastern border of the apophysis is even, while the western one is indented. The western compartment of the fault was strongly uplifted as revealed by the outcropping of Tg3 Formation and by the small granitic intrusions, as well as the extended contact phenomena. The lower position of the eastern compartment is shown by the outcropping of the upper sequences of Tg4 Formation and by the absence of the intrusions and hornfelses. Subsequently, a system of minor cross-cut faults, WNW - ESE orientated, has affected the metamorphics and the apophysis.

The apophysis is built up by granites and syenites, both alkaline and alkalifeldspathic. The transition from one petrographic type to another is gradual. A few alkaline vein rocks occur in the southern and middle parts of the apophysis. To the south - west of the root zone a monzonite complex occurs. The small

Institutul Geologic al României

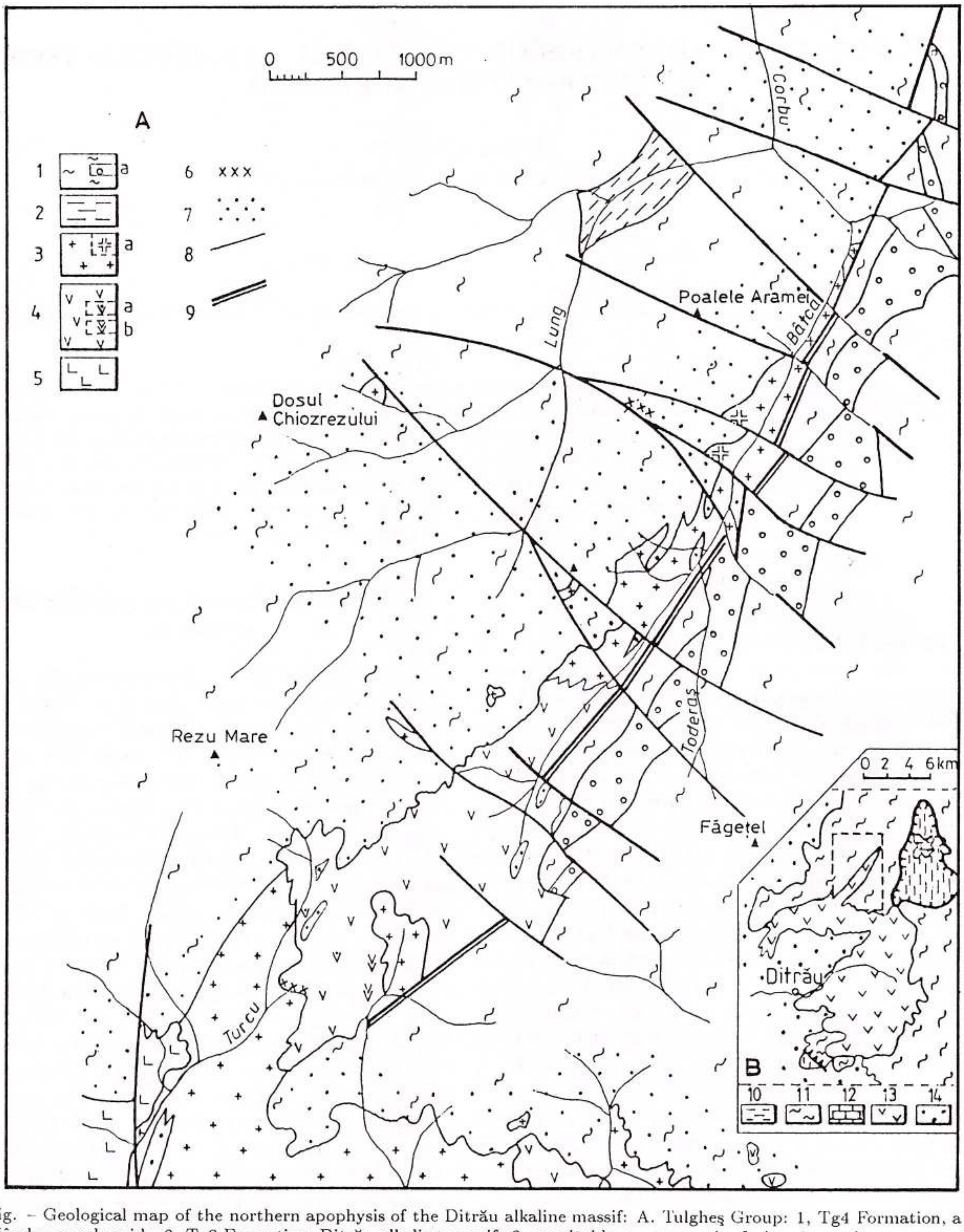

Fig. – Geological map of the northern apophysis of the Ditrău alkaline massif: A. Tulgheș Group: 1, Tg4 Formation, a - Mândra porphyroids; 2, Tg3 Formation; Ditrău alkaline massif: 3, granitoids, a - pegmatite facies; 4, syenites, a - quartz syenites, b - foid syenites; 5, monzonites; Other symbols: 6, mineralizations; 7, hornfelses; 8, faults; 9, mylonites. B. 10, medium grade metamorphitcs; 11, greenschist facies metamorphitcs; 12, Bucovinian Mesozoic sedimentary; 13, Ditrău alkaline massif; 14, Neogene andesitic volcanics.

intrusions of the western part are built up by granites. The eastern contact with the crystalline schists is achieved by a mylonite zone.

Granites. These rocks crop out at the northern border of the massif (in the southern part of the apophysis) and yield small intrusions to the west.

Institutul Geologic al României

They are built up by K-feldspar (microcline, orthose, perthite = 30 - 54 %), quartz (21 - 30 %, as isolated grains or as aggregated crystals), tabular crystals or short prisms of plagioclase (oligoclase + albite = 5 - 40 %), chloritized biotite, muscovite with fine opaque grains along cleavage planes (probably resulted from the expelled iron of a former biotite) and, rarely, epidote.

Alkalin granites. They crop out mostly in the central-northern part and in the southern part of the apophysis. Their composition is dominated by the K-feldspars with secondary sericite (perthite, microcline, orthose = 33 - 64 %) and plagioclase (oligoclase + albite =9-31 %), sometimes intensely argillized and sericitized. Subordinately, hipidiomorphic quartz grains (10 - 16 %) with undulatory extinction and chloritized biotite (5 - 18%) occur.

Across two small areas from the northwestern part of the apophysis these granites show a pegmatoid facies.

Syenites. They occur in the northern part of the Ditrău Massif, in the southern and middle parts of the apophysis, and in some small isolated intrusions in the metamorphic schists from the south-eastern extremity of the studied zone. Their composition is dominated by K-feldspars (microcline, perthite, orthose = 20 - 90 %) as well-developed crystals, locally intensely sericitized, and short prismatic or tabular plagioclase crystals (oligoclase + albite = 5 - 7 %). The hipidiomorphic grains of quartz are less abundant (3 - 10 %). The chloritized biotite flakes (1 - 8 %) have formed on riebeckite. Apatite, zircon, epidote and muscovite may occur sometimes.

Foid bearing syenites. These rocks crop out in the southern extremity of the apophysis. They are dominated by plagioclase (oligoclase + albite = 25 - 58 %) and K- feldspar (microcline + orthose = 26 - 42 %), that occur as large aggregates which may contain clear riebeckite and biotite crystals. Sometimes small sericitized nepheline grains, analcite and cancrinite occur. Zircon, apatite and orthite are very rare.

Vein rocks. In the southern and middle parts of the apophysis two bostonite dykes and a microgranite dyke were found.

The bostonites are built up by slightly orientated sericitized plagioclase prisms (65 - 75 %). Chlorite occurs subordinately, probably at the expense of former mafics. Zircon is the common accessory.

The microgranite, with an orientated texture, is built up by quartz, plagioclase (oligoclase, albite), muscovite and chloritized biotite. Cancrinite invades the rock, forming clusters.

Mylonites. These rocks occur on the eastern border of the apophysis, which represents an old shear zone, now healed. Typical mylonites massively crop out on both sides of the Toderaş creek, near the joint with the Bâtca creek (Fig.). The rock looks as a greenish - black tectonized mass, with contorted whitish little bands. Under the microscope the quartz occurs as strongly flattened and deformed porphyroblasts, polygonized, crushed, and enclosed in a mixed mass built up by sericite flakes, chlorite and fine quartz and feldspar crystals.

Contact phenomena

Around the apophysis the thermal aureole crops out only on the western part, being cut, to the east, by the above mentioned fault. The thermal influence can be observed over a distance of 2.5 km from the apophysis, its effect being increased by the small granitoid intrusions.

Our observations allowed the separation of three zones with respect to the intensity of the transformations, in good agreement with the facial zones described by Voicu et al. (1990). Starting from the massif, they are as follows:

The intensely affected zone. It contains the following contact paragenesis: andalusite ± sillimanite - muscovite - biotite ± cordierite ± garnet ± corundum ± K - feldspar. This zone extends from the contact with the massif up to several hundreds meters, but sometimes it may thin out. The former rock is difficult if not impossible to recognize. These rocks are blackish due to the abundance of biotite which, in the innermost parts of the aureole, may form monomineral separations. The mica-rich bands may alternate with feldspathic ones, generating a banded texture. The andalusite and the sillimanite may be seen with the naked eye on the schistosity planes as elongated blackish-gray crystals or as rounded, radiated spots. These hornfelses have a granolepidoblastic structure, containing quartz, feldspar and andalusite grains between the phyllosilicatic bands. Frequently, the andalusite is replaced by sericite and the biotite is replaced by chlorite. The occurrence of two generations of andalusite, biotite or muscovite, is common. The younger mica generations are randomly orientated.

The alkaline metasomatism that has affected the regionally metamorphosed rocks at the contact with the massif produced important quantities of potassic feldspars and only seldom some cancrinite and tourmaline.

The moderately affected zone. It is the best represented, defined by the following contact mineral assemblage: muscovite - biotite ± andalusite ± K - feldspar. The former regionally metamorphosed rocks can be easier to recognize. The abundance of biotite and muscovite varies very much. On the hile between Bâtca creek and Turcu creek the hornfelses

Institutul Geologic al României

are built up almost exclusively by quartz and muscovite, having the looking of metavolcanics in which the phenocrysts are missing. In these rocks, two biotite and muscovite generations may occur. The younger generation developed along shear cracks that cross the schistosity. As Voicu et al. (1990) remarked, the quartz-feldspar rocks are much less affected than the neighbouring schists. The occurrence of the feldspathic rocks as continuous thick lithons represents, after the mentioned authors, lithological screens which considerably diminish the contact phenomena.

In the hornfelsed blastodetrital rocks the quartz porphyroblasts are recrystallized, having usually anormal extinction, while the microgranular quartz has undulatory extinction. Feldspar porphyroblasts are sericitized to various degrees and the biotite flakes are partly chloritized.

The weakly affected zone. It represents the outer zone of the aureole, in which the only contact mineral is the biotite. Biotite has formed in schists while the quartz - feldspathic rocks are not affected. The biotite is chloritized (perhaps a retrograde process during the cooling of the massif). Sometimes the biotite occurs as rounded aggregates that may be seen on the schistosity planes, generating the spotted schists varieties.

Mineralizations

Ionescu et al. (1992) identified two epigenetic mineralizations in the studied apophysis. They are high temperature metasomatic-hydrothermal mineralizations, generated by the Ditrău magmatism.

One mineralization, containing molybdenum and rare earths, represent the easternmost known occurrence of Jolotca-type vein mineralization. In the syenites from the left side of the Turcu creek (Fig. 1), we identified fragments of a vein, intensely altered, with the following contents: Mo = tens to 100 ppm; Yb - Sc - Nb = tens ppm; Y - Gd - La = hundreds ppm; Ce - Nd - Th = thousands ppm.

The other mineralization occurs in the saddle from the crest between the Batca creek and the Pârâul Lung creek southwards from Poalele Aramei Peak (Fig. 1), at the intersection of several faults. The mineralization occurs in hornfelsed schists, as blocks of intensely circulated rocks that led to a strong alteration of the surrounding rocks. Under the vegetal soil, fault gauge occurs. The following contents have been found: Au = 0.5 - 0.6 g/t; Ag = 100 - 160 g/t, Cu = 0.15 - 0.2 %; Pb = 1 - 2.5 %; Zn = 0.15 - 0.2 %; S = 0.1 - 2%; Bi = hundreds ppm; Sn = tens to 100 ppm. A similar but poorer mineralization occurs on the same crest at about 1.2 km southwards.

References

Ionescu, L., Kasztl, C., Torok, T., Zolya, L. (1992) Report (in Romanian). Geolex SA Archive, Miercurea Ciuc.

Voicu, G., Runceanu, M., Voicu, C., Munteanu, M., Popa, G. N. (1990) Report (in Romanian). Archives of the Geological Institute of Romania, Bucharest.

Received: February 24, 1998
Accepted: October 30, 1998

Institutul Geologic al României

LAMPROPHYRES IN THE HAGOTA - TULGHEŞ ZONE (EAST CARPATHIANS)

Lucian IONESCU

GEOLEX S.A., str. Körösi Cs. 7, 4100 Miercurea Ciuc

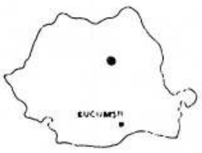

Key words: East Carpathians. Tulgheş. Lamprophyres.

Abstract: In the Hagota-Tulgheş zone about 200 lamprophyre veins have been identified, which penetrate mostly the epimetamorphic formation of the Tulgheş Group. All the wells in the area penetrated lamprophyres, amounting to 2.27 % of the total length drilled. Most of the analysed lamprophyres represent spessartites, odinites, beerbachites. Vogesites, kersantites, malchites and camptonites are found subordinately. The majority of lamprophyres are intensely altered, being affected especially by carbonatations and subordinately by limonitizations, chloritizations, serpentinizations, epidotizations, albitizations and argillizations. Locally, they contain enclaves from the metamorphic formations penetrated and more rarely from older syenites and lamprophyres. All lamprophyres occur on fissures. They are grouped in fields, within which the position of the veins is relatively constant. Most of the lamprophyre bodies are oriented after a system of conjugated directions, N-S (with eastern dippings) and E-W (with northern dippings). The distribution of the minor elements in these rocks does not depend significantly on the spatial position of the veins or on sampling site, it pointing to the common origin of all lamprophyres. In the whole area, the lamprophyres are found in association with epigenetic mineralisations. This fact can be explained by the use of the same access ways. The age of the lamprophyres in the Hagota-Tulgheş zone is probably Upper Jurassic-Cretaceous.

The study zone is situated in the Giurgeu Mts, south of the Bistricioara River, covering the lower basins of the Asod, Rezu Mare and Putna valleys. The geologic setting is dominated by the epimetamorphic formations of the Tulgheş Group, that constitute the Putna Nappe, developed in the central part of a wide antiform (Valea Putnei antiform). The Tg_3 and Tg_4 formations are cropping out here. Between the Asod and Rezu Mare valleys, due to a secondary tectonic plane (Asod-Rezu Mare digitation), the Tg_3 and Tg_4 suite is doubled. In the eastern and southern parts, the Tulgheş Group is overlain by the Balaj Nappe (formed of sericite-muscovite±biotite±feldspar quartzitic schists) and overlies the Rarău Nappe (formed of diverse mesometamorphic rocks and metagranitoids of the Bretila Group) (Fig. 1). The metamorphics are penetrated by lamprophyres and subordinately by alkaline vein rocks affiliated to the alkaline Ditrău Massif (situated south-west of the study region).

In the Hogota-Tulgheş zone about 200 lamprophyres veins have been identified. The first description of the lamprophyres in the Tulgheş zone (which is the object of an ample study) occurs in the geologic study of the Tulgheş zone (Atanasiu, 1929). Later on, the nonmetamorphosed vein rocks from the same zone were presented by Chelărescu (1937, 1938), Bercia, Bercia (1954), Ionescu et al. (1962), Arion et al. (1963), Jakab (1981), Condurache et al. (1985), Vodă, Vodă (1985). The vein rocks identified in wells in the Hagota-Tulgheş zone were mentioned or described by Mureşan, Mureşan (1989-1992), Mureşan (1993-1995), Airinei, Funkenhauser (1993), and Airinei (1994).

1. Petrography

Lamprophyres are, in general, microcrystalline, massive, of a grey or blackish, sometimes smoky colour, within which, in most cases, melanocrate and leucocrate phenocrysts are visible. Very rarely, lamprophyres contain large-sized (5-20 mm) mafic phenocrysts, e.g. in Baratul Mare Valley. In case of thicker veins an increase of the grain size to their central zone has been noticed. No thermal contact phenomena (hornfelsizations) of the host rocks have been observed at the contact with the lamprophyres.

Institutul Geologic al României

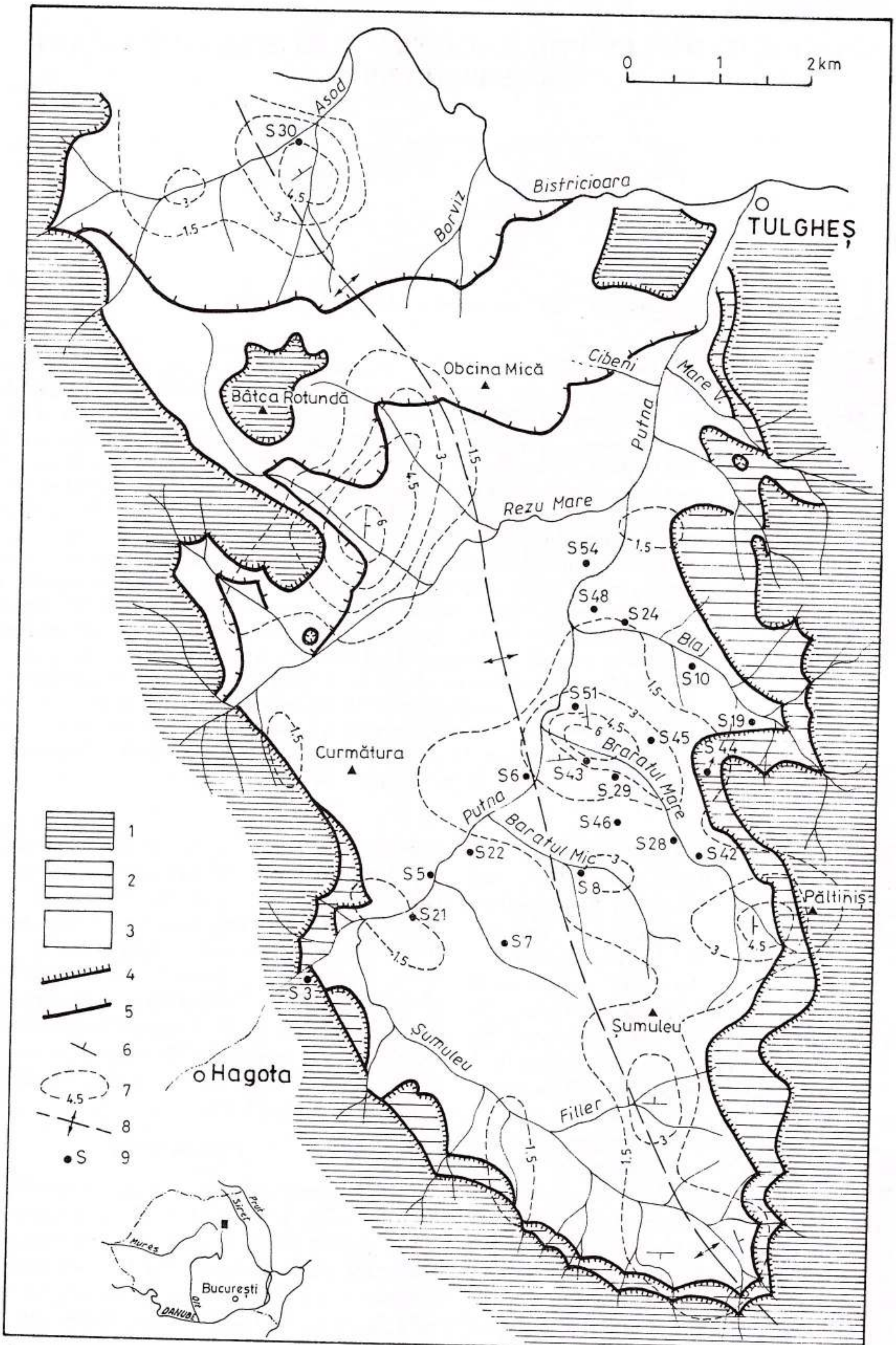

Fig. 1 – Spreading of the lamprophires in the Hagota-Tulgheş zone: 1, Rarău Nappe (Bretila Group, Precambrian); 2, Balaj Nappe (Balaj Formation); 3, Putna Nappe (Tulgheş Group, Cambrian); 4, overthrust; 5, Asod-Rezu Mare Digitation; 6, predominant position of the veins in the lamprophyre fields; 7, contour lines of the lamprophyres frequency (per cent); 8, Valea Putnei antiform; 9, boreholes.

Institutul Geologic al României

Table 1
Modal mineralogical composition of lamprophyres

Type of lamprophyre	Family	No.	Major minerals					Sporadic minerals
			Fp	Amf	Carb	Cl	M.O.	
Vogesite	Syenite	1		16	18	6	10	Fk=34 Serp=16
Spessartite	Diorite	12	18-52	0-38	0-40	0-38	2-28	Serp=0-10 Q=0-10 Bi=0-7
Kersantite	Diorite	1		22	8		6	Bi=18
Malchite	Diorite	1		18	29	22	5	Q=18
Odinite	Gabbro	4	16-66		8-42	8-35	10-22	Bi=8(1probă)
Beerbachite	Gabbro	2	50-54		0-6	2-11	36	Py=8-18
?		1	44			18	18	Ab=30 Q=6
Camptonite?	Alk. gab.	1	34	18	16		8	Bi=10 Py=12 Ol=3

Legend:No-number of analysed samples; Fp-plagioclase feldspars; Amf-amphiboles; Carb-carbonates; Cl-chlorite; M.O.-opaque minerals; Fk-potash feldspar; Serp- serpentinic minerals; Q-quartz; Bi-biotite; Py-pyroxenes; Al-albite; Ol-olivine.

In general, the veins are steeply dipping and are grouped into fields within which the veins display a relatively constant spatial position.

Almost all lamprophyres are affected by carbonatations (mostly calcitizations); calcite occurs as veins, masses or impregnations in the rock mass. Mureşan (1991) considered that the pink carbonate veinlets are genetically related to the Ditrău alkaline massif.

Lamprophyres are often pyritized. Pyrite occurs, in general, as idiomorphic grains, disseminated in the rock and locally concentrated on fissures. The pyritizations and limonitizations of the lamprophyres can be spread on a restricted distance in the adjacent rock. In very many cases, lamprophyres are intensely altered, appearing as a friable aggregate formed of carbonates, limonite, chlorite and serpentinic minerals.

In some cases, one could observe that lamprophyres include angular fragments of epimetamorphic rocks belonging to the Tulgheş Group and in one case, in the Sumuleu Valley, a fragment of pink syenite, similar to those known in the Ditrău alkaline massif.

The majority of studied lamprophyres from the Hagota-Tulgheş zone belong to the diorite family, being of spessartite type and one kersantite sample and one malchite sample, and subordinately to the gabbro family, of the odinite, beerbachite, possibly camptonite type (from the alkali gabbro family). One lamprophyre rich in potash feldspar was assigned to the vegesites, that belong to the syenite family. The modal mineralogical composition of the lamprophyres studied under the microscope is presented in Table 1.

1.1 Vogesite

The rock consists of long prismatic amphibole phenocrysts, partly chloritized and opacitized, included in a feldspathic-carbonatic mass, locally serpentinized. Other melanocrate phenocrysts, entirely substituted by carbonates, chlorite and limonite,could represent pyroxenes. These rocks include large nests, visible macroscopically, formed of carbonatic xenomorphic grains.

The groundmass consists of small, xenomorphic grains of perthitic potash feldspar, often forming aureoles around the carbonatic nests. Beside them fine carbonatic masses, serpentinic minerals and magnetite are noticed.

In 1929 Atanasiu described, in the Tulgheş zone, a lamprophyre, possibly a vogesite, formed of amphibole (entirely altered), in association with feldspar (orthose ?). The phenocrysts are chloritized or substituted by calcite.

1.2 Spessartite

The matrix of these rocks consists of intermediary plagioclase feldspars and amphiboles, beside reduced amounts of biotite, potash feldspar, quartz, olivine and magnetite. When present, the phenocrysts are represented by amphiboles and plagioclase feldspars; these minerals are decomposed, being replaced by carbonates, serpentinic minerals, opaque minerals and limonite.

The groundmass is generally altered. Thus, the plagioclase feldspars occur as rods and polysynthetically twinned prisms, replaced partially by calcite, sericite and serpentine; in places, they are saussuritized. Potash feldspar (orthose) is found sporadically, being partially or totally altered into sericite. The presence of sodium feldspar, as xenomorphic grains, points to albilization phenomena. Amphiboles are found as prisms and rods, partially or totally opacitized, replaced by chlorite and epidote. Biotite scales and lamellas are corroded and randomly spread in the

Institutul Geologic al României

rock mass. Olivine is totally replaced by serpentinic minerals. The opaque minerals are represented by magnetite, locally replaced by hematite or completely leached. Calcite is almost omnipresent, frequently occurring in very large amounts; it replaces the phenocrysts or invades the rock mass. Quartz is locally observed as veinlets or nests formed of xenomorphic, angular grains, with normal to weakly undulatory extinction.

In 1929 Atanasiu identified a spessartite in the Tulgheş zone. The described rock is of a greenish colour, with a silky luster, a rusty alteration crust, and slightly schistous. Under the microscope, one can observe a network of elongated crystals of twinned feldspars, interfingered with short amphibole prisms. Oligoclase-andesine is altered into calcite and epidote, and the brown hornblende into chlorite and epidote. The meshes of the network are filled with chlorite, epidote and calcite, the primary minerals being unrecognizable. Another spessartite displays large-sized feldspar phenocrysts and the amphibole phenocrysts are entirely altered.

The spessartites described by Ionescu et al. (1962) in the Tulgheş-Corbu zone display a panidiomorphous-granulated structure, being formed of a network of elongated crystals of twinned feldspars intercalated with brown amphiboles, as idiomorphic prisms. Chlorite, epidote and calcite occur in the meshes of the network. Feldspar develops as prismatic crystals of maximum 0.5 mm long and it is often calcitized and epidotized. Amphibolite is, generally, altered into chlorite and epidote. Opaque minerals are abounding (5% of the rock mass).

1.3 Kersantite

Kersantites are rocks of a blackish colour and contain relict phenocrysts which, according to the hexagonal contour, seem to have been a biotite replaced by secondary minerals (carbonates, chlorite). Other intensely serpentinized and carbonatated minerals, initially probably an olivine, are very rarely found.

The groundmass consists of idiomorphic lamellas of biotite, short prisms of amphiboles, with intercalations of xenomorphic grains of intermediary plagioclase feldspars and possibly of albite. The rock also contains opaque minerals (magnetite?) and is penetrated by thin carbonatic veinlets.

1.4 Malchite

Relict phenocrysts of quartz and calcitized feldspars are observed under the microscope. The groundmass is altered, the prismatic amphiboles being opacitized and replaced by chlorite. The matrix includes short lamellas of chlorite, xenomorphic grains of calcite, cubic or xenomorphic crystals of opaque minerals, fine grains of quartz. Carbonatic bands are crossing the rock mass.

1.5 Odinite

These rocks are intensely altered, being invaded by carbonates, chlorite and limonite. The phenocrysts, after contours initially pyroxenes, feldspars and amphiboles, are totally replaced by secondary minerals. In one section, plagioclase feldspar is fresher, generally being replaced by carbonates and sericite. The mafic phenocrysts are entirely substituted by chlorite and carbonates. Xenomorphic relicts of biotite occur in one case.

The primary minerals of the groundmass are replaced by carbonates, chlorite and limonite. The opaque minerals are found as square or skeletic forms (ilmenite?). Carbonates invade the rock mass or occur as veinlets.

The lamprophyre veins, possibly odinites, described by Atanasiu (1929) in the Tulgheş zone, have a greenish colour and a rusty alteration crust. They display a massive texture and a holocrystalline-porphyric structure. The phenocrysts are represented by oligoclase-andesine. The matrix consists of feldspar and altered amphibole crystals, that form a network whose meshes are filled with chlorite.

1.6 Beerbachite

The mafic minerals of these quasi-echigranular rocks are represented by partly chloritized pyroxenes (augite), and the salic ones by carbonatated and sericitized plagioclase feldspars. The main opaque mineral is represented by pyrite, found as limonitized cubic crystals or as xenomorphic aggregates. As secondary minerals, carbonates are found in relatively small amounts, beside clayey minerals and limonite.

1.7 Camptonite

An identified lamprophyre, possibly a camptonite, consists of crystals of feldspars, amphiboles, pyroxenes and olivine, strongly altered and invaded by secondary minerals.

The camptonites described by Atanasiu (1929) in the Tulgheş zone are rocks with a basaltic aspect. They display a massive texture and a holocrystalline-porphyritic structure. The phenocrysts are represented by titanaugite (partially or totally substituted by chlorite and calcite), barkevikite, and locally olivine (altered into antigorite and calcite) or quartz (as masses surrounded by a pink rim formed of fine rods of iron oxides ?). The microcrystalline matrix is constituted of barkevikite, pyroxene, opaque minerals (abounding), calcite and small amounts of feldspar,

Institutul Geologic al României

analcime and apatite. The author considered that these rocks differ from the normal camptonites by the absence of biotite and the presence, only sporadical, of feldspar.

These rocks, described by Ionescu et al. (1962) in the Tulgheş-Corbu zone, display a massive texture and a holocrystalline structure. The olivine and pyroxene phenocrysts occur in a microcrystalline mass, formed of augite, barkevikite, plagioclase, zoisite, opaque minerals,sphene and apatite. Quartz occurs sporadically as white-greenish 3-4 mm thick masses, surrounded by a pinkish rim formed of fine rods of iron oxides.

Camptonites presented by Arion et al. (1963) contain phenocrysts of pyroxenes, olivine and, locally, barkevikite, included in a microcrystalline matrix, constituted of augite, plagioclase, barkevikite, and opaque minerals.

1.8 Monchiquite

Monchiquites described by Atanasiu (1929) in the Tulgheş zone are compact, basaltic-like rocks, of a grey-blackish colour. They display an alteration crust of a rusty colour. In places, fine pyrite grains and calcite spherules are observed with the naked eye. Monchiquites show a massive texture and a hypocrystalline porphyric structure. The phenocrysts of augite (altered into chlorite, calcite and sphene), olivine (altered into serpentine and calcite), locally barkevikite, basic plagioclase feldspar and biotite are included in a matrix formed of barkevikite, opaque minerals, analcime, and sporadically glass, sphene and apatite. It is to note the absence or reduced presence of biotite and the prevalence of augite and olivine.

Atanasiu (1929) assigned to the camptonite and monchiquite series some strongly altered lamprophyres, of a green or grey-greenish colour, with a cryptocrystalline-porphyric structure. The phenoelements, locally large-sized (more than 1 cm), are totally altered, being replaced by chlorite (former pyroxenes ?) or serpentine (at the expense of olivine ?). Remains of unaltered biotite are found very rarely. The cryptocrystalline matrix is invaded by calcite, the primary minerals being completely altered.

Chelărescu (1937) described several monchiquites, intensely altered hydrothermally (frequently propylitized), which occur beside the polymetallic sulphides in the Tulgheş zone. The primary phenocrysts are, at present, substituted: feldspar by calcite, sericite and quartz, augite by pennine, and olivine (or analcime) by serpentine, calcite, quartz and iron oxides. The groundmass is a mixture of calcite, iron oxides and, more seldom, antigorite, pennine and zoisite.

Ionescu et al. (1962) described monchiquite in the Tulgheş-Corbu zone. These rocks are of a dark grey colour and display a hypocrystalline-prophyric structure, with a basaltic aspect. The augite and olivine phenocrysts are included in a microcrystalline mass, constituted of augite, barkevikite, opaque minerals (ilmenite, pyrite), sphene and apatite. The pyroxene phenocrysts occur as short prisms, up to 2-3 m long, twinned, with clinochlore and calcite on fissures. Olivine is almost completely transformed into serpentine and calcite.

Monchiquites described by Arion et al. (1963) contain rare phenocrysts of olivine and pyroxene included in a hypocrystalline matrix of barkevikite, pyroxene and opaque minerals. In places pyrite is abounding.

1.9 Other lamprophyres

They are rocks hard to define either due to the advanced mineralogical alterations or to the impossibility to assign them to the accepted petrographic classifications.

Thus, a lamprophyre contains, beside plagioclases, a large amount of albite (about 30%), both feldspars being easily sericitized. The chlorite scales preserve the long-prismatic contour of some former mafic minerals, possibly pyroxenes.

A lamprophyre with enclaves of crystalline schists has been sampled from the peak between the Balaj and Baratul Mare valleys. The lamprophyre mass includes: very large (up to 1 cm), tabular-prismatic phenocrysts, completely serpentinized and partially calcitized, probably initially pyroxene; the minerals with a hexagonal contour, entirely serpentinized and carbonatated, probably representing former amphiboles; very large grains, serpentinized, with rows of opaque minerals on fissures, formed at the expense of pre-existent olivine. All these strongly altered phenocrysts are included in a groundmass formed of clayey minerals, carbonates, serpentinic minerals. The rock is penetrated by calcite veinlets. The enclosed angular elements represent up to 40% of the rock and are formed of quartzites, quartz-sericite schists and quartz-graphite schists.

Mureşan (1991, 1994, 1995) described schists enclaves in lamprophyres, in the wells 8-Baratul Mic (here, the lamprophyre has a fluidal texture), 1-Hagota (calcite epigenetic crosses the lamprophyre and quartz schist), 47-Putna, 7-Beche, 21-Putna, 43-Baratul Mare. In the well 43-Baratul Mare, Mureşan (1995) identified a highly altered lamprophyre that contains an enclave in an older lamprophyre.

Institutul Geologic al României

Table 2
Average contents in minor elements (in p.p.m.) of the lamprophyres grouped according to their spatial position (azimuth of the dipping sense)

Position	No.	Ag	As	B	Co	Cr	Cu	Mn	Mo	Ni	Pb	Sn	Zn
340-20^0	11	0.03	0	10	34	104	53	289	2.2	156	29.8	1.1	220
80-115^0	10	0.03	20	27	35	76	59	391	2.1	149	18.3	1.0	285
210-230^0	5	0.08	20	0	41	130	70	150	2.6	160	32.0	0.8	128
260-280^0	5	0.20	40	36	40	79	36	224	2.0	132	21.6	1.0	110
300-320^0	7	0.04	29	33	20	82	40	80	1.4	93	19.7	0.6	44

No. = number of analyses

1.10 Other vein rocks

In the Hagota-Tulgheş zone, other vein rock types have been described, some of them of the diabase type and others, more numerous, affiliated to the Ditrău massif.

1.10.1 Diabases

Atanasiu (1929) considered that in the Tulgheş zone diabases occur beside melaphyres as intercalations interbedded in the Mesozoic sedimentary deposits overlying the crystalline.

Chelărescu (1937) described veins of porpylitized diabases beside the epigenetic mineralisations in the Asod Brook zone. Diabases consist of feldspar, olivine, augite, antigorite, pennine, sericite, calcite, and quartz. Olivine, the oldest mineral, is found as idiomorphic crystals, locally substituted by antigorite, calcite and quartz. Feldspar is altered in the interior, with neoformation of sericite and saussurite. Augite is altered into brown hornblende towards the periphery.

Ionescu et al. (1962) mentioned the presence of the diabases in the Tulgheş-Corbu zone, in the north-eastern part of the Barasău Valley basin. These diabases are described in general; they have a grey colour with greenish hues, an ophiolitic structure and a massive texture.

Arion et al. (1963) described four diabase veins, of less than 1m thick, unconformable versus the epimetamorphic crystalline schists from the right side of the Putna Valley, in the zone of the Hagota village. These rocks display a grey colour and a massive aspect. They have and intersertal structure, within which prismatic-acicular crystals of basic plagioclase feldspar include crypto-crystalline or glassy masses, probably of pyroxenic origin. These masses are strongly altered and calcitized. Partly altered lamellas of biotite, as well as granular clusters of opaque minerals beside secondary minerals are also frequently observed.

Mureşan & Mureşan (1990, 1991) identified diabases in the wells 3-Putna and 1-Hagota. Thus, the diabase intercepted in the well 3-Putna, in the interval 1042-1045m, consists of feldspars, pyroxenes and amphiboles. The melanocrates are chloritized. In the well 1-Hagota three diabase veins are described in the intervals 629-631m, 828-833m and 968-970m. The first diabase is altered and displays an ophitic structure. Hypidiomorphic feldspars, partly sericitized and calcitized, can be noticed, within which amphiboles partly altered into biotite are developed. The second vein has a diabase strucutre due to the hypidiomorphic plagioclase feldspars, with different trendings, between which opacitized and chloritized melanocrates are developed. The third diabase shows a similar structure. Feldspars are saussuritized and partly calcitized, and melanocrates are opacitized and chloritized.

1.10.2 Alkaline vein rocks

These rocks, associated or not with mineralisations, were identified in boreholes by Mureşan (1989-1995) and Funkenhauser, Airinei (1992, 1993). Thus, Mureşan described: a syenitic rock with monazite, related to the metallogenesis of the Ditrău massif, in the well 5-Hagota; two veins of calcitized tinguaites, in the well 29-Baratul Mare; a massive, fine-grained vein rock (with an enclave of a pyritous, probably syngenetic, metamorphosed mineralisation), that is also found upwards in the borehole column as an enclave included in a lamprophyre, in the well 22-Putna.

Fukenhauser, Airinei (1992, 1993) described: syenites and microsyenites in the wells 5-Putna, 22-Putna and 43-Baratul Mare; an intrusive, more acid rock, with a porphyric structure, beside lamprophyres, in the well 24-Balaj; liebneritic syenites in the well 7-Beche.

2. Geochemical considerations

92 out of the 200 lamprophyres identified in the Hagota-Tulgheş zone have spectrally been analysed

Institutul Geologic al României

for 16 elements. It it to note that, Bi, Cd, Sb and W are usually below the detection limit.

The data presented in the above table do not indicate any law of any preferential geochemical component of the lamprophyres grouped according to their spatial position (azimuth of the dipping sense), regardless of the sampling site.

Table 3 presents the average contents (in p.p.m.) of the lamprophyres grouped according to their geographic spreading (Fig. 1), in certain fields, presented from north to south, regardless of the vein position.

Table 3

Average contents of the minor elements (in p.p.m.) of the lamprophyres grouped according to their geographic spreading

Zone	No.	Ag	As	B	Co	Cr	Cu	Mn	Mo	Ni	Pb	Sn	Zn
Asod	6	0.03	0	41.7	50	91	76	191	4.16	138	32.2	1.16	157
Rezu Mare	17	0.02	0	21.4	29	62	42	551	2.17	62	13.5	0.58	248
Putna-B.M.	22	0.07	18	6.4	21	139	76	296	3.72	184	30.1	0.86	99
B.M. upstream	15	0.06	20	27.0	35	132	69	167	2.93	214	21.2	1.00	170
Sumuleu	23	0.03	17	9.6	26	81	57	309	2.93	130	31.4	1.65	166

No. = number of analyses, B.M. = Baratul Mare

Table 4

Contents of major elements of some lamprophyres in the Tulgheş zone (Atanasiu, 1929)

Oxydes (%)	1	2	3	4	5	6	7
SiO_2	37.24	34.72	38.78	39.10	33.74	26.48	45.81
TiO_2	3.40	3.02	5.10	4.08	2.86	1.61	2.78
Al_2O_3	12.62	9.82	11.64	13.84	14.12	15.72	19.02
Fe_2O_3	2.47	3.24	4.22	5.41	4.78	3.77	1.44
FeO	13.37	11.39	12.30	8.39	9.84	11.28	8.72
MnO	0.86	1.56	0.85	0.90	0.60	1.51	0.93
MgO	6.59	8.43	8.24	9.11	13.23	10.14	6.76
CaO	13.96	10.92	9.24	8.88	6.00	9.67	5.52
BaO+SrO	0.09	traces	0.19	traces	ndt	ndt	ndt
Na_2O	2.04	2.47	0.93	3.93	5.15	3.10	2.90
K_2O	1.29	0.65	0.10	ndt	ndt	0.55	168
P_2O_5	0.13	traces	0.11	0.76	0.16	0.27	ndt
SO_3	1.44	0.84	0.67	1.40	3.64	0.49	ndt
H_2O	0.40	2.06	0.62	0.34	0.49	0.77	0.25
CO_2+H2O^+	4.97	11.04	6.78	4.64	6.34	13.73	*1.80
TOTAL	100.87	100.16	99.77	100.78	100.95	99.09	100.65

1, camptonite, Piatra Roşie Românească; 2, monchiquite, Magyaros; 3, monchiquite, Fuges; 4, camptonite-monchiquite, Baratul Mic; 5, camptonite-monchiquite, Putna Brook; 6, camptonite-monchiquite, Putna Brook; 7, spessartine, Stejii Mount (*losses=3.04 %); ndt=undetermined.

The resulting values do not indicate any law concerning the variation of the contents of the analysed elements according to their regional spreading.

Atanasiu (1929) grouped the lamprophyres and diabases in the Tulgheş zone into two rock series, according to the chemistry of the rocks: the camptonite-monchiquite series, representing differentiation products of the alkaline magmas, of Atlantic type; the vogesite-spessartine-odinite and diabase melaphyre series, representing differentiation products of the alkali-calcic, granito-dioritic and gabbro-peridotitic magmas, of Pacific type. Table 4 presents the results of the chemical analyses (major elements) effectuated by Atanasiu (1929) on some lamprophyres from the Tulgheş zone. They have been defined on the basis of the petrographic analyses. In sample 2, and possibly samples 5 and 6, the apparent lower contents in SiO_2 have been regarded at the expense of some high contents in CO_2 and H_2. Because of the small number of analyses, it is difficult to characterize and define the lamprophyre types from the chemical point of view.

Institutul Geologic al României

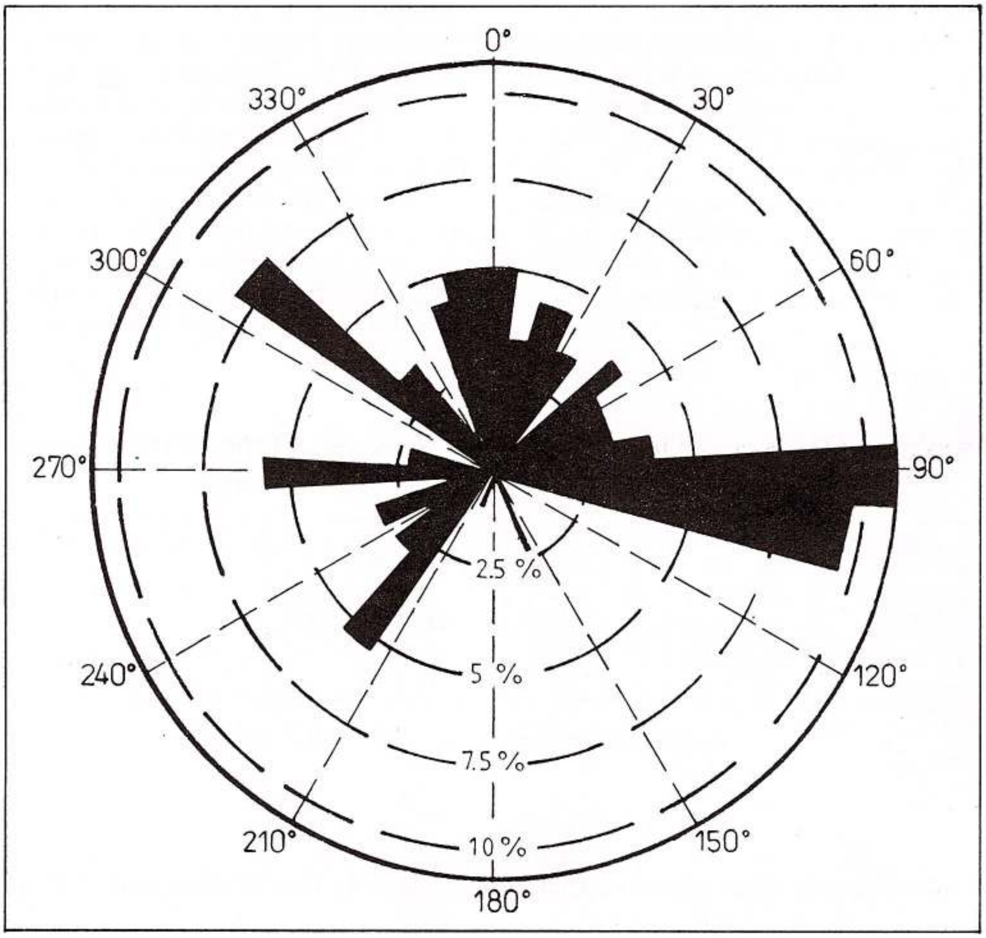

Fig. 2 - Diagram of the lamprophyre veins positions (azimuth of the dipping sense) in the Hagota-Tulgheş zone (per cent).

The data presented in tables 2, 3 and 4 point out that in the Hagota-Tulgheş zone the contents of lamprophyres in the analysed elements do not depend significantly either on the spatial position or on the geographic spreading of these rocks. All this suggests the common origin of all lamprophyres in the study zone.

3. Spreading and position of lamprophyres

In the Hagota-Tulgheş zone lamprophyres are grouped into several fields (Fig. 1), situated in the Asod, Rezu Mare, Putna-Baratul Mare, Baratul Mare, Filler-Şumuleu valleys zones. The lamprophyre fields occur mostly in the spreading area of the Tulgheş Group formations, showing a tendency to close at their contact with the Balaj and Rarău nappes.

The spatial position of 98 out of 200 identified lamprophyres could be determined either directly, with the compass, or indirectly, biogeophysically (with the angular rod). The position of the lamprophyres differ from one field to another, being, however, relatively constant within the same field (Fig. 1). With a few exceptions, the dipping of the lamprophyres is sharp ($60\text{-}90^0$). The diagram with the percentage representation of the lamprophyre positions (azimuth of the dipping sense) has been drawn up based on the 98 positions measured (Fig. 2).

The above-mentioned diagram indicates that the majority of the lamprophyres are assigned to a system of conjugated directions, corresponding to a system of fractures with a N-S trend and eastern dips, that is a fracture system with an E-W trend and N dips.

4. Dimensions and volume (in percentage) of the lamprophyres

In the Hagota-Tulgheş zone, lamprophyres are quite frequently found (Atanasiu, 1929). At the surface, the thickness of the veins is in general submetric

Institutul Geologic al României

(usually 20-50m), very seldom more than 1m. Along the strike, these rocks could be followed at the surface on limited distances (of metres order). The lamprophyre bodies are usually unconformable versus the crystalline schists and quite rarely they occur as concordant veins.

All the wells drilled in the Hagota-Tulgheş zone intercepted lamprophyres. The thickness of the lamprophyre veins in the drilling columns is, in general, of the metres order, even smaller. Apparently great thicknesses have been found in the wells: 1-Hagota (13 m), 21-Putna (19 m), 43-Baratul Mare (11 m), 47-Putna (11 m, 30 m, 11.5 m).

zone, the author considered that the genetic association of these rock is less probable. The mentioned lamprophyre series and the diabase-melaphyre series, by their very similar chemistry, made the mentioned author to conclude that they represent products of the same magmatic phase, of Upper Triassic age.

Chelărescu (1937) considered the mineralizations in the Tulgheş zone as post-metamorphic, associated with a hydrothermal activity related to the granodioritic massifs and lamprophyre veins. Later on, in 1953, he associated those mineralisations with the Neogene volcanic activity in the Călimani-Gurghiu-Harghita chain.

Table 5
Lamprophyres spreading in the wells in the Hagota-Tulgheş zone (according to Mureşan, 1989-1995; Airinei, 1993, 1994)

Well	Loc.	Depth	No.	Thickness	%	Well	Loc.	Depth	No.	Thickness	%
S1	Hagota	994	13	42.0	4.23	S28	Bar. Mare	659	6	11.2	1.70
S3	Putna	1200	12	29.0	4.23	S29	Bar. Mare	645	1	3.5	0.54
S5	Putna	1410	10	17.7	1.26	S30	Asod	655	4	10.5	1.60
S6	Putna	1335	14	45.0	3.37	S42	Bar. Mare	700	2	2.0	0.29
S7	Beche	750	10	23.0	3.07	S43	Bar. Mare	550	10	29.4	5.35
S8	Bar. Mic	700	4	7.0	1.00	S44	Bar. Mare	720	1	5.0	0.69
S9	Bar. Mare	675	2	3.5	0.52	S45	Bar. Mare	602	2	7.5	1.25
S10	Balaj	650	6	20.0	3.08	S46	Bar. Mare	650	5	12.0	1.85
S19	Balaj	1165	6	21.5	1.85	S47	Putna	400	11	79.2	19.80
S21	Putna	476	4	26.0	5.46	S48	Putna	450	1	12.0	2.67
S22	Putna	662	15	43.3	6.54	S51	Putna	406	4	15.9	3.92
S24	Balaj	1114	6	18.0	1.62	S54	Putna	353	1	3.5	0.99

(Sd-well; Loc.=locations; Ad.=depth of the well; No.=number of lamprophyre veins intercepted; Thickness=total apparent thicknesses; %-share of the lamprophyre intercalations in the lithologic column of the well; Bar.=Baratul)

Table 5 presents the systematic data on the spreading of the lamprophyres intercepted by wells drilled in the Hagota-Tulgheş zone. Considering these data, it results that out of the 17,921m drilled, 487.7m have been crossed by lamprophyres, totalizing about 150 veins, with an apparent average value of 3.25m. They represent about 2.72% of the rock investigated by drillings.

5. Age, genesis and relationships of lamprophyres with the epigenetic mineralisations

In the Tulgheş zone, the alkaline character of the lamprophyres from the camptonite-monchiquite series is assigned by Atanasiu (1929) to the affiliation of these rocks to the Ditrău alkaline massif, considered by the mentioned author of Upper Cretaceous age at most. Camptonites and monchiquites should be younger, that is post-Aptian in age. Although the chemistry of the vogesite-spessartine-odinite and diabase-melaphyre series show affinities with the granodioritic intrusive massifs in the Tulgheş

Savul (1954) mentioned in the Corbu zone a close association between the lamprophyres and mineralisations, and considered that they originate in hydrothermal solutions differentiated at depth, which represented access ways of the fractures on which the lamprophyres are situated.

In 1954, Bercia and Bercia pointed out that, for the mineralisations situated north-east of Tulgheş, the absence of marcasite indicates their formation at great depths and in relation to the zones on which the lamprophyres were injected.

Koczur (1973) mentioned that the mining works carried out in the Şumuleu-Filler zone, proved that the mineralisations are closely related to a lamprophyre which presents, in the contact zone with the schists, pyrite and chalcopyrite impregnations.

Anastasiu and Constantinescu (1980) highlighted the association of the lamprophyres in the Jolotca zone with some mineralised veins.

In the Hagota-Tulgheş zone there is a good spatial association of the lamprophyres with the epigenetic mineralisations (Şumuleu, Baratul Mare, Cibeni, Barasău, Sângeroasa).

Institutul Geologic al României

Nearby Tulgheş, although the density of the lamprophyres is reduced, two of them are closely related to the epigenetic mineralisations. Thus, the common sulphide mineralisation in quartz gangue, identified in the Cibeni Valley, occurs beside an intensely pyritized lamprophyre, both veins having a N-S trend. In the Ohaba Peak zone one of the two weakly mineralised veins with sphalerite-galena and lantanides in carbonate-quartz gangue occurs, in the hanging wall, at a distance of ca 20 cm beside an intensely altered lamprophyre, and displays the same position ($260^0/50^0$).

In the Borsec-Tulgheş zone, within the Tulgheş Group, there occur several vein lead-zinc mineralisations related to lamprophyres. From this point of view, the situation of the lamprophyres is, as follows: lamprophyres are bordering on or they are in the vicinity of the mineralized veins, at Paltin, Sangeroasa, Obcina Mică , Baratul Mare; lamprophyres occur as fragments in the mineralised breccias at Paltin; lamprophyres are hosting the mineralisations at Paltin, Pârâul cu Linia (Barasău), Argintăria. This association was argued (Jakab, 1981; Vodă, Vodă, 1985) by the fact that both lamprophyres and the mineralised solutions used the same access ways.

As regards the age of the lamprophyres, we consider that they are younger than the epimetamorphics of the Tulgheş Group (Cambrian), younger than the overthrusts in the area and than the Asod-Rezu Mare digitation, younger than the Paltin-type mineralisations for which Jakab, Popescu (1981) estimated a Cretaceous age, possibly Upper Jurassic, on the basis of the isotopic age analyses, $^{205}Pb/^{205}Pb$=0.17-0.18.

Received: February 24, 1998
Accepted: October 30, 1998

References

Airinei, I., Funkenhauser, P. (1983) Report, Archives of "Geolex" S.A., M. Ciuc.

— **(1984)** Report, Archives of "Geolex" S.A., M. Ciuc.

Anastasiu, N., Constantinescu, E. (1980) Report, Archives of "Geolex" S.A., M. Ciuc.

Arion, M., Rişa, E., Nedelcu, V. (1983) Report, Archives of "Geolex" S.A., M. Ciuc.

Atanasiu, I. (1929) Cercetări geologice în împrejurimile Tulgheşului (judeţul Neamţ) *An. Inst. Geol. Rom.*, v. XIII, p. 165-371, Bucureşti.

Bercia, E., Bercia I. (1954) Report, Archives of "Geolex" S.A., M. Ciuc.

Chelărescu, A. (1937) Gisements metalliferes de Tulgheş. Ann. *Sc. Univ. Jassy*, XXIII, II, p. 265-393, Iaşi.

Condurache, C., Dudnic, G., Strugaru, T. (1985) Report, Archives of "Geolex" S.A., M. Ciuc.

Funkenhauser, P., Airinei, I. (1980) Report, Archives of "Geolex" S.A., M. Ciuc.

Ionescu, C., Gheruci, O., Costache, P., Micu, C., Popa, Gh., Puiu, V., Puiu, M., Arion, M., Teucă, I. (1962) Report, Archives of "Geolex" S.A., M. Ciuc.

Jakab, G. (1981) Contribuţii la cunoaşterea mineralizaţiilor plumbo - zincifere de la Valea Seacă - pîrîul Paltin (Carpaţii Orientali) *D.S. Inst. Geol.*, LXVI/2, p. 21-35, Bucureşti.

— **, Popescu, G. (1981)** Date noi privind vîrsta şi geneza mineralizaţiilor hidrotermale din cristalinul seriei de Tulgheş, zona Gheorgheni-Bilbor (Carpaţii Orientali). *D.S. Inst. Geol.*, LXVI/2, p. 37-44, Bucureşti.

Mureşan, M., Mureşan, G. (1989) Report, Archives of "Geolex" S.A., M. Ciuc.

— **(1990)** Report, Archives of "Geolex" S.A., M. Ciuc.

— **(1991)** Report, Archives of "Geolex" S.A., M. Ciuc.

— **(1992)** Report, Archives of "Geolex" S.A., M. Ciuc.

Mureşan, M., (1993) Report, Archives of "Geolex" S.A., M. Ciuc.

— **(1994)** Report, Archives of "Geolex" S.A., M. Ciuc.

— **(1995)** Report, Archives of "Geolex" S.A., M. Ciuc.

Vodă, Al., Vodă, D. (1985) "Consideraţii asupra unor mineralizaţii epigenetice din zona cristalino-mezozoică a "Carpaţilor Orientali" *Stud. cerc. geol., geof., geogr., Geologie*, 30, p. 53-57, Bucureşti.

Institutul Geologic al României

ZIRCON IN ALBEŞTI GRANITE (LEAOTA MOUNTAINS), SOUTH CARPATHIANS, ROMANIA

Ion Niculae ROBU, Lucia ROBU

Institutul Geologic al României, str. Caransebeş nr. 1, 79678 Bucureşti 32.

Key words: Granitoid. Zircon. Morphology. Prism. Pyramid. Petrogenetic significance. Temperature.

Abstract: Albeşti granite is hosted in the Leaota crystalline formations. It has a tabular form and occupies a fixed stratigrafical position within the metamorphic pile. There are two genetical hypotheses: (1) anatexis processes and in situ crystallization due to the ultrametamorphism of the some material of granitic composition, (2) magmatic origin and emplacement facilitated by the tectonic plane. The chemical composition of this granite has a peraluminous, calc-alkaline character. Zircon morphology has been considered according to the original typological classification for zircon proposed by J. P. Pupin, G. Turco (1972). Q and S types have been identified (100) prism and (211) pyramids are more developed than (110) and (101) ones. Zircons are colourless, light and dark pink, or brown and inside of them apatite, opaque and mafic minerals, and gaseous-fluid inclusions are visible. A few metamictized crystals have been observed. Sometimes zonal and overgrown zircons have been identified. The crystallization temperature values vary between 850^0 and 750^0 C. Pupin's morphological classification of zircon crystals points out a crustal or hybrid (crust + mantle) origin for the Albeşti granitic rocks.

Introduction

Due to its mineralogical and petrographical characteristics and to its spatial position in the crystalline formations that contain it, the study regarding the morphology of zircon crystals from this granite, tries to give some information about conditions of zircon crystallization, and by this way some data about the granitic rocks which host zircons; this one is supported by the theory which supposes that the changes of chemical and physical parameters of the crystalization environment determine changes of the crystal morphology.

Geological considerations

The Albeşti granite is hosted by the Leaota crystalline formations. It has a tabular form and occupies a fixed stratigraphical position within the metamorphic pile. There are two genetical hypotheses: - the Albeşti granite formed as a result of the anatexis and in situ crystallization due to ultrametamorphism of some material of granitic composition (Gheucă, Dinică, 1981, 1983);

- its emplacement has been facilitated by the presence of a tectonic plane reactivated during and after the granitic intrusion; the mineralogical characters (oscillatory zoning in the plagioclase) point out the existence of a magmatic chamber which generated the Albeşti granite (Tatu, Săbău, 1987).

Chemical characteristics

The chemical composition of this granite has a peraluminous-calc-alkaline character, a variable and generally sub-unitary Na_2O/K_2O ratio and the sum of Na and K oxides, ranging between 5 and 8.66; according to the CIPW normative composition, the Albeşti granite plots in the field of monzogranites, close to the granodiorites boundary (Tatu, Săbău, 1987).

Modalities of samples preparing

Ten samples, weighting 5 kg each, were taken off from this granite. Each sample was crushed at 1 mm fraction; zircon has been found in the fractions of about 0.2-0.5 mm.

Institutul Geologic al României

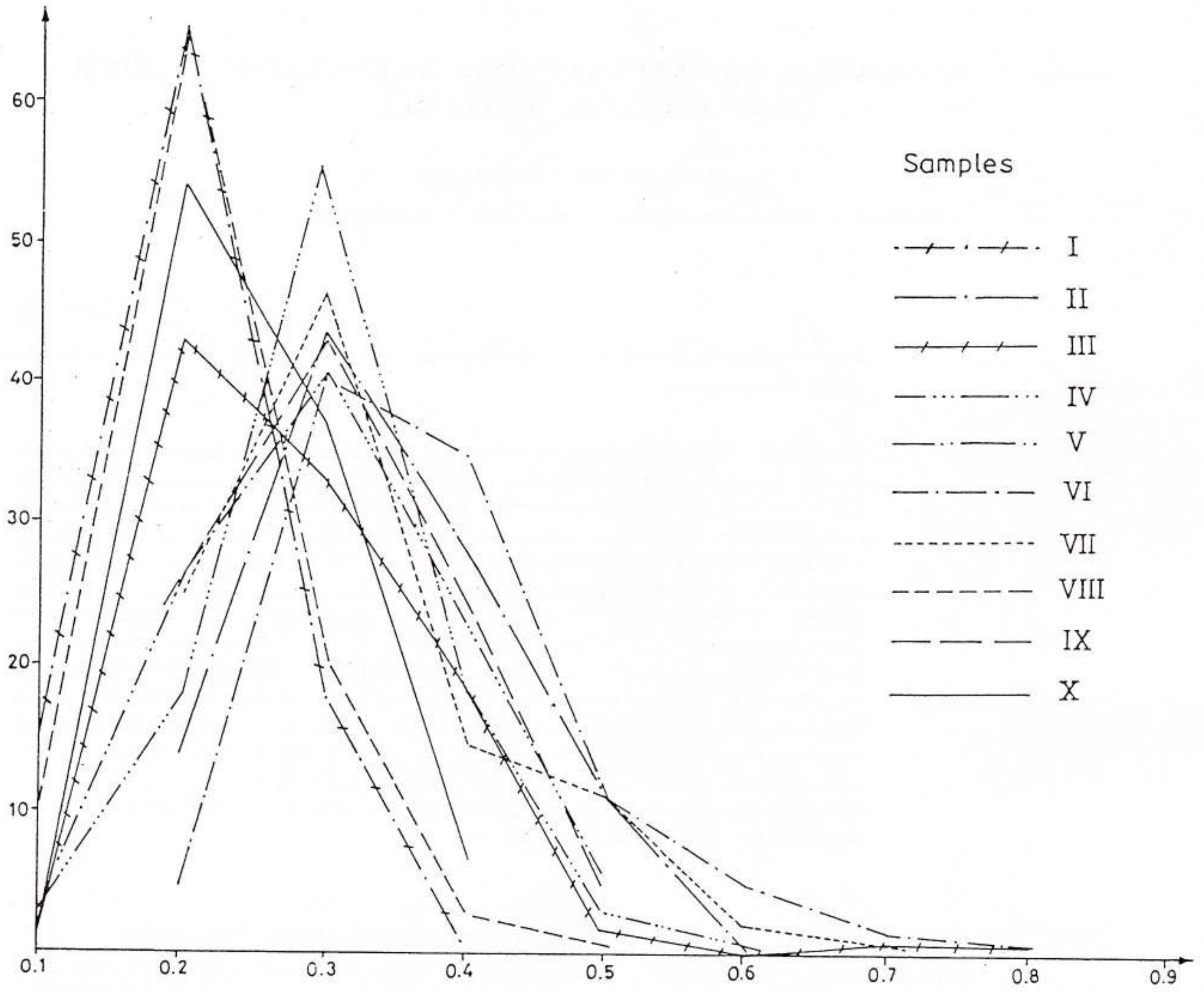

Fig. 1 – The length variation of the zircon crystals.

The morphological study under binocular microscope has been made using zircon crystals, separated according to the specific heavy minerals methods. All morphological and typological consideratins have been made according to Pupin, Turco (1972) and Pupin (1980).

The typological distribution has been established on the basis of the examination of 100 unbroken zircon crystals from each granite sample.

Zircon morphological features

Zircons in the Albeşti granite consist of fine crystals, colourless, light-pink to dark-pink, seldom brown, with long or short prismatic habit; the colourless crystals and long prismatic ones prevail.

No more variations of the lengh or the elongation exist (Figs. 1, 2).

Zircon morphological types, according to Pupin's classification, are represented mainly by the Q_3, Q_4, Q_5 and less by S_{16}, S_{17} or S_{13}, S_{14}, S_{18}, S_{19} types (Fig. 3).

The (100) prism faces and (211) pyramidal ones are well-developed, whereas the faces (110) and (101) appear subordinately.

In transmitted light, zircon crystals have a complicated structure; there are some visible inclusions of minute prismatic crystals, most probably of apatite, as well as gaseous-fluid ones or opaque minerals (probably magnetite or ilmenite). The inclusions exhibit a chaotic distribution in the crystals, concentrating mainly in the prism development zone.

A few metamictic crystals have been observed; the process is weak few crystals are isotrope.

Sometimes zircons are zoned and some of them are overgrown.

Typological frequency distribution (Fig. 4) is very

Institutul Geologic al României

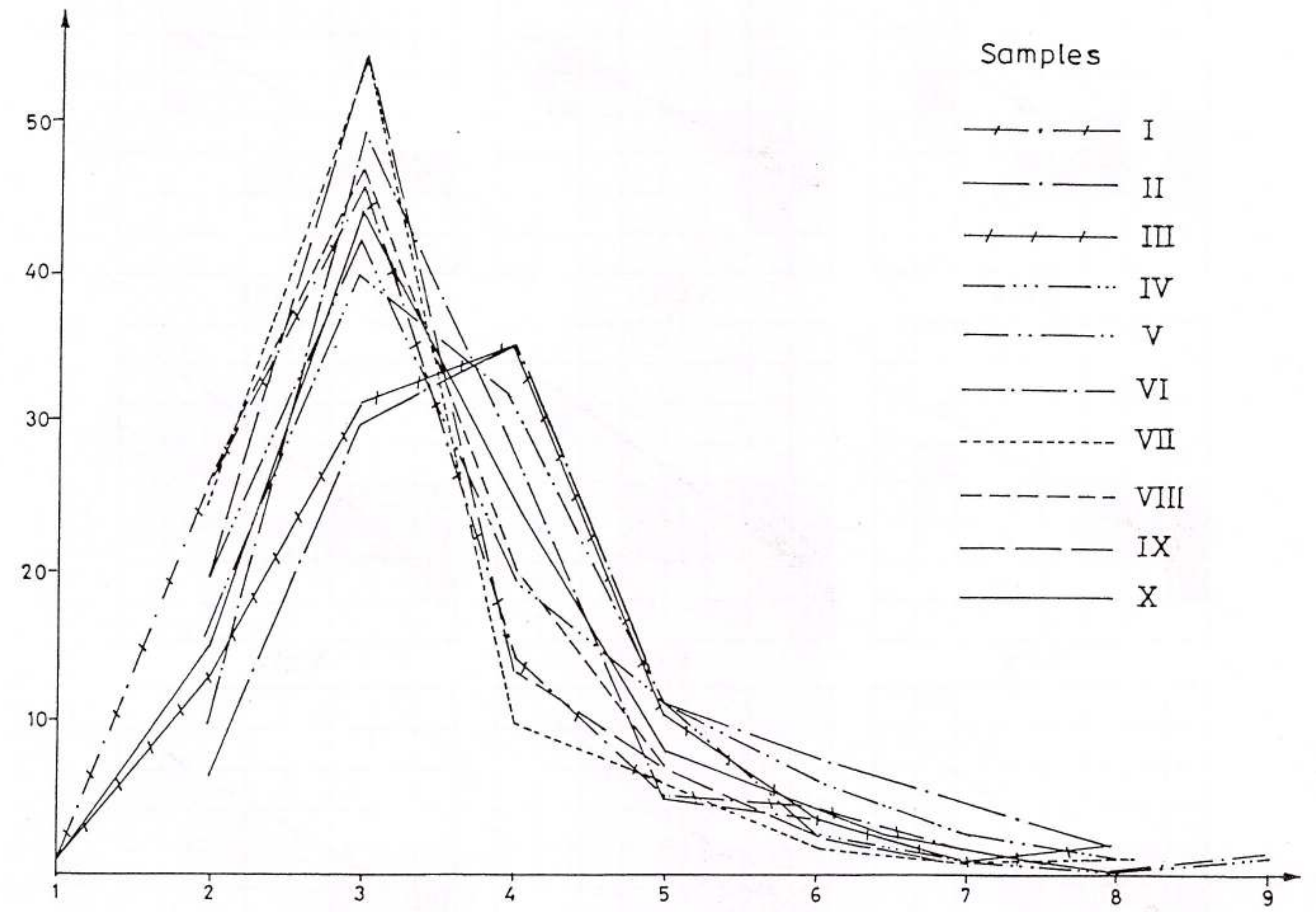

Fig. 2 - The elongation of the zircon crystals.

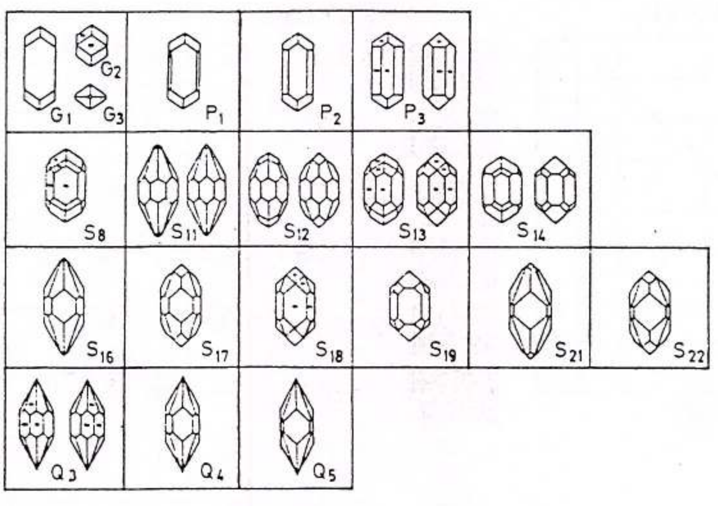

Fig. 3 - Main morphological types of the zircons.

Institutul Geologic al României

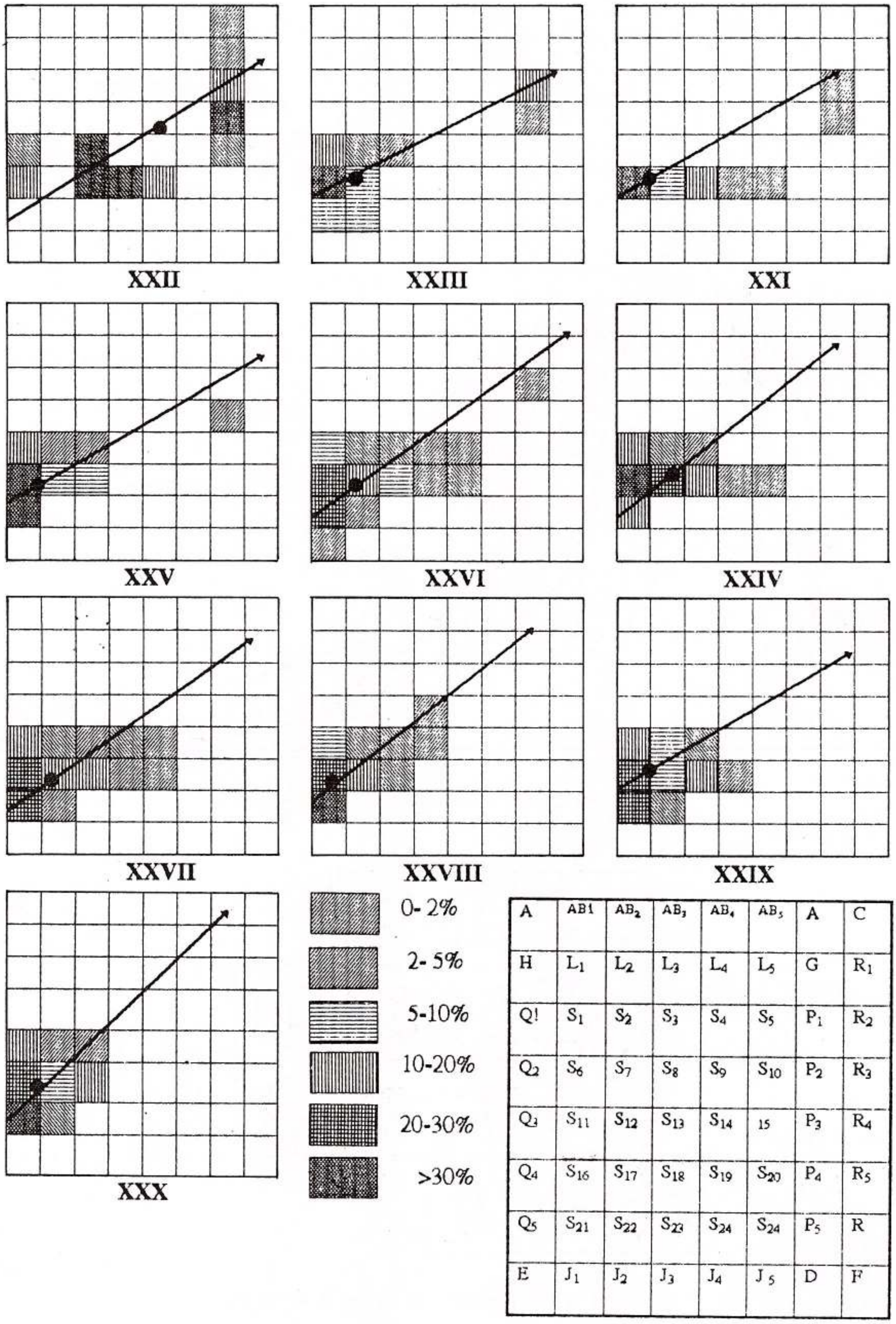

A	AB1	AB_2	AB_3	AB_4	AB_5	A	C
H	L_1	L_2	L_3	L_4	L_5	G	R_1
Q!	S_1	S_2	S_3	S_4	S_5	P_1	R_2
Q_2	S_6	S_7	S_8	S_9	S_{10}	P_2	R_3
Q_3	S_{11}	S_{12}	S_{13}	S_{14}	15	P_3	R_4
Q_4	S_{16}	S_{17}	S_{18}	S_{19}	S_{20}	P_4	R_5
Q_5	S_{21}	S_{22}	S_{23}	S_{24}	S_{24}	P_5	R
E	J_1	J_2	J_3	J_4	J_5	D	F

Fig. 4 – Typological frequency distribution of zircon.

Institutul Geologic al României

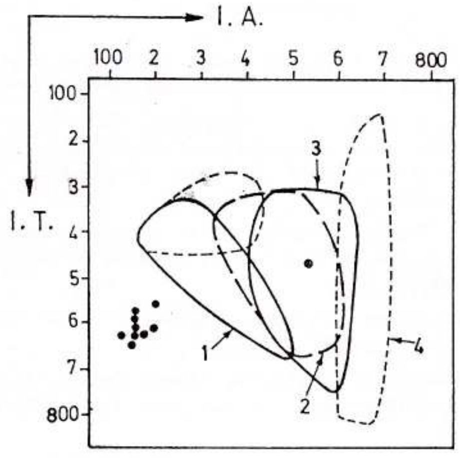

Fig. 5 – Mean calculated points and mean typological evolutionary trend

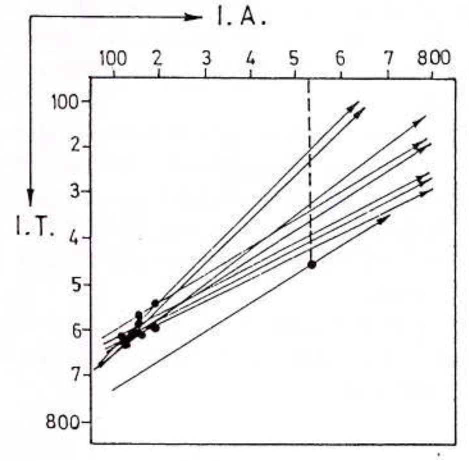

Fig. 6 – Distribution of plutonic rocks in the typological diagram: (1) diorites, gabbros, tonalites; (2) granodiorites; (3) monzogranites and monzosyenites; (4) alkaline and hyperalkaline syenites and granites.

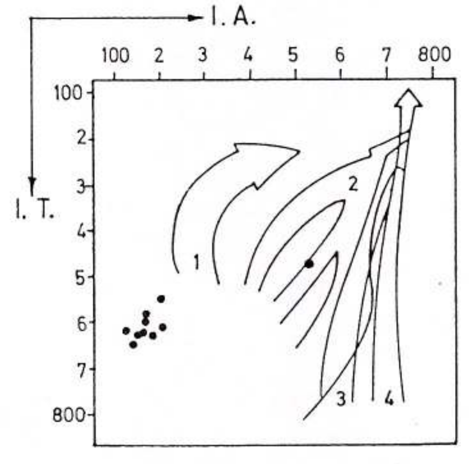

166990

Fig. 7 – Distribution of mean points and mean T.E.T. of zircon from (1) granites of crustal or mainly crustal origin; (2+3) granites of crustal + mantle origin, hybrid granites; (4) granites of mantle or mainly mantle origin.

similar for all studied samples, poining out the same fields (peraluminous) of the diagram for the majority of zircon populations. Some samples present two different fields (peraluminous and peralkaline), which could be interpretated as two different crystallization moments, the first one being predominant.

According to Pupin's typological method, the mentioned morphological observations point out zircon crystallization temperature values ranging between 850 and 750^0 C.

The mean calculated points from Albeşti granites (Fig. 5) plot on the T.E.T. diagram of plutonic rocks near diorites, gabbros and q-diorites field (Fig. 6).

The peraluminous - calc-alkaline character and the mean typological evolution tendency point out a crustal origin (except one sample with hybrid origin -crust + mantle) for these granitic rocks (Fig. 7).

Conclusions

Morphological and optical characteristics of the zircon populations emphasize the peraluminous-calc-alkaline character of the magma where zircon crystallized and which have determined some specific

Institutul Geologic al României

morphological features, as: good development of the (100) prism faces and (211) pyramidal ones, but the subordinated appearance of the (110) prisms and (101) pyramids.

The small content of radio-active elements determined few metamictic phenomena, but the presence of different kinds of inclusions (solid, liquid, or gaseous) emphasize a nearly crystallization for opaque minerals or apatite, and some gas content in the parental magma.

The sporadical appearance of zoning and overgrown crystals point out few processes of assimilation or magmatic corrosion.

References

Gheuca, I., Dinică, I. (1981) Asupra genezei granitului de Albeşti. *D. S. Inst. Geol. Geofiz.*, LXVIII/1, Bucureşti.

— **, Dinică, I. (1983)** Litostratigrafia şI tectonica cristalinului Leaotei între Albeşti-Valea Ghimbav-Valea Bădeanca (Iezer-Leaota). *D. S. Inst. Geol. Geofiz.*, 70, 71/5, Bucureşti.

Pupin, J. P., Turco, G. (1972 a) Une typologie originale du zircon accessoire. *Bull. Soc. Fr. Mineral. Cristallogr.*, 95; p. 348-359, Paris.

— **(1980)** Zircon and Granite Petrology. Contrib. Mineral. Petrol, 73, p. 207-220, Paris.

Tatu, M., Săbău, G. (1987) The Albeşti Granite: Petrogenetic considerations. *D. S. Inst. Geol. Geofiz.*, 72, 73, Bucureşti.

Received: August 28, 1996
Accepted: December 20, 1996

Institutul Geologic al României

PETROGENETIC SIGNIFICANCE OF ZIRCON IN RETEZAT GRANITOID PLUTON, SOUTH CARPATHIANS, ROMANIA

Lucia ROBU, Ion Niculae ROBU

Institutul Geologic al României, str. Caransebeş nr. 1, 79678 Bucureşti 32.

Key words: Granitoid. Zircon. Morphology. Petrogenetic Considerations

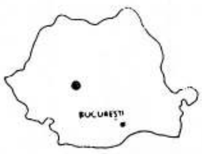

Abstract: The Retezat Massif is intruded in crystalline formations belonging to the Drăgşan Group, from the Danubian Lainici Nappe, a very important Alpine tectonic unit of the South Carpathians. Petrographically, there is a small variability of petrotypes (diorites, tonalites, granodiorites, and granites), showing a specific chemical evolution for silicic rocks, arising from a low differentiated calc-alkaline magma. No major difference exists between the major, minor and REE element concentrations in different zones of the massif. Optical and morphological characteristics of the zircon crystals are very similar for all studied samples. All zircon populations contain different coloured crystals (colourless, light and dark pink or brown), sometimes zoned, opaque or translucent. Two inclusion types are observed in zircon crystals: (1) elongated or ovoid gaseous inclusions and (2) very small zircon crystals. The main morphological types (according to Pupin, 1980) are Q, S, P, L, G, D, presenting an obvious subtype variability, induced by the variation of alkalinity and temperature during zircon growth. Typological Evolutionary Trend (T.E.T.) points to a calc-alkaline tendency and a mixed origin (crust+mantle).

Introduction

The morphology of zircon crystals in the granitoid rocks was a constant preoccupation of many researchers for establishing its petrogenetic segnificance. However, Poldervaart (1950) and, more recently, Pupin (Pupin, Turco, 1972; Pupin 1980) have established connections between the zircon morphology and the chemical charactertistics of the granitic magmas.

In the present paper, zircon populations have been studied by morphological and optical criteria, trying to determine the evolution trend of the magma from the Retezat granitoid massif.

Geological setting

Retezat granitoid massif is intruded in the crystalline formations belonging to Drăgşan Group, from the Danubian Nappe, a lower Alpine tectonic unit of the South Carpathians (Berza et al., 1988) (Fig. 1).

The Drăgşan Group contains garnet amphibolites, associated to augen gneisses, biotite ± garnet gneisses, biotite+muscovite±kyanite±sillimanite±garnet gneisses, actinolitic schists and serpentinites.

All the metamorphic rocks are affected by the retrograde processes (low degree metamorphism), which determined the appearance of the chlorites, epidote and fine-grained white micas.

In whole exposed area of the granitoid massif, but especially at its borders, mylonitic foliations, determined by Alpine or pre-Alpine tectonics, are obvious.

The northern and southern parts of the granitoid body are covered by the sedimentary formations (Lower, Middle and Upper Jurassic, and Lower-Middle Cretaceous).

Techniques of study

The optical and morphological data have been obtained using the following methods:

- twenty-three samples, each of them weighting about 5 kg, which have been crushed under 1 mm;
- the heavy minerals have been separated with Frantz isodynamic magnetic separator and then with dense liquids (bromoform);
- crystal faces have been indexed using Caruba's method (Caruba, Turco, 1971);

Institutul Geologic al României

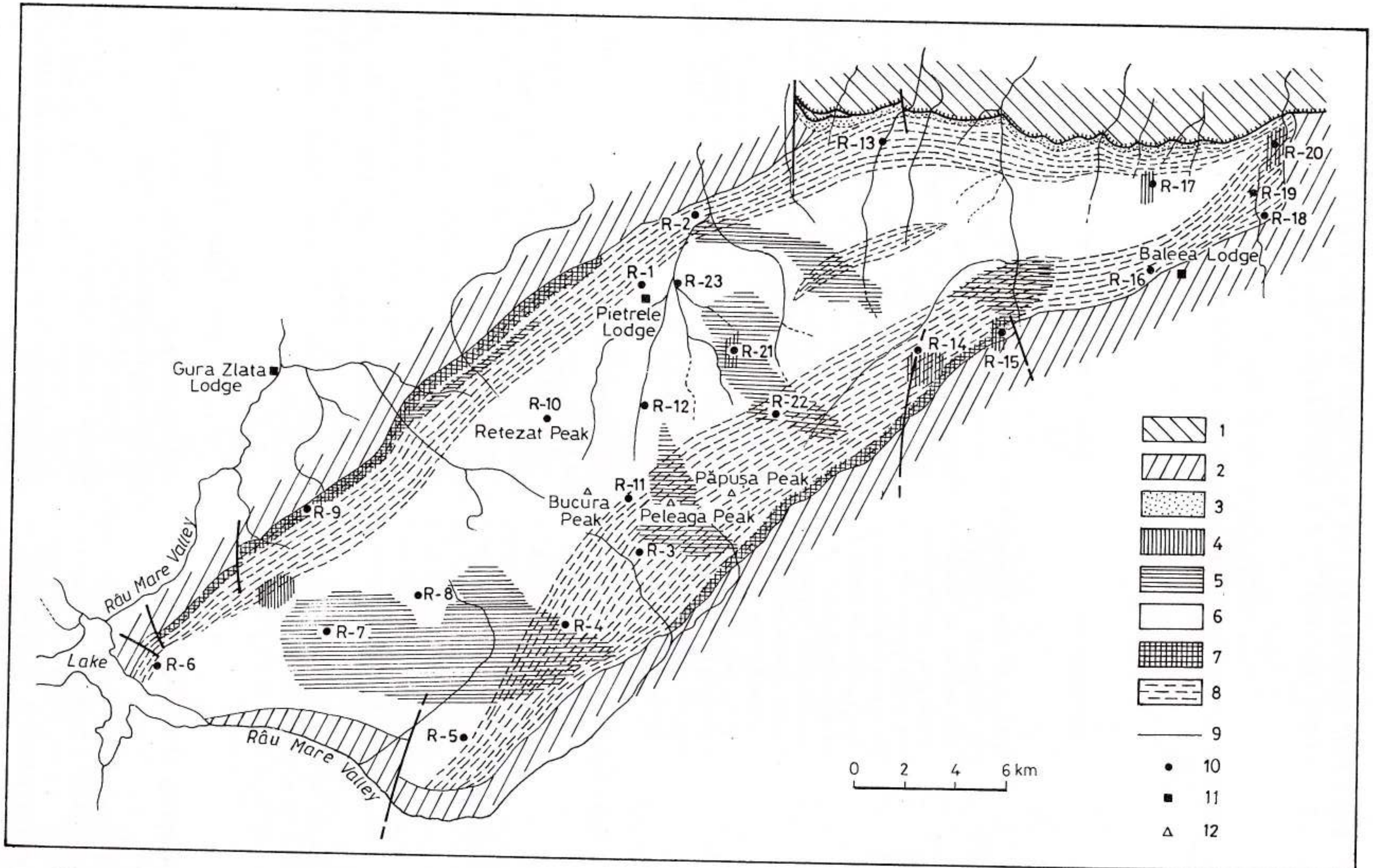

Fig. 1 – Geological sketch of the Retezat massif (according to Berza et al., 1989) and sample location of the Danubian Realm: Upper Danubian Napes: 1, Urdele Nappe mylonites; Lainici Nappe; Lower Danubian Nape; 2, Drăgşan amphibolites; Sedimentary Formations: 3, Jurassic -Cretaceous Deposits;

Retezat massif: 4, biotite-muscovite-epidote granites; 5, biotite-muscovite-epidote tonalites; 6, biotite-muscovite-epidote granodiorites; 7, biotite±hornblende diorites; 8, shear zones; 9, general geological limit; 10, fault; 11, sample.

Institutul Geologic al României

- optical characteristics were established using the Jenapol microscope and the stereo-microscope;
- morphological features have been considered according to Pupin's tyopological method (Pupin, Turco, 1972).

Petrographical and mineralogical characteristics of the Retezat massif

The previous authors (Pavelescu, 1953; Macaleţ, 1983, 1991; Berza et al., 1988) separated some petrotypes, having a pronounced leucocrate character, as follows:

- *biotite-muscovite-epidote granites* include: K-feldspars, plagioclase feldspar (albite), biotite, muscovite and epidote, as magmatic minerals and albite, clay minerals, carbonates, as secondary minerals;
- *biotite-muscovite-epidote tonalites and biotite-muscovite-epidote granodiorites* composed of the same magmatic minerals, but in different proportions: plagioclase feldspar (oligoclase), K-feldspar, muscovite, biotite, epidote and quartz; all primary minerals are affected by post-magmatic phenomena, determining the appearance of chlorites, secondary albite, clay minerals, carbonates;
- *biotite ± hornblende diorites* observed in the north-western and south-eastern parts of the massif, as very narrow strips, are composed of plagioclase feldspar (andesine), biotite, quartz, all minerals being totally or partially substituted by secondary minerals (epidote, chlorites, albite) formed during the post-magmatic stages.

The presence of magmatic epidote is the main characteristic of these rocks. All petrotypes of the Retezat massif are crossed by aplitic and pegmatitic dykes, representing a later acid phase of the magmatic activity.

The considered samples were selected from various petrotypes and zones of the massif, so that they are representative for it (Table 1).

Chemical composition of the rocks

Chemical variations from basic to acid ends (according to Berza et al., 1993), reflected by mineralogical and petrographical characteristics, are as follows: SiO_2 and K_2O increasing, CaO, MgO, FeO, Fe_2O_3, TiO_2 decreasing and small Al_2O_3 and Na_2O variations.

The correlation between $SiO_2/CaO+MgO/Al_2O_3+Fe_2O_3$ points out a characteristic tendency of high-silica rocks, evolving from diorites to granites. The increasing of the alkali contents and a decreasing of Fe and Mg amounts point out a short magmatic differentiation of the calc-alkaline type (Berza et al., 1993).

The Zr content of the samples is variable: tonalites (92 ppm), diorites (160 ppm), grandiorites (92-190 ppm) and granites (57-225 ppm). No correlation exists between Zr content variation and petrotype (Table 2).

Morphological and optical features of zircon crystals

No evident difference exists between the morphological and optical properties of the studied zircon populations from granites, grandiorites, diorites and tonalites; they are presented in table 3 and illustrated in Figure 2.

Similar morphological characteristics for the zircon crystals were remarked: the good-development of the (110) and (100) prismatic faces together with bad-development or absence of one of the pyramidal faces (211) or (101).

The terminations of the crystals are simple (one of the (211) or (101) pyramidal faces) (Fig. 2) or complicated (both (211) and (101) pyramidal faces) (Fig. 2), according to the chemical changes of the crystallization medium.

The crystal faces are smooth and glossy, without corrosion or etching traces.

Morphological variations of the zircon crystals were used for a study of the typological frequency distribution of the zircon populations from each rock sample. In the typological diagrams (Fig. 3), the studied zircons plot in two distinct fields: (1) hyperaluminous and hypoalkaline field and (2) hypoaluminous and hyperalkaline one, but calculated mean points and Typological Evolutionary Trend (T.E.T) evidence a calc-alkaline tendency (Fig. 3). Their morphology is specific to a diorite-tonalite-granodiorite-monzogranite-monzonite suite of granitoid rocks (Fig. 4) and a hybrid origin (crust+mantle) (Fig. 5).

The optical features (colour, transparency, zoning, core and inclusions) are not specific to a certain petrotype. We remarked a large variability of colour (colourless, light and dark pink or brown), a predominance of the translucent crystals, the sporadic appearance of zoned and overgrown crystals and a predominance of the primary gaseous inclusions (Pl., Table 3); and sporadical appearance of globular opaque inclusions and smaller included zircon crystals.

Petrogenetic implications

All data obtained, according to the study of zircon populations, permit some suppositions regarding the magma evolution in the Retezat massif. It is to note the following aspects: 1, similar physico-chemical

Institutul Geologic al României

Table 1
Number, petrotype and location of samples

Sample	Petrotype	Location of sample
R-4	T	Slăvei Crest
R-9	LD	Piciorul Radeșului Crest
R-1	Gd	Pietrele Lodge
R-12	Gd	Pietrele Lake
R-23	Gd	Pietrele Valley
R-10	Gd	Retezat Summit
R-7	Gd	Zlata Summit
R-8	Gd	Zănoaga Lake
R-5	mGd	Slăvei Crest
R-6	mGd	Lăpușnic Crest
R-2	LGd	Câlnic Summit
R-13	LGd	Paroș Valley
R-16	LGd	Baleea Lodge
R-22	LGd	Galeșu Lake
R-11	LGd	Bucura Saddle
R-3	LGd	Bucura Lake
R-17	G	Serel Crest
R-21	G	Galeșu Valley
R-14	gG	Lancițiu Saddle
R-15	gG	Lancițiu Top
R-19	gG	Bărbat Valley
R-20	LG	Bărbat Valley
R-18	LG	Bărbat Valley

T = tonalite; LD = mylonitic diorite; Gd = granodiorite; mGd = microgranodiorite; LGd = mylonitic granodiorite; G = granite; gG = foliated granite; LG = mylonitic granite

Table 2
Zr content (ppm) of the granitoid rocks*

Sample	R-4	R-9	R-1	R-12	R-23	R-10	R-7	R-8	R-5	R-6	R-2	R-13
Zr	92	100	145	140	85	100	135	190	92	100	100	140
Petrotype	T	LD	Gd	Gd	Gd	Gd	Gd	Gd	mGd	mGd	LGd	LGd

Sample	R-16	R-22	R-11	R-3	R-17	R-21	R-14	R-15	R-19	R-20	R-18
Zr	120	150	150	110	110	60	57	225	160	150	160
Petrotype	LGd	LGd	LGd	LGd	G	G	gG	gG	gG	LG	LG

The same legend as in table 1; *(The samples have been analysed in the IGR laboratory, using spectrographic method).

Institutul Geologic al României

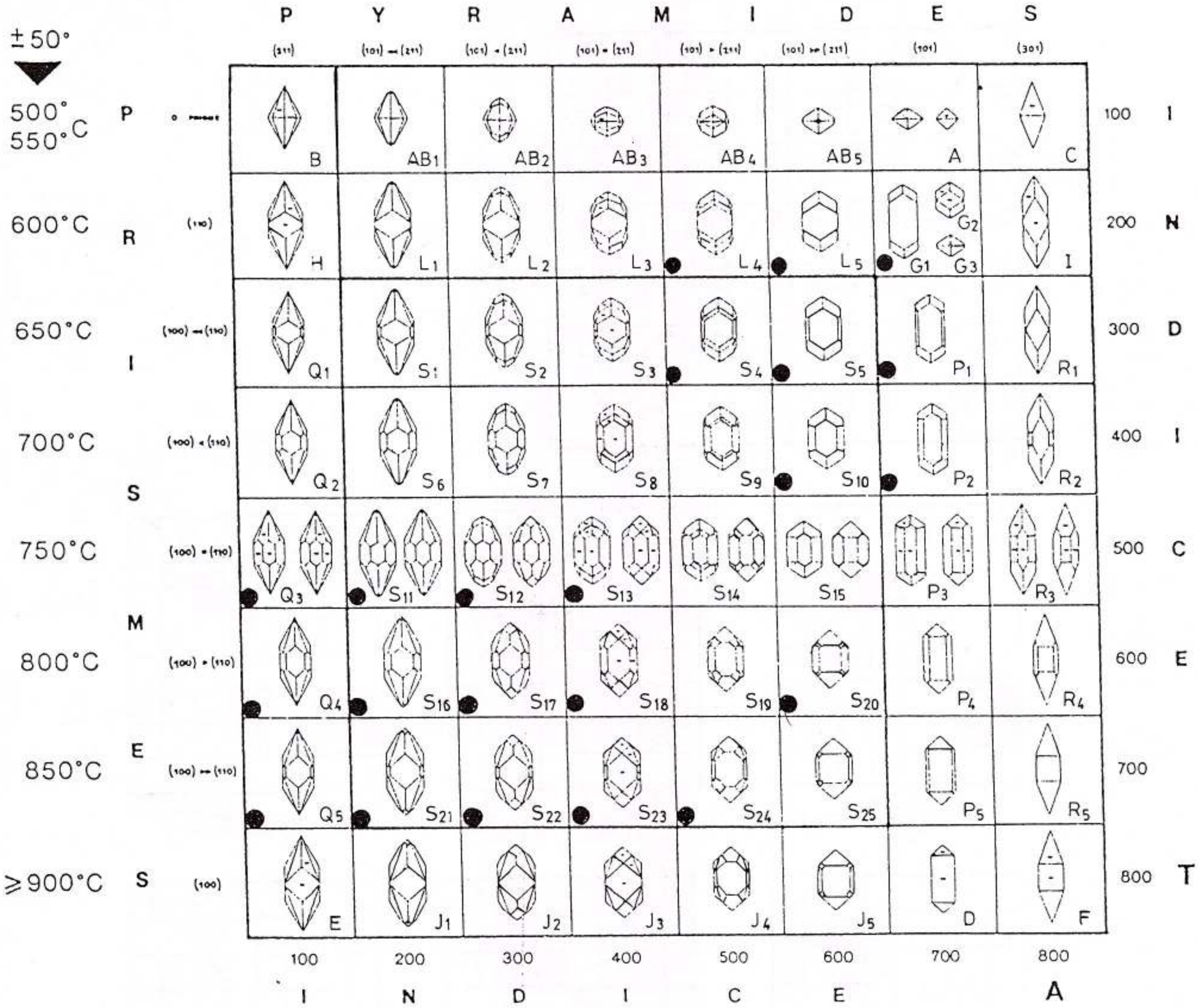

Fig. 2 – Main zircon morphological types and subtypes. (according to Pupin, Turco, 1972)
● = zircon crystals from Retezat massif.

conditions for all differentiated rock types, because all studied populations of zircon crystals contain crystals with similar morphology (the same Pupin's types), differentiated one from another by their subtypes and frequency (Figs. 2, 3); 2, a calc-alkaline tendency of magma evolution in the whole area of the Retezat massif; 3, a magmatic source including two components: (a) a hyperaluminous and hypoalkaline component, and (b) hyperalkaline and hypoaluminous one; 4, a high content of the volatile elements, which determined the formation of the gaseous inclusions in the majority of the crystals, from all studied samples, but most frequently met in zircon crystals from granites; 5, a dry magma character, indicated by the lack of well-developed pyramidal faces and the good development of the prismatic ones (according to experimental studies Caruba, 1975; Duchesne et al., 1984); 6, a high content of the radio-active elements, which determined, in time, metamictic phenomena in the majority of the zircon crystals; 7, few contaminations, assimilation phenomena or magmatic corosions, determining a small overgrowth of the zircon crystals (Plate); 8, mixing of two magma types or magmatic segregations, determining the appearance of two different zircon type generations that include one another (S_4 crystal type included in the S_{17} one) (Plate).

Hypotheses of the magma evolution

Three possible hypotheses of the magma generation arise, according to the morphological and optical data of the zircon populations:

Institutul Geologic al României

B	AB_1	AB_2	AB_3	AB_4	AB_5	A	C
H	L_1	L_3	L_3	L_4	L_5	G1	I
Q_1	S_1	S_2	S_3	S_4	S_5	P_1	R_1
Q_2	S_6	S_7	S_8	S_9	S_{10}	P_2	R_2
Q_3	S_{11}	S_{12}	S_{13}	S_{14}	S_{15}	P_3	R_3
Q_4	S_{16}	S_{17}	S_{18}	S_{19}	S_{20}	P_4	R_4
Q_5	S_{21}	S_{22}	S_{23}	S_{24}	S_{25}	P_5	R_5
E	J_1	J_2	J_3	J_4	J_5	D	F

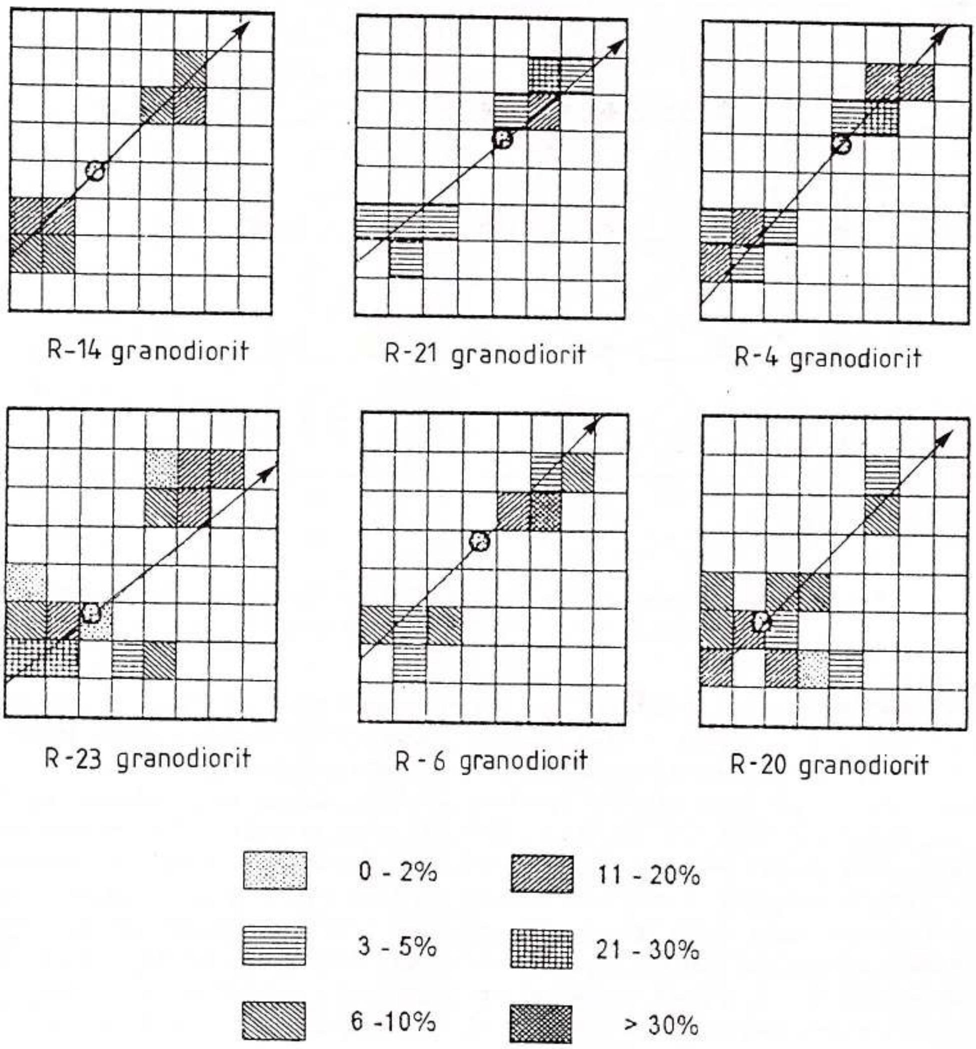

Fig. 3 a – Typological frequency distribution of zircon crystals.

Institutul Geologic al României

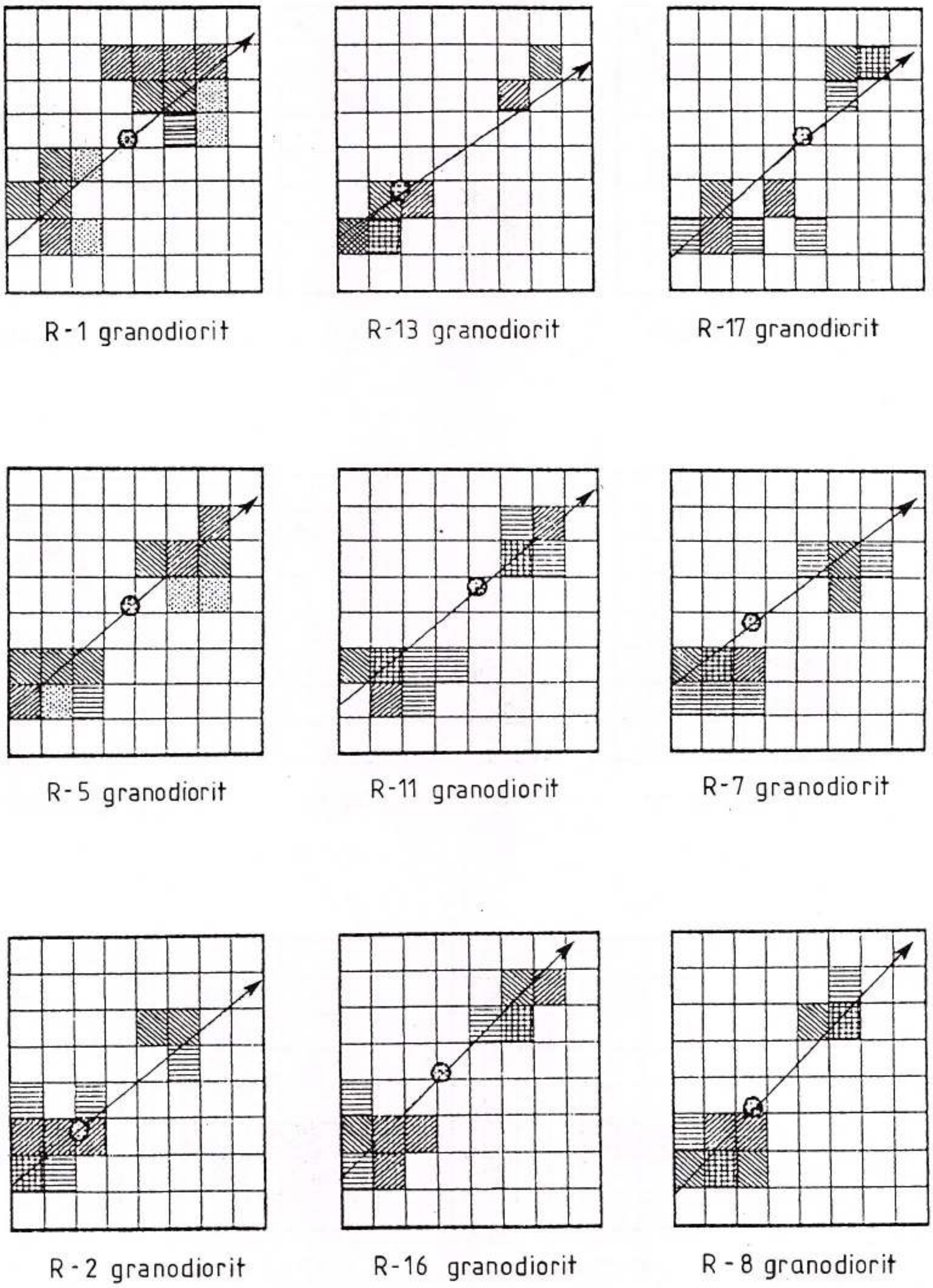

Fig. 3 b – Typological frequency distribution of zircon crystals.

Institutul Geologic al României

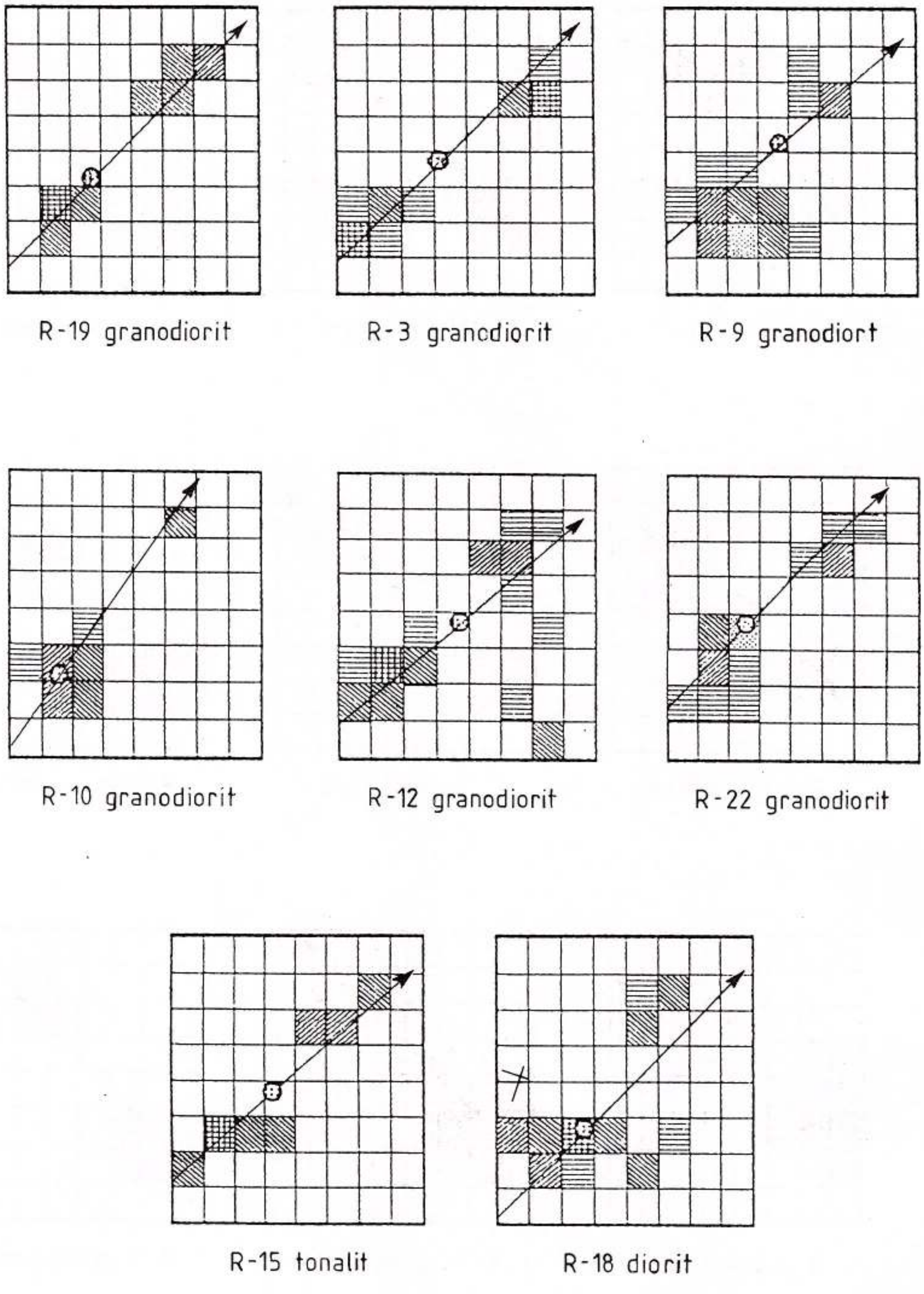

Fig. 3 c – Typological frequency distribution of zircon crystals.

Institutul Geologic al României

Table 3
Morphological and optical features of zircons

Sample	Colour*	Inclusions**	Zoning	Core	Transparence***	Morphology
R-4	Cl, LP, LB	-	+	-	T, Td	Q, S, L, G_1
R-9	LP, DP, LB	-	-	+	T, Td	S, L, G_1
R-1	Cl, LB	G	+	+	T, Td	Q, S, L, G_1, P
R-12	Cl, LP, LB, DB	-	-	-	T, Td	Q, S, L, G_1, D
R-23	Cl, LP, LB, DB	-	-	-	T, Td	Q, S, L, G_1
R-10	Cl, LP, LB	G	-	-	T, Td	Q, S, L
R-7	Cl, DP, LB	G	-	-	T, Td	Q, S, L, G_1
R-8	LP, DP, LB, DB	G, Zr	-	+	T	Q, S
R-5	Cl, LP, LB	G	-	-	T, Td	Q, S, L, G_1, P
R-6	Cl, LB, DB	-	+	-	T, Td	Q, S, L, G_1, P
R-2	Cl, LP, DB	G	-	+	T, Td	Q, S
R 13	Cl, LP, DB	G	-	+	T, Td	Q, S, G_1
R-16	Cl, LP, DP, LB	G	+	-	T, Td	Q, S, L, G_1
R-22	Cl, LP, LB	-	-	-	T, Td	Q, S, L, G_1
R-11	LP, DP	G, O	-	-	T, Td	O, S, L, G_1
R-3	Cl, LP, LB	-	-	-	T, Td	Q, L
R-17	Cl, LB, LB, DB	-	-	-	T, Td	Q, S, L, G_1
R-21	LP, LB, DB	G	-	-	T, Td	Q, S, L, G_1
R-14	LP, LB	G	-	-	T, Td	Q, S, L
R-15	Cl, LP, DP	-	-	-	T	Q, S, G_1
R-19	LP, DP, LB	G	-	-	T, Td	Q, S, L
R-20	Cl, LP	-	-	-	T	Q, S, L
R-18	Cl, LP	G	-	-	T, Td	Q, S, L, G_1

* = Colour: Cl = colourles; LP = light pink; DP = dark pink; LB = light brown; DB = dark brown.
** = Inclusions: G = gaseous; O = opaque; Zr = zircon.
*** = Transparence: T = transparence; Td = translucent. Core and Zoning: - = no; + = yes

1 – *the anatectic processes*, developed at the deep crust level, involving melting of some peraluminous and hyperalkaline rocks, without reaching zircon melting temperature. This is revealed by (1) these two distinct zircon groups, which have been observed in each population of each studied sample, and (2) the sporadic overgrowth of crystals;

2 – *the mixing of two magma types* (hyperaluminous and peralkaline types), supported by the morphological features of the zircon crystals (Q and L, G, P, D types and the presence of the S_4 type included in the S_{17} one);

3 – *a two stage magma evolution* at different levels of the crust: (i) first, a deep one, at the lower crust level and (ii) the second one, much upper in the crust.

Conclusions

The study of zircon crystals from the Retezat granitoid massif emphasized some characteristic features of the investigated zircon crystals, proper for this massif, which pointed out some petrogenetic significances, generally in agreement with chemical, mineralogical and petrographical aspects.

The prismatic habit, determined by the well-developed prismatic faces, suggests a dry environment of the zircon crystallization; no corrosion and etching processes affected the faces.

The intensity of the colour and the variable degree of metamictic processes point out the presence of considerable radio-active element contents.

The gaseous (majority) and opaque (few) inclusions reveal the high amount of volatile in the magma, during zircon growth.

The morphological characteristics of the crystals reveal three possible processes of magma evolution: (1) crustal anatexy, (2) a mixing of two different magma types, or (3) in two stages , at the different levels in the crust.

Institutul Geologic al României

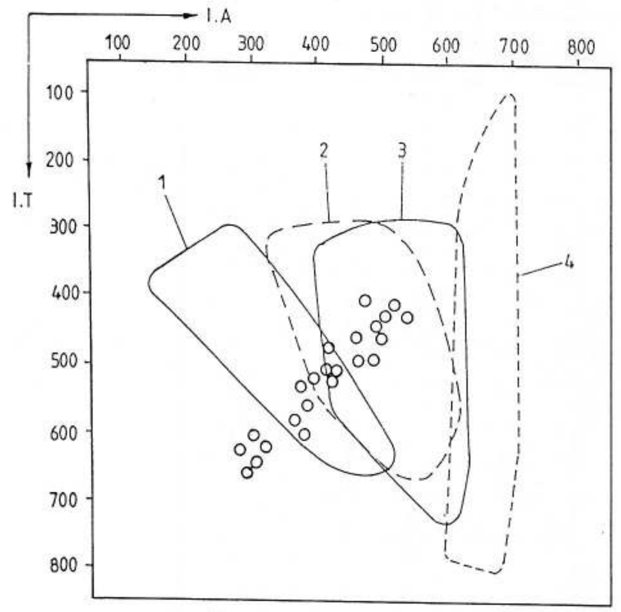

Fig. 4 – Distribution of plutonic rocks in the typological diagram (Pupin, 1980): 1, diorites, quartz gabbros and diorites, tonalites; 2, granodiorites; 3, monzogranites and monzonites; 4, alkaline and hyperalkaline syenites and granites.

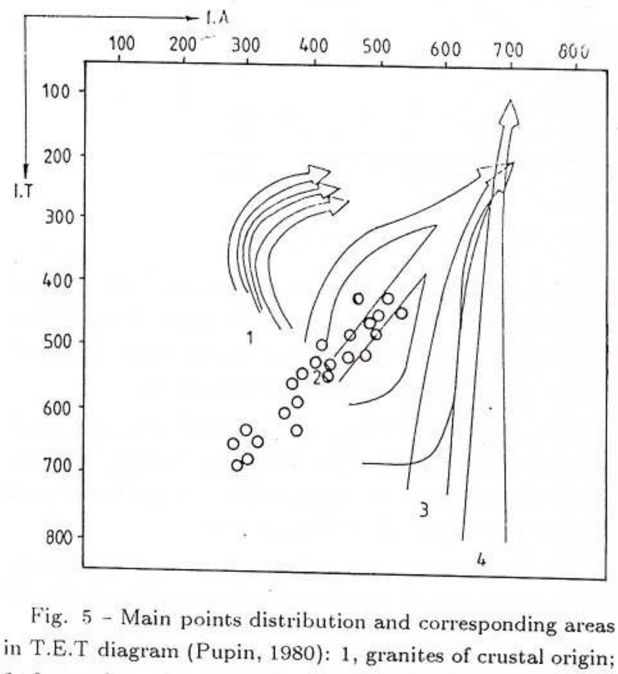

Fig. 5 – Main points distribution and corresponding areas in T.E.T diagram (Pupin, 1980): 1, granites of crustal origin; 2+3, granites of crustal+mantle origin (hybrid granites); 4, granites of mantle origin.

References

Berza, T., Seghedi, A., Stănoiu, I. (1988) Unităţile danubiene din partea estică a munţilor Retezat (Carpaţii Meridionali) *D.S. Tectonică-Geologie Regională* (5), vol. 72-73), p. 5-20, Bucureşti.

— , **Dimitrescu, R., Dimitrescu, M., Tatu, M., Strusievicz, O. R., Pop, G., Popescu, G., Bandrabur, T. (1989)** *Harta geologică a Romaniei*, sc. 1.50 000, Foaia Retezat, I.G.R., Bucureşti.

— , **Macaleţ, V., Andăr, P., Udrescu, C. (1992)** Retezat granitoid pluton (South Carpathians) a geological approach. *Rom. J. Petrology*, 76/2, p. 1-18, Bucureşti.

Caruba, G. C. (1975) Étude experimentale de la cristallographie, de la morphologie, de la stabilité et de la genèse du zircon et des zircon silicates en vue d'applications petrogénetiques. *Thesis University of Nice*, 324 p., Nice.

Duschesne, J. C., Caruba, R., Iacconi, I. (1984) Zircon in charnockitic rocks from Rogaland (Southwest Norway); petrogenetic implications. *Lithos* 20. p. 357-368.

Macaleţ, V. (1983) Considerations regarding the geological structure of the northern part of the Retezat Mountains (South Carpathians) *An. Inst. Geol. Geofiz.*. LXI, p. 35-102, Bucureşti.

— **(1991)** Geological and petrographical study of North Retezat Mountains *An. Inst. Geol. Geofiz.*, 68, p. 115, Bucureşti.

Pavelescu, L. (1953) Studiul geologic şi petrografic al regiunii centrale şi de Sud-Est a Munţilor Retezatului. *An. Com. Geol.*. XXV, 119 p, Bucureşti.

Poldervaart, A. (1950) Statistical studies of zircon as a criterion in granitization. *Nature G.B.* 165, p. 574-584.

Pupin, J. P., Turco, G. (1972) Une typologie originale du zircon accesoire. *Bull. Soc. Cr. Mineral. Cristallogr.*, 95, p. 348-359.

— **(1980)** Zircon and granite petrology. *Contrib. Mineral. Petrol.*, 73, p. 207-220.

Received: August 6, 1997
Accepted: February 9, 1998

Institutul Geologic al României

Plate - Optical and morphological characteristics of zircon crystals

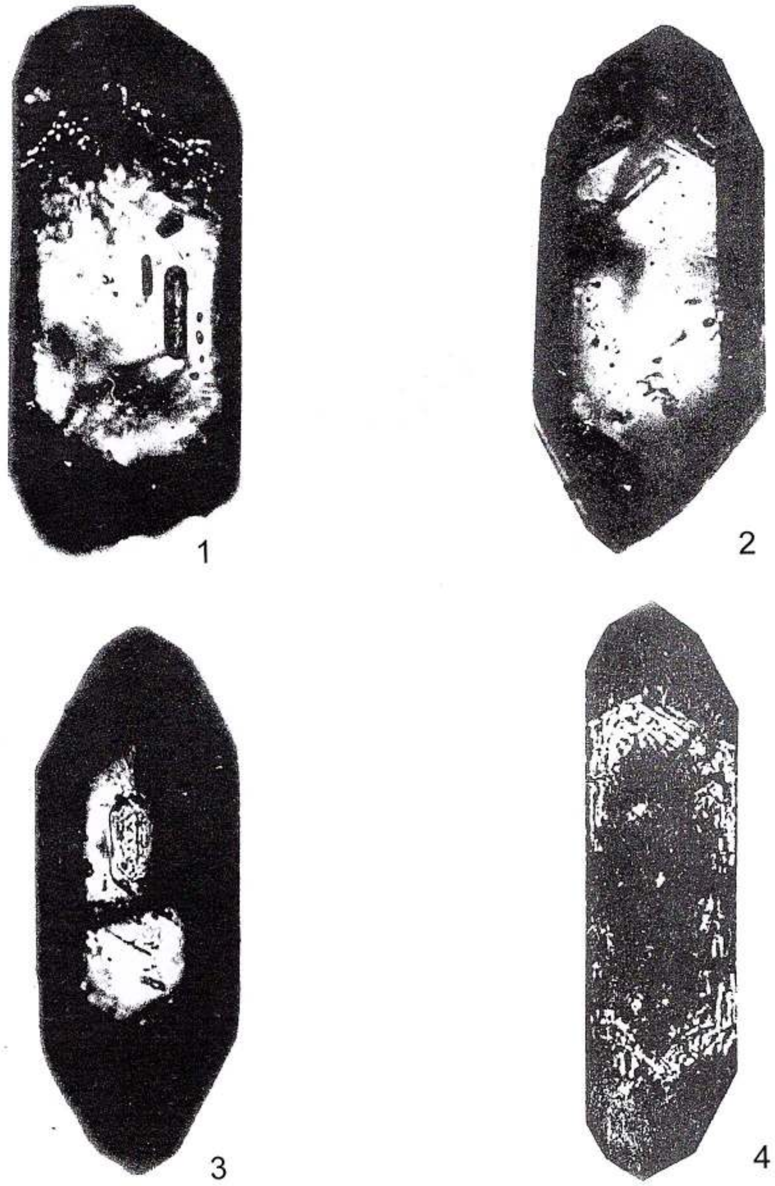

1. Metamictized S5 zircon crystal, enclosing gaseous inclusions disposed parallelling prismatic faces;
2. Metamictized S22 zircon crystal type, characterized by gaseous inclusions orientated parallel with pyramidal faces;
3. S4 zoned crystal, included in an S17 one;
4. Overgrown finely zoned crystal

Institutul Geologic al României

CORRELATIONS BETWEEN ZIRCON MORPHOLOGY AND CHEMICAL CHARACTERISTICS OF ALKALINE MAGMATITES (GRANITES, RHYOLITES, SYENITES) FROM TURCOAIA-PIATRA ROŞIE ZONE, NORTH DOBROGEA

Ion Niculae ROBU, Lucia ROBU

Institutul Geologic al României, str.Caransebeş nr. 1, 79678 Bucureşti 32.

Key words: Zircon. Morphology. Typology. Frequency. Prism. Pyramid. Elongation. Alkaline magmatites.

Abstract: Morphological variations of zircons from alkaline magmatites, Turcoaia-Piatra Roşie zone, North Dobrogea, emphasized some aspects specific to the identified petrotypes: riebeckite-aegirine granites, riebeckite granites, alkali granites and alkali rhyolites, quartz syenites and syenites. All investigated rocks have similar zircon morphological types (D, P_5 K_1, S_5); the differences, when they exist, are determined by (1) different degree of prism or pyramid face development, or (2) different frequency of these types in each studied petrotype. A large variability of the crystal elongation has been observed. The elongation is differentiated in studied petrotypes, varying as follows: (1) very elongated crystals (long prismatic habit) in alkali granites; (2) long, medium and short in riebeckite-aegirine granites and rhyolites; (3) medium in alkaline rhyolites; (4) medium and short in syenitic rocks. No significant differences exist between the physical properties of the zircon crystals from different rocks: generally dark or brown colour, no zoning, no cores, frequently translucent or opaque, including mafic or opaque minerals. Morphological and physical properties of zircons point to a common source of the studied alkaline magmatites, with a deep origin (upper mantle-lower crust), including high alkali content, a variable water content, small U, Th, Y, and REE amount, enough Zr to be fixed as zircon crystals characterized by well-developed (100) prism and (101) pyramidal faces.

Introduction

The influence of the crystallization environment on the growth of crystals is well known. This has been proved by many researchers (Poldervaart, 1950; Pupin,Turco, 1972; Pupin, 1980), who studied the morphology of the zircon crystals and their probable physical and chemical conditions of crystallization, according to chemical features of the parental magma.

This paper tries to establish (1) the connections between the morphology of zircon crystals and chemical composition of the rocks including them and (2) the relations between morphology of zircons, chemical features of the rocks and the magmatic processes which generated, in given time and space, identified petrotypes from an initial magma.

Geological Setting

The studied alkaline magmatites belong to the Măcin Unit of the North Dobrogea, cropping out in the Turcoaia-Piatra Roşie zone.

They intruded and determinated the thermic metamorphism of the Paleozoic formations and are covered by Cretaceous and Quaternary sedimentary formations.

The alkaline magmatites form irregular bodies, composed of granites and alkaline granites, in the central part, but rhyolites exist in the marginal zones of granitoid bodies.

The Paleozoic formations are represented by the Carapelit (coarse- to fine-grained sandstones, conglomerates, pelites) and Cerna (pelites, micasandstones, lime-sandstones) formations.

All observed petrotypes are characterized by high alkalinity, being recognized: quartz syenites, riebeckite-aegirine granites, granophyric alkali granites, alkali rhyolites, riebeckite - aegirine - alkali hornblende rhyolites (Table 1).

All previous petrographical and mineralogical studies (Cantuniari, 1912; Stefan, in Seghedi, 1990)

Institutul Geologic al României

Table 1
Petrotypes and sample location

No.	Sample	Petrotipe	Location
1	3335	riebeckite-aegirine granite	Turcoaia
2	3332	riebeckite granite	Turcoaia
3	3331	alkali granite	Turcoaia
4	3329	riebeckite - aegirine granite	Iacobdeal
5	3327	riebeckite granite	Piatra Roșie
6	3326	alkali granite	Piatra Roșie
7	3324	alkali granite	Turcoaia
8	3325	alkali rhyolite	Turcoaia
9	3322	alkali rhyolite	Iglicioara
10	3333	quartz syenite	Turcoaia
11	3330	syenite	Iacobdeal

Table 2
The optic and physical properties of zircon crystals

No.	Sample	Colour	Zone	Core	Inclusions	Transparence
1	3335	DB	no	no	O, M	t, o
2	3332	LB, DB	no	no	mgt	t, o
3	3331	LB, DB	no	no	O, M	t, o
4	3329	LB, DB	no	no	O, M	t, o
5	3327	DB	no	no	O, M	t, o
6	3326	DB	no	no	O, M	t
7	3324	LB, DB	no	no	O, M	t, o
8	3325	CS	no	no	O, M	t
9	3322	LB, DB	no	no	O, M	t, o
10	3333	DB	no	no	O, M	o
11	3330	DB	no	no	O, M	t, o

LB = light brown; DB = dark brown; CS = colourless; O = opaque inclusions; M = undetermined mafic inclusions; T = transparent; t = translucent; o = opaque; mgt = magnetite

point out a genetical connection between granites, syenites and rhyolites.

Chemical features of the rocks

Alkaline magmatites of the Turcoaia - Piatra Roşie zone present the following chemical characteristics (Stefan, in Seghedi, 1990): • high SiO_2 and alkali sum, up to 8 %; • a small CaO content (under 1%), excepting quartz syenites; • high Zr-Nb-Y contents and small Sr-Ba ones; • REE amounts point out a partial melting process followed by the small differentiated magmatic phenomena.

Sample preparation and methods of study

The sample rocks were crushed under 1 mm and zircons were obtained using vibration table, Frantz isodynamic magnetic separator and dense liquids.

Crystal faces were indexed according to Caruba's abaque method (Caruba, Turco, 1971) and their morphological features were established in concordance

Institutul Geologic al României

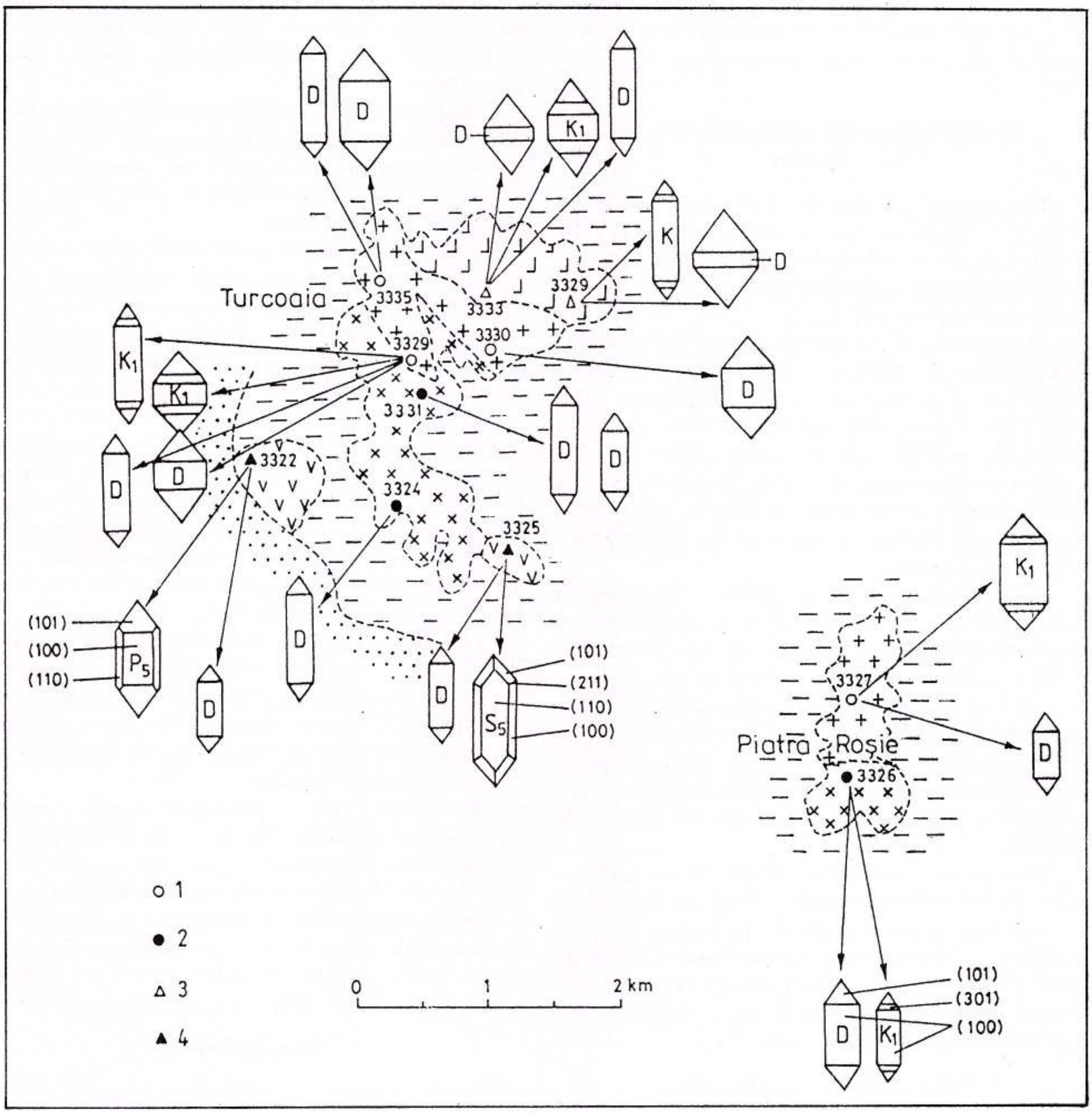

Fig. – Geological sketch of Turcoaia-Piatra Roşie Zone (according to Geological Map of Romania, 1:50000, Peceneaga) and zircon typology (zircon morphology according to Pupin, Turco, 1972): 1, riebeckite-aegirine granites; 2, alkali granites; 3, syenites; 4, rhyolites.

Institutul Geologic al României

with Pupin's typological method (Pupin, Turco, 1972).

The optical and morphological properties of zircon crystals were observed at the stereo-microscope (x oc. 12.5; x ob. 7) and Jenapol microscope (x oc.10; x ob. 20).

Morphological and optical properties of zircons

The morphological study of zircons (according to Pupin, 1980) from alkaline rocks of the North Dobrogea region included zircons from alkali granites, riebeckite-aegirine granites, quartz syenites, syenites and alkali rhyolites (Table 1).

The typological analyses point out the same morphological types for each petrotype (Fig.).

So, the main type is D, which represents about 100% for granitic rocks and 98% for the alkali rhyolites; P_5 and S_4 types were met only in the alkali rhyolites. Sometimes the (301) pyramidal face has been observed which points to (Pupin, Turco, 1972) a very high alkaline environment for the growth of the zircon crystals.

There are some obvious differences regarding the elongation of the zircon crystals composing zircon populations from different petrographical types (Fig.), as follows: • alkali granites contain very elongated zircon crystals; • riebeckite-aegirine granites and syenites have all types of the elongation (long, medium and short zircon crystals); • alkali rhyolites are characterized by the medium elongated zircon crystals; • syenites contain medium and short zircon crystals.

Some physical properties (Table 2) are very similar for all studied samples: dark or light brown colour (sometimes colourless), no zoning, no cores, frequently translucent or opaque (sometimes transparent) inclusions of mafic or opaque mineral, no obvious dimension variations (between 0.15/0.10/0.10 and 0.0155/0.0125/0.0125 mm).

Petrogenetic implications

It is well known now that the variations of some physico-chemical parameters of the crystallization environment determine exchanges of zircon morphology. So, it could be mentioned, as follows:

1. Aluminium and alkali content variations in concordance with temperature changes determine (according to Pupin, 1980) a large variability of zircon morphology, as (1) the well-developed (100) prism face and (101) pyramidal one, crystallize in high alkaline medium and high temperature (up to 800^0C), reached at a deep level, probably at the upper mantle and lower crust, and (2) the appearance and development of the (110) prism face and (211) pyramidal ones in a -Al-rich crystallization environment and at low temperature (up to 500^0 C);

2. Low Zr, Hf contents and small U, Y, Th and REE amounts (Benisek and Finger, 1993; Vavra, 1990) point to favourable conditions for the (100) prism faces;

3. H_2O content of crystallization medium (Caruba, 1975; Caruba et al., 1971, fide Duchesne, 1984) determines size variations of crystal faces, namely a dry environment favors the growth of zircons without well-developed pyramidal faces.

For the zircon studied populations, their morphological characteristics emphasize some specific features of the crystallization environment, that will be mentioned bellow. Crystallization of zircons especially with well-developed (100) prism faces and (101) pyramidal one points to: • Al and high alkali contents; • Al and alkali variations in concordance with the temperature changes; • a deep source for the initial material, probably upper mantle-lower crust; • low Zr, Hf, small U, Th, contents; • high water content variation, responsible for the high variation of the face growth process, determining especially the well-development of the prism faces, when the crystallization environment was a dry one; • a high temperature, about 900^0 C, for zircon growth in granites and syenites, the rhyolities including two zircon types, specifically for high (about 900^0 C) and lower (about 650^0 C) temperatures; • the same physico-chemical crystallization conditions for syenites and riebeckite-aegirine granites.

The changes in the morphological aspects of zircon crystals show two important moments of magma evolution: 1. the variation of magma water content during the crystallization of the mentioned petrotypes; 2. obvious temperature decrease during the crystallization of rhyolites, or some low contamination processes, emphasized by the appearance of two zircon types, characteristic of low and high temperatures.

Conclusions

The study of zircon morphology points to genetical connections between all alkali magmatites from Turcoaia-Piatra Roşie Zone. They could form from the same deep material (upper mantle-lower crust), which in the beginning (about 900^0C) have been (1) high alkaline, (2) sufficient Zr supersaturated for the crystals with well-developed (100) prism faces, (3) with a variable water content, and (4) small U, Y, Th and REE amounts during zircon growth, but higher in the final magmatic stage evolution.

References

Benisek, A., Finger, F. (1993) Factors controlling the development of prism faces in granite zircons: a microprobe study. *Contr. Mineral. Petrol.*, 114, p. 441-451.

Institutul Geologic al României

Cantuniari, St. N. (1912) Masivul eruptiv Muntele Carol-Piatra Roşie. *An. VI*, p. 1-160.

Caruba, G. C., Turco, G. (1971) Mise au point la notation des faces du zircon. Elaboration d'une méthode d'identification rapide des faces des zircons accessoires des roches par utillization d'abaque. *Bul. Soc. Fr. Mineral Cristallogr.*, 64 (4), p. 427-436

— **(1975)** Étude experimentale de la crystallographie de la morphologie, de la stabilité et de la génèse du zircon et des zircon silicates en vue d'applications pétrógenétiques. *Thesis University of Nice*, 324 p, Nice.

Duschesne, J. C., Caruba, R., Iacconi, I. (1984) Zircon in charnockitic rocks from Rogaland (Southwest Norway); petrogenetic implications. *Lithos 20*, p. 357-368.

Poldervaart, A. (1950) Statistical studies of zircon as a criterion in granitization Nature, G, B, 165, p. 574-585.

Pupin, J. P., Turco, G. (1972) Une typologie originale du zircon accessoire. *Bull. Soc. Cr. Mineral. Cristallogr.*, 95, p. 348-359.

— **(1980)** Zircon and granite petrology. *Contrib. Mineral. Petrol.*, 73, p. 207-220.

Seghedi, A., Baltreş, A., Nedelcu, L., Szasz, L., Seghedi, I., Ştefan, A., Ion, J., Rădan, S. (1990) *Rap.. Arch. IGR.*, Bucureşti.

Vavra, G. (1990) On the kinematics of zircon growth and its petrogenetic significance: a cathodoluminiscence study. *Contrib. Mineral. Petrol.*, 106, p. 90-99.

Received: August 6, 1997
Accepted: January 27, 1998

Institutul Geologic al României

Institutul Geologic al României

METAMORPHIC FORMING AND EVOLUTION CONDITIONS OF THE ECLOGITES IN THE TOPOLOG COMPLEX, FĂGĂRAŞ MOUNTAINS

G. SĂBĂU, E. NEGULESCU

Institutul Geologic al României, str. Caransebeş nr.1, 79678 Bucureşti 32.

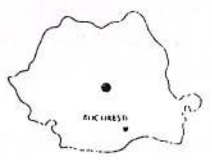

Key words: Făgăraş Mountains. Topolog Complex. Kyanite-bearing eclogites. Garnet zonation. Thermobarometry. Isobaric heating.

Abstract: The median amphibolites belonging to the Topolog "Formation" (Gheuca, 1988) contain scattered eclogite lenses. Besides the eclogitic omphacite-garnet assemblage, other phases like kyanite, zoisite or phengite may be present. Accidentally the silicate phases have a high-Cr content. Chemical zonation of garnet indicates coalescence of crystals during their growth, accomplished over an unusually large temperature interval. Plagioclase inclusions as well as frequent well-developed radial cracks around quartz inclusions prove an episode of considerable heating in the final stages of the eclogitic assemblage formation. Consistent equilibrium reactions could be derived in the CFMAS anhydrous system for the kyanite bearing assemblages, while for zoisite-bearing assemblages equilibria involving dehydration reactions indicate small and increasing water activities as the dehydration proceeds. Calculated equilibrium conditions show different paths for each sample, with peak pressures at 2.1-2.6 GPa. A good fit of estimated temperatures implies an evolution of equilibrium pyroxene from disordered high-jadeite omphacite towards ordered lower-jadeite pyroxene, during a high-pressure near-isobaric heating episode (from ca. 650^0 C to over 750^0 C), in agreement with garnet zonation and radial cracks around quartz inclusions. The pT-paths derived for individual samples show burial along a low thermal gradient, which significantly increases at peak pressures. This array may most probably have been accomplished through decoupling and crustal residence before uplift of portions of the downgoing slab. The presence of highly deformed sialic rocks with contrasting metamorphic grade as against the medium-grade host rocks also supports this model.

Several eclogite lenses, first mentioned by Hann and Gheuca (in Ştefănescu et al., 1982), occur at about the middle part of the Topolog "Formation", consisting mainly of mica gneiss, but including various gneisses and amphibolites in a level named "the median amphibolites" (Gheuca, 1988). The mineralogy and geochemistry of a few eclogite pods located in this level (thought not mentioned as such) have recently been investigated by Costin and Menot *(in press)*, who also derived minimum peak conditions. In order to improve knowledge about the eclogitic assemblage and its forming conditions we sampled four eclogite lenses, as follows: on the Iedu-Podeni road (sample 6554), at about 3 Km N from the Cumpăna chalet to the end of the lake (sample 812), at the Capra-Buda confluence, and on the road from Cernat saddle to Preotesele summit (samples 17432, 17433, 16809). The eclogites are usually associated with gneisses and amphibolites; only near the Capra-Buda confluence ultrabasites also occur.

1. Mineral assemblages

The mineralogical composition of the studied samples consists in a uniform garnet-clinopyroxene-quartz assemblage, more or less overprinted by retrogression. Abundant kyanite is in most instances also present; some samples may contain zoisite or phengite. Minor amphibole, rutile and chromite are quite widespread.

Garnet appears as milimetric optically zoned porphyroblasts. Two domains are easily distinguishable: one containing abundant small quartz and pargasitic or magnesiotaramitic amphibole inclusions, and another clear one, usually free of inclusions, which may, however, enclose larger quartz, pyroxene, sulphides, rutile and even plagioclase. Careful optical inspection suggests that the garnet "porphyroblasts" have

Institutul Geologic al României

a composite structure and result from agglutination of smaller individuals that contain a core blurred with small inclusions and a limpid outer shell (Pl. I, Figs. 1-4). As garnet crystals join during growth, they may enclose voids in the resulting aggregates. These voids are frequently and characteristically bounded by idiomorphic contours of the converging crystals and eventually contain the larger sized inclusions (Pl. I, Figs. 3-4). The external contour of the aggregates often shows concave euhedral portions consistent with this interpretation. Usually the clear shells which extend towards the inner portions of the aggregates are narrower than those which grow towards the margins. Chemical zonation (Pl. II) of the garnet reveales a complicate picture, which is consistent with optical zoning:

- the zone containing abundant small inclusions represents euhedral or equant areas of higher Ca content in which the Mg/Fe ratio radially increases;

- the clear zone mantles these nuclei and evolves to higher Mg/Fe ratios during growth;

- the zonation pattern is at some extent blurred (upper right) or truncated (upper left) by subsequent irregular or concentric Mg increase starting from the margin and propagating inwards, most probably due to prograde diffusion, during which Ca distribution is less affected;

- around pyroxene entrapped in garnet a narrow Fe-richer halo develops, making evidence of retrograde Mg-Fe exchange between the two phases.

The above - mentioned picture as well as the important chemical variation inside the porphyroblast indicate a large duration of garnet growth, which started with rapid growth of several nuclei coeval with early silica-producing eclogitization reactions. At first garnet coexisted with amphibole now found as small inclusions and continued to grow along a prograde path until the income of pyroxene, when the grossular contents as well as the growth rate of garnet significantly decreased. At near-peak conditions garnet continued to grow slowly along with pyroxene and kyanite. The conspicuous diffusion interpreted from the chemical zonation indicates relatively high peak temperatures, while significant increase in pyrope to the margin shows considerable heating in the final stages.

Pyroxene is usually unzoned omphacite; nevertheless omphacites enclosed in garnet have jadeite contents up to 43 %, while matrix omphacite can go down to around 35 %, or even lower in some samples. Coexistence in the same sample of unzoned omphacites with variable jadeite contents could suggest that omphacite crystallised in both ordered and disordered state. An unusual Cr-rich omphacite appears together with Cr-kyanite and chromite in sample 812 (Pl. I, Figs. 5-6). It may form nodules up to 1 cm in the common eclogite matrix. In hand specimen these nodules have a characteristic bright grass-green to apple-green colour, while in thin section Cr-omphacite displays a conspicuous pleochroism in yellow-bright green hues. Symplectites around Cr-omphacite are narrower than those around the normal omphacites.

Kyanite is usually abundant, even making up monomineralic layers. Quite seldom, but at several locations, an unusual Cr-kyanite appears (e.g. points 812, 17433), which may associate with Cr-bearing omphacite (Negulescu & Săbău, *in preparation*). It has a strong (bluish) emerald-green pleochroism with a patchy character and encloses or abuts on chromite grains.

Primary **amphibole** (usually pargasite, but also magnesiotaramite or barroisite) is often included in garnet cores, but sometimes textural relations indicate that also matrix barroisitic amphibole could have formed in equilibrium with the eclogitic assemblage.

Plagioclase appears only enclosed in garnet and is chemically close to pure albite. The textural relationships indicate its equilibrium growth with garnet rims (Pl. I, Fig. 4). This situation precludes pre-eclogitic plagioclase preservation in "pressure vessels" provided by enclosing garnet crystals. On the other hand, the absence of plagioclase in the matrix shows that this phase is out of equilibrium with the entire assemblage. The only explanation could be that plagioclase crystallised from chemical microdomains segregated from the system (*e.g.* via partial melting) and enclosed in the growing garnet, where they attained local equilibrium.

Retrograde alteration produced symplectitic decomposition of pyroxene and kyanite, as well as growth of large amphibole. Symplectites around omphacite consist of diopside and plagioclase. Symplectites around kyanite are composed of very fine-grained ($< 10\ \mu m$) equant blebs of corundum or spinel in a plagioclase groundmass. Corundum and spinel may appear in different symplectites in the same sample, or even coexist in the same symplectite. Despite reduced grain-size, distinction of the Al-rich phase involved in symplectites around kyanite is straightforward, as corundum, unlike spinel, appears less reflective than coexisting plagioclase on BSE images. Since plagioclase-producing isochemical breakdown of kyanite is not possible, and the symplectite has a constant thickness around the relict kyanite, it is apparent that some reactants (Na_2O, CaO, FeO, MgO) are supplied by intergranular ionic diffusion to reacting kyanite grain margins. Appearance of spinel vs. corundum depends on the amount of ferromagnesian elements locally available,

Institutul Geologic al României

Plate I

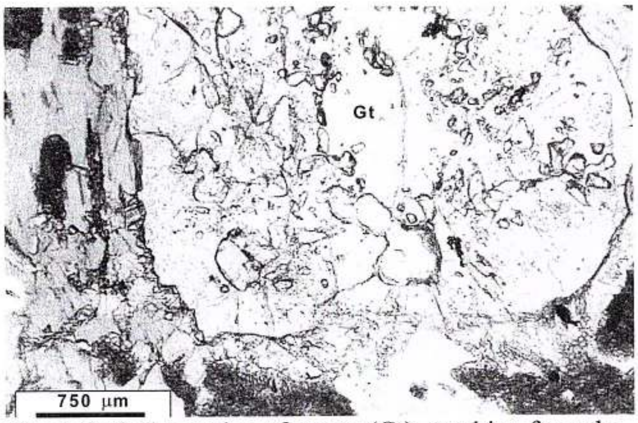

Fig. 1 Optical zonation of garnet (Gt), resulting from the size and distribution of incusions. Sample 6554, N II

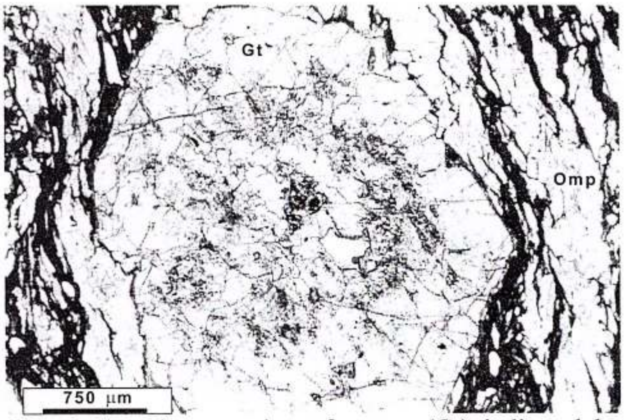

Fig. 2 Complex zonation of garnet (Gt) indicated by inhomogeneous distribution of inclusions. Sample 17432, N II

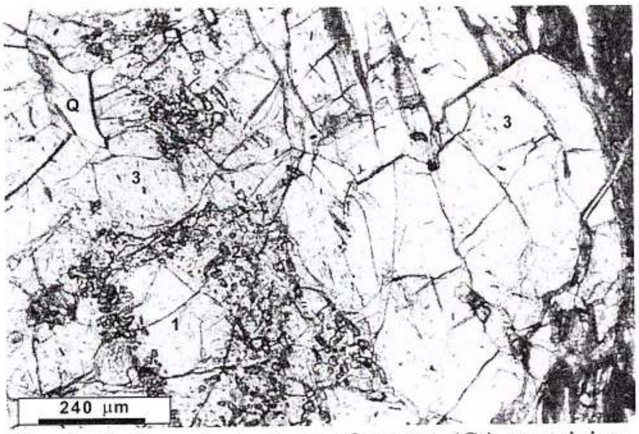

Fig. 3 Coalescent structure of garnet (Gt) containing several individual zoned crystals. Consecutive zones are numbered 1 to 3. Q – quartz hosted in a void surrounded by coalescing crystals. Sample 17432, N II

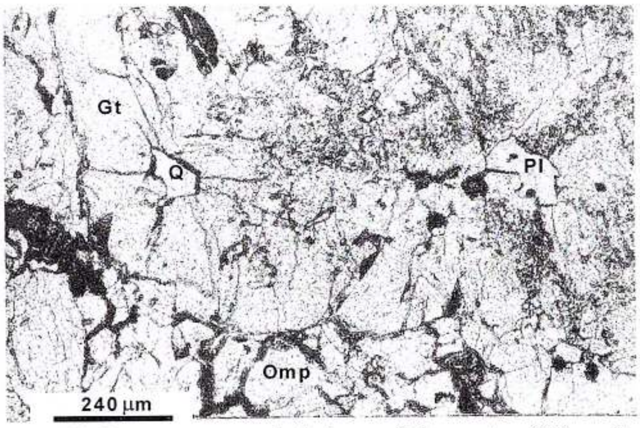

Fig. 4 Quartz surrounded by radial cracks (Q) and plagioclase (Pl) preserved in intergranular voids. Note euhedral garnet contour at lower left boundary of plagioclase. Sample 17432, N II

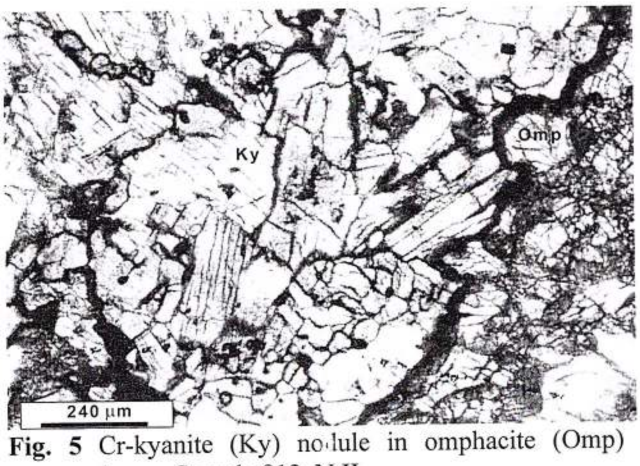

Fig. 5 Cr-kyanite (Ky) nodule in omphacite (Omp) groundmass. Sample 812, N II

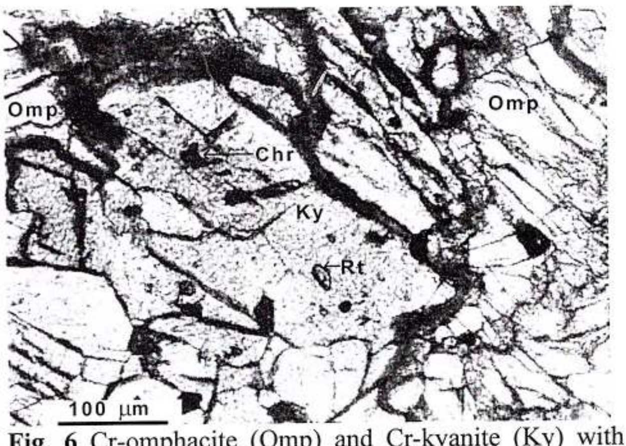

Fig. 6 Cr-omphacite (Omp) and Cr-kyanite (Ky) with rutile (Rt) and chromite (Chr) inclusions. Kyanite colour is more intense (grey) in inclusion-rich patches. Sample 812, N II

Institutul Geologic al României

Table 1 Mineral compositions used for estimation of equilibrium conditions

Garnet	6554	6554	6554	6554	6554	6554	6554	6554	17432	17432	17432	17432	17432	17432	16809	16809	16809	16809
analysis #	1867 133	1867 95	1867 96	1867 99	1867 94	1867 111	1867 118	1867 129	1864 51	1865 11	1865 13	1864 39	1865 2	1865 5	1867 47	1867 46	1867 69	1867 85
SiO_2	38.29	39.05	38.71	38.95	38.78	38.72	38.59	38.46	39.52	39.25	39.64	39.57	39.15	39.93	40.05	39.72	39.31	39.69
TiO_2	0.11	0.08	0.08	0.06	0.10	0.61	0.15	0.11	0.03	0.03	0.01	0.04	0.05	0.02	0.04	0.04	0.46	0.02
Al_2O_3	21.57	21.80	21.87	21.77	21.91	21.60	21.92	21.74	22.35	22.52	22.37	22.60	22.50	22.62	22.25	22.34	22.54	22.35
Fe_2O_3*	0.82	0.61	0.39	0.55	0.80	0.74	0.35	0.91	0.46	0.09	0.53	0.56	1.03	0.24	0.68	0.84	0.72	1.01
Cr_2O_3	0.15	0.00	0.05	0.02	0.00	0.07	0.05	0.08	0.07	0.01	0.03	0.02	0.03	0.00	0.00	0.05	0.10	0.10
MgO	5.54	6.05	5.84	5.83	6.14	7.31	5.42	6.55	11.39	10.62	12.29	12.32	11.81	12.27	11.11	10.16	10.43	10.88
ZnO	0.07	0.00	0.03	0.26	0.03	0.09	0.17	0.04	0.00	0.00	0.05	0.04	0.10	0.14	0.00	0.00	0.06	0.07
FeO*	22.24	22.18	22.49	21.87	22.23	20.94	22.96	21.74	16.66	19.03	17.11	17.01	17.01	16.46	18.23	19.13	18.21	18.78
MnO	0.77	0.75	0.77	0.94	0.75	0.75	0.51	0.90	0.40	0.37	0.29	0.33	0.33	0.33	0.24	0.33	0.28	0.43
CaO	10.32	10.11	9.96	10.16	9.96	9.23	10.28	9.43	7.84	6.97	6.46	6.56	7.08	7.04	7.40	8.03	8.39	7.21
BaO	0.20	0.00	0.00	0.00	0.06	0.11	0.00	0.00	0.02	0.00	0.00	0.00	0.00	0.00	0.00	0.04	0.00	0.00
Na_2O	0.01	0.04	0.03	0.05	0.03	0.03	0.02	0.04	0.04	0.00	0.01	0.02	0.06	0.02	0.04	0.00	0.02	0.02
K_2O	0.00	0.03	0.02	0.08	0.02	0.03	0.02	0.01	0.02	0.00	0.01	0.03	0.02	0.03	0.05	0.01	0.01	0.02
F	0.01	0.00	0.00	0.06	0.00	0.00	0.03	0.00	0.00	0.00	0.00	0.05	0.08	0.06	0.01	0.00	0.00	0.01
Cl	0.00	0.00	0.00	0.01	0.01	0.00	0.02	0.00	0.00	0.00	0.01	0.00	0.01	0.00	0.01	0.00	0.00	0.00
H_2O*	0.05	0.03	0.04	0.02	0.06	0.01	0.03	0.07	0.05	0.04	0.04	0.06	0.11	0.02	0.02	0.05	0.07	0.07
Σ	100.15	100.73	100.28	100.61	100.87	100.25	100.51	100.08	98.87	98.94	98.84	99.19	99.33	99.18	100.13	100.73	100.59	100.67
Si	2.9672	2.9919	2.9828	2.9923	2.9701	2.9669	2.9756	2.9627	2.9805	2.9787	2.9832	2.9677	2.9434	2.9888	2.9971	2.9756	2.9410	2.9669
Alt	0.0328	0.0081	0.0172	0.0077	0.0299	0.0331	0.0244	0.0373	0.0195	0.0213	0.0168	0.0323	0.0566	0.0112	0.0029	0.0244	0.0590	0.0331
Σ	3.0000	3.0000	3.0000	3.0000	3.0000	3.0000	3.0000	3.0000	3.0000	3.0000	3.0000	3.0000	3.0000	3.0000	3.0000	3.0000	3.0000	3.0000
Alo	1.9338	1.9604	1.9693	1.9631	1.9480	1.9121	1.9610	1.9365	1.9677	1.9925	1.9677	1.9655	1.9374	1.9849	1.9595	1.9475	1.9230	1.9362
Ti	0.0094	0.0044	0.0046	0.0037	0.0058	0.0409	0.0156	0.0061	0.0018	0.0017	0.0005	0.0021	0.0026	0.0013	0.0023	0.0023	0.0308	0.0011
Cr	0.0090	0.0000	0.0032	0.0011	0.0000	0.0042	0.0030	0.0047	0.0044	0.0009	0.0020	0.0010	0.0016	0.0003	0.0001	0.0028	0.0059	0.0060
Fe^{3+}	0.0479	0.0352	0.0228	0.0321	0.0462	0.0429	0.0204	0.0526	0.0261	0.0049	0.0298	0.0314	0.0584	0.0136	0.0381	0.0474	0.0403	0.0567
Σ	2.0000	2.0000	2.0000	2.0000	2.0000	2.0000	2.0000	2.0000	2.0000	2.0000	2.0000	2.0000	2.0000	2.0000	2.0000	2.0000	2.0000	2.0000
Zn	0.0038	0.0000	0.0018	0.0147	0.0017	0.0052	0.0096	0.0022	0.0000	0.0000	0.0026	0.0021	0.0058	0.0080	0.0000	0.0000	0.0032	0.0040
Fe^{2+}	1.4408	1.4214	1.4492	1.4051	1.4237	1.3422	1.4803	1.4008	1.0508	1.2077	1.0769	1.0670	1.0696	1.0303	1.1410	1.1987	1.1392	1.1737
Mn	0.0507	0.0488	0.0504	0.0614	0.0484	0.0486	0.0333	0.0588	0.0259	0.0240	0.0185	0.0211	0.0210	0.0212	0.0154	0.0209	0.0181	0.0272
Mg	0.6399	0.6906	0.6703	0.6674	0.7007	0.8353	0.6223	0.7526	1.2809	1.2016	1.3788	1.3774	1.3239	1.3692	1.2396	1.1339	1.1635	1.2120
Ca	0.8570	0.8298	0.8224	0.8366	0.8172	0.7576	0.8492	0.7785	0.6337	0.5666	0.5207	0.5275	0.5702	0.5649	0.5934	0.6443	0.6727	0.5775
Ba	0.0061	0.0000	0.0000	0.0000	0.0017	0.0034	0.0000	0.0000	0.0006	0.0000	0.0000	0.0000	0.0000	0.0000	0.0000	0.0012	0.0000	0.0000
K	0.0002	0.0033	0.0020	0.0064	0.0020	0.0032	0.0019	0.0013	0.0018	0.0000	0.0008	0.0024	0.0015	0.0025	0.0037	0.0010	0.0009	0.0019
Na	0.0015	0.0060	0.0040	0.0070	0.0046	0.0045	0.0034	0.0059	0.0063	0.0000	0.0016	0.0023	0.0081	0.0033	0.0062	0.0000	0.0025	0.0033
Σ	3.0000	3.0000	3.0000	2.9986	3.0000	3.0000	3.0000	3.0000	3.0000	3.0000	2.9998	2.9998	3.0000	2.9994	2.9993	3.0000	3.0000	2.9996
F	0.0023	0.0001	0.0001	0.0127	0.0001	0.0001	0.0079	0.0001	0.0001	0.0001	0.0001	0.0109	0.0182	0.0127	0.0014	0.0001	0.0001	0.0016
Cl	0.0000	0.0000	0.0000	0.0008	0.0008	0.0005	0.0020	0.0000	0.0000	0.0000	0.0011	0.0000	0.0010	0.0000	0.0014	0.0000	0.0000	0.0004
OH	0.0269	0.0130	0.0184	0.0121	0.0303	0.0057	0.0159	0.0383	0.0257	0.0197	0.0182	0.0297	0.0540	0.0190	0.0098	0.0231	0.0366	0.0366
$Ca_3Cr_2Si_3O_{12}$	0.0045	0.0000	0.0016	0.0006	0.0000	0.0021	0.0015	0.0024	0.0022	0.0004	0.0010	0.0005	0.0008	0.0001	0.0001	0.0014	0.0029	0.0030
$Ca_3Fe_2Si_3O_{12}$	0.0240	0.0176	0.0114	0.0160	0.0231	0.0214	0.0102	0.0263	0.0130	0.0025	0.0149	0.0157	0.0292	0.0068	0.0191	0.0237	0.0202	0.0284
$Ca_3Al_2Si_3O_{12}$	0.2593	0.2590	0.2611	0.2623	0.2499	0.2302	0.2714	0.2308	0.1962	0.1860	0.1576	0.1596	0.1600	0.1814	0.1787	0.1901	0.2011	0.1611
$Mn_3Al_2Si_3O_{12}$	0.0169	0.0163	0.0168	0.0205	0.0161	0.0162	0.0111	0.0196	0.0086	0.0080	0.0062	0.0070	0.0070	0.0071	0.0051	0.0070	0.0060	0.0091
$Mg_3Al_2Si_3O_{12}$	0.2094	0.2291	0.2214	0.2214	0.2360	0.2716	0.2042	0.2462	0.4232	0.3968	0.4564	0.4529	0.4306	0.4541	0.4125	0.3738	0.3753	0.3983
$Fe_3Al_2Si_3O_{12}$	0.4716	0.4715	0.4786	0.4662	0.4672	0.4364	0.4859	0.4582	0.3472	0.3989	0.3565	0.3508	0.3479	0.3418	0.3797	0.3952	0.3675	0.3857
Others	0.0143	0.0065	0.0091	0.0130	0.0137	0.0221	0.0157	0.0165	0.0096	0.0074	0.0074	0.0135	0.0245	0.0087	0.0048	0.0088	0.0270	0.0144
Xmg	0.3075	0.3270	0.3162	0.3220	0.3298	0.3836	0.2960	0.3495	0.5493	0.4987	0.5615	0.5635	0.5531	0.5706	0.5207	0.4861	0.5053	0.5080

Institutul Geologic al României

Table 1 (continued)

Clinopyroxene	6554	6554	6554	6554	6554	17432	17432	17432	17432	17432	17432	17432	16809	16809	16809	16809
analysis =	1867 132	1867 97	1867 110	1867 119	1867 131	1864 50	1864 34	1865 12	1865 14	1864 38	1865 15	1865 1	1867 44	1867 87	1867 68	1867 83
SiO_2	53.89	55.83	55.36	55.41	54.91	54.73	54.80	55.18	55.45	54.93	55.40	55.01	54.34	55.79	55.28	56.04
TiO_2	2.43	0.05	0.05	0.07	0.05	0.03	0.07	0.05	0.03	0.04	0.06	0.05	0.07	0.03	0.06	0.00
Al_2O_3	9.70	10.55	9.79	9.18	10.74	8.89	10.57	10.77	10.77	10.02	11.78	9.82	8.13	9.02	9.96	8.80
Fe_2O_3*	0.00	0.00	0.00	0.00	0.00	0.00	0.00	0.00	0.00	0.00	0.00	0.00	0.00	0.24	0.20	0.00
Cr_2O_3	0.14	0.08	0.00	0.09	0.06	0.03	0.04	0.20	0.04	0.08	0.11	0.08	0.03	0.11	0.16	0.07
MgO	9.40	9.39	9.35	9.51	9.88	11.04	9.69	9.48	9.71	10.39	8.87	10.59	11.30	10.82	10.19	10.87
ZnO	0.06	0.01	0.00	0.06	0.04	0.01	0.00	0.08	0.09	0.17	0.00	0.05	0.00	0.04	0.11	0.00
FeO*	3.09	3.21	3.66	4.18	2.23	1.57	2.64	1.83	1.49	1.41	1.89	1.63	2.99	1.91	2.31	2.27
MnO	0.04	0.03	0.02	0.06	0.09	0.04	0.01	0.04	0.01	0.03	0.00	0.04	0.01	0.10	0.06	0.00
CaO	14.49	14.44	14.61	14.93	16.06	16.72	14.77	14.62	14.43	15.65	13.35	15.60	17.33	16.37	15.79	16.44
BaO	0.00	0.00	0.07	0.04	0.00	0.06	0.06	0.06	0.01	0.08	0.08	0.04	0.00	0.09	0.02	0.07
Na_2O	5.67	5.94	5.79	5.56	4.99	4.74	5.84	6.00	5.96	5.40	6.54	5.33	4.04	5.29	5.43	5.01
K_2O	0.03	0.03	0.01	0.00	0.04	0.04	0.02	0.03	0.04	0.04	0.03	0.05	0.07	0.01	0.03	0.03
F	0.00	0.09	0.00	0.07	0.00	0.00	0.00	0.03	0.00	0.00	0.11	0.00	0.06	0.04	0.00	0.03
Cl	0.00	0.00	0.01	0.01	0.01	0.01	0.00	0.00	0.01	0.01	0.01	0.02	0.38	0.00	0.01	0.02
Σ	95.89	99.62	98.73	99.13	99.09	97.91	97.85	98.36	98.05	98.26	98.18	98.31	98.64	99.84	99.61	99.62
Si	1.9347	1.9868	1.9956	1.9961	1.9643	1.9826	1.9792	1.9820	1.9908	1.9777	1.9841	1.9795	1.9698	1.9857	1.9724	1.9967
Alt	0.0653	0.0132	0.0044	0.0039	0.0357	0.0174	0.0208	0.0180	0.0092	0.0223	0.0159	0.0205	0.0302	0.0143	0.0276	0.0033
Σ	2.0000	2.0000	2.0000	2.0000	2.0000	2.0000	2.0000	2.0000	2.0000	2.0000	2.0000	2.0000	2.0000	2.0000	2.0000	2.0000
Alo	0.3451	0.4293	0.4117	0.3857	0.4171	0.3619	0.4292	0.4378	0.4465	0.4030	0.4813	0.3962	0.3170	0.3639	0.3911	0.3664
Ti	0.0782	0.0017	0.0016	0.0023	0.0016	0.0010	0.0024	0.0016	0.0009	0.0014	0.0019	0.0016	0.0024	0.0009	0.0019	0.0000
Cr	0.0040	0.0023	0.0000	0.0026	0.0016	0.0010	0.0011	0.0058	0.0012	0.0024	0.0031	0.0024	0.0010	0.0031	0.0044	0.0019
Zn	0.0000	0.0003	0.0000	0.0017	0.0009	0.0002	0.0000	0.0021	0.0024	0.0044	0.0000	0.0014	0.0000	0.0010	0.0028	0.0000
Fe^{3+}	0.0000	0.0000	0.0000	0.0000	0.0000	0.0000	0.0000	0.0000	0.0000	0.0000	0.0000	0.0000	0.0000	0.0064	0.0054	0.0000
Fe^{2+}	0.0927	0.0944	0.1163	0.1251	0.0667	0.0475	0.0616	0.0549	0.0446	0.0426	0.0557	0.0490	0.0882	0.0566	0.0689	0.0671
Mn	0.0013	0.0009	0.0007	0.0018	0.0026	0.0011	0.0003	0.0012	0.0003	0.0010	0.0000	0.0011	0.0003	0.0030	0.0019	0.0000
Mg	0.5031	0.4990	0.5026	0.5119	0.5267	0.5962	0.5216	0.5078	0.5198	0.5578	0.4745	0.5679	0.6129	0.5741	0.5420	0.5775
Ca	0.5574	0.5506	0.5641	0.5761	0.6154	0.6490	0.5717	0.5625	0.5551	0.6037	0.5121	0.6014	0.6731	0.6243	0.6038	0.6277
Ba	0.0000	0.0000	0.0010	0.0005	0.0000	0.0009	0.0000	0.0009	0.0002	0.0011	0.0011	0.0005	0.0000	0.0012	0.0003	0.0010
Na	0.3950	0.4100	0.4047	0.3881	0.3460	0.3328	0.4088	0.4176	0.4152	0.3769	0.4538	0.3719	0.2841	0.3651	0.3759	0.3459
K	0.0015	0.0016	0.0006	0.0001	0.0018	0.0016	0.0010	0.0014	0.0017	0.0017	0.0016	0.0024	0.0030	0.0004	0.0016	0.0011
Σ	1.9782	1.9962	1.9973	1.9959	1.9804	1.9932	1.9977	1.9935	1.9879	1.9969	1.9850	1.9959	1.9819	2.0000	2.0000	1.9885
$NaAlSi_2O_6$	0.3256	0.3964	0.4025	0.3750	0.3420	0.3302	0.4053	0.4067	0.4123	0.3722	0.4358	0.3666	0.2499	0.3497	0.3638	0.3390
$CaMgSi_2O_6$	0.4630	0.4510	0.4584	0.4618	0.4984	0.5799	0.4928	0.4877	0.4909	0.5343	0.4423	0.5322	0.5711	0.5593	0.5108	0.5530
$CaFeSi_2O_6$	0.0853	0.0764	0.0999	0.1050	0.0623	0.0456	0.0581	0.0493	0.0414	0.0398	0.0397	0.0446	0.0532	0.0501	0.0644	0.0594
$CaAlAlSiO_6$	0.0000	0.0115	0.0028	0.0017	0.0341	0.0164	0.0184	0.0164	0.0083	0.0209	0.0139	0.0189	0.0278	0.0134	0.0257	0.0033
$(Mg,Fe,Mn)_2Si_2O_6$	0.0243	0.0282	0.0269	0.0308	0.0172	0.0089	0.0162	0.0111	0.0157	0.0126	0.0176	0.0196	0.0229	0.0088	0.0184	0.0136
Rest	0.1018	0.0366	0.0093	0.0256	0.0461	0.0190	0.0091	0.0289	0.0314	0.0201	0.0507	0.0181	0.0749	0.0187	0.0170	0.0317
X_{Mg}	0.8444	0.8529	0.8208	0.8125	0.8888	0.9270	0.8945	0.9077	0.9222	0.9305	0.9155	0.9224	0.9107	0.9171	0.8879	0.9022

Plagioclase	17432	17432
analysis =	1865 22	1865 3
SiO_2	62.25	67.49
TiO_2	0.02	0.00
Al_2O_3	21.78	19.27
Fe_2O_3*	0.00	0.19
Cr_2O_3	0.00	0.01
MgO	0.09	0.00
ZnO	0.07	0.00
FeO*	0.27	0.00
MnO	0.00	0.01
CaO	3.46	0.16
BaO	0.00	0.08
Na_2O	9.02	11.63
K_2O	0.08	0.07
F	0.00	0.13
Cl	0.02	0.00
Σ	97.05	99.00
Si	2.8384	2.9807
Al	1.1708	1.0031
Ti	0.0007	0.0000
Cr	0.0000	0.0004
Fe^{3+}	0.0000	0.0063
Zn	0.0023	0.0000
Mg	0.0062	0.0000
Fe^{2+}	0.0102	0.0000
Mn	0.0000	0.0003
Ca	0.1692	0.0078
Ba	0.0000	0.0015
Na	0.7976	0.9963
K	0.0045	0.0042
F	0.0001	0.0183
Cl	0.0013	0.0000

Phengite	16809
analysis =	1867 81
SiO_2	48.57
TiO_2	0.04
Al_2O_3	28.78
Fe_2O_3*	0.00
Cr_2O_3	0.22
MgO	3.14
ZnO	0.02
FeO*	2.39
MnO	0.05
CaO	0.08
BaO	0.05
Na_2O	0.14
K_2O	10.73
F	0.08
Cl	0.01
H_2O*	4.38
Σ	98.65
Si	3.2943
Al	0.7057
Σ	4.0000
Alo	1.5952
Ti	0.0021
Cr	0.0119
Fe^{3+}	0.0000
Zn	0.0011
Fe^{2+}	0.1353
Mn	0.0030
Mg	0.3178
Σ	2.0664
Ca	0.0058
Na	0.0187
K	0.9287
Ba	0.0013
Σ	0.9545
F	0.0175
Cl	0.0014
O	0.0000
OH	1.9811
$KMgAlSi_4O_{10}(OH)_2$	0.1801
$KFeAlSi_4O_{10}(OH)_2$	0.0767
$KMg_3AlSi_3O_{10}(OH)_2$	0.0452
$KFe_3AlSi_3O_{10}(OH)_2$	0.0193
$KAl_2AlSi_3O_{10}(OH)_2$	0.5980
$NaAl_2AlSi_3O_{10}(OH)_2$	0.0187
Rest	0.0620

* calculated

Institutul Geologic al României

Plate II
Compositional maps of garnet in Pl. I, Fig. 2

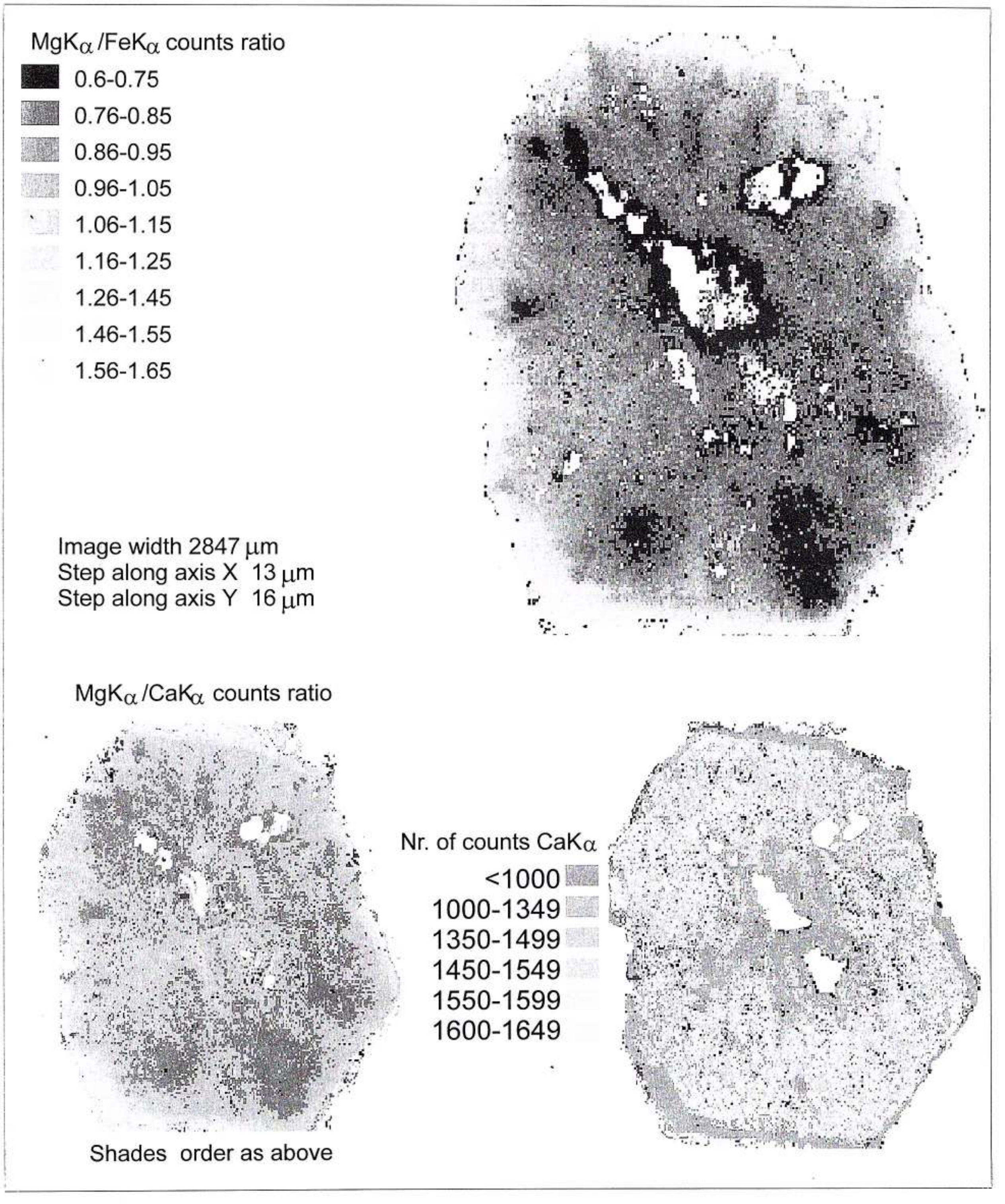

Institutul Geologic al României

in such a way that spinel is usually formed nearby breaking-down garnet, while more efficient diffusion of Na_2O and CaO allows formation of corundum also at relatively Fe, Mg-poorer locations. Sometimes the former kyanite grains are completely replaced by an annealed aggregate of sub-millimetric barrel-shaped corundum intergrown with polygranular plagioclase. Retrograde amphibole of barroisite to magnesiohornblende composition, obviously postdating symplectite formation, corrodes and includes earlier phases.

2. Thermobarometry of the eclogitic assemblage

Estimation of P-T conditions is a very difficult task in assemblages containing strongly zoned phases as is garnet in the analysed sample, apart from post eclogitic alternation. For instance, analysed garnets in sample 17432 cover a wide composition interval (Alm_{34-44}, Py_{32-46}, Gro_{24-15}) - which may for sure not represent the entire compositional field, since the analyses were aimed to investigate rather coexisting phases than chemical variability of individual phases. Under these circumstances, it is critical for correct derivation of equilibrium conditions that the grains be truly in equilibrium, as inaccurate choice dramatically affect the results. Therefore, only mineral pairs consisting of points less distant than 100 μm from one another, belonging to contiguous grains, were selected for thermodynamic calculations. Even with this provision taken, mineral chemistry may be significantly altered in the very eclogitic stage, due to high compositional gradients in minerals. To avoid the effects of retrograde alterations, only samples with a well-preserved eclogitic assemblage were selected for mineral chemistry determination.

Analyses were performed on a Cameca SX50 microprobe using synthetic silicate crystals and glasses, at the Ruhr University in Bochum. Operating conditions were: accelerating potential - 15 kV, sample current 15 nA, counting time 20 s. For pyroxene a sample current of 10 nA and a defocused beam were employed, in order to avoid Na volatilisation during the analysis. Mineral formulae were recalculated assuming charge balance of eight cations p.f.u. for garnet, simultaneous cation charge balance and Na balance among Na-bearing end-members ($NaTiAlSiO_6$ -$NaAlSi_2O_6$ - $NaFeSi_2O_6$) for pyroxene respectively. Thermobaric estimates were made (when possible) in the dry CFMAS system, involving silica and kyanite besides garnet and pyroxene end-members (viz. grossular, pyrope, almandine, diopside, hedenbergite, Ca-Ts pyroxene). Thermodynamic data for pure phases were mostly taken from the internally consistent dataset of Berman (1988). Excess solution properties (and some end-member data) were chosen according to Massonne (1992), using an asymmetric nonideal ionic model for garnet (a least-square refinement of the data of Berman (1990)), and an asymmetric molecular model for C2/c and/or P2/n omphacite. Calculation routine was that described by Berman (1991) allowing, in the above- mentioned system, determination of both equilibration conditions and degree of equilibration. In kyanite-free assemblages, thermobaric investigations were performed in the CFMASH system, using hydrous equilibria involving zoisite (a_{Zo}= .9), anchored to the dry garnet-pyroxene-silica CFMAS invariat system. In this case the calculations also yielded (rather by need than by choice) an estimation of water activity. Phengite-bearing assemblages were used for independent pressure estimates based on the Si p.fu. content of Mg- and Fe-celadonite in equilibrium with garnet, quartz and kyanite (Massonne, 1995).

Sample 6554 is a kyanite-free, zoisite-bearing eclogite. The assemblage does not allow any additional control on the position of the CFMAS invariant point (kyanite is absent), while the compositional range of pyroxene clearly indicates, at least for the initial stages, the presence of P2/n ordered omphacite. Calculated reactions (Tab. 2) yield very good intersections 575-580^0 C and 1.8-1.84 GPa at low water activities (a_{H2O}=.17). Poorer intersections most probably indicate, according to the position of the exchange reactions as compared with net transfer reactions, either overstepping of the equilibrium conditions by heating, or retrograde Fe-Mg exchange during cooling. For these, apparent temperatures derived from the clinopyroxene-garnet Fe-Mg exchange thermometer were bracketed for both ordered and disordered omphacite between 2.1-2.7 GPa, for estimates of either maximum temperatures at which the system evolved (Pl. III), or minimum temperatures recorded along the retrograde path. Because some of the brackets pertaining to disordered omphacite indicate cooling temperatures, most of them group together, and some equilibria for P2/n omphacite imply unrealistically low water activities or unrealisitically low retrograde Fe-Mg exchange temperatures, it is probable that omphacite P2/n-C2/c boundary was crossed during the prograde path around peak temperatures. Calculations for some mineral pairs under this assumption yield consistent values at 683-692^0 C and 2.62-2.64 GPa. The associated water activity is .74. This inferred prograde path is fully consistent with the jadeite-augite pseudobinary proposed by Carpenter & Smith (1981), but is conflicting with the phase diagrams of Carpenter (1978) and Massonne (1991).

For sample 17432 the kyanite-bearing assemblage allowed internal checking of the position of the cal-

Institutul Geologic al României

Table 2
Thermobarometric estimates for the analysed samples

Sample	Garnet	Omphacite		T, °C	P, GPa	a_{H_2O}
6554: P,T-fields						
6554_2	1867/95	1867/97	P2/n	**575**	**1.8**	**0.17**
6554_3	1867/96	1867/97	C2/c	**683**	**2.63**	**0.743**
6554_4	1867/99	1867/97	C2/c	**684-692**	**2.62-2.64**	**0.743**
6554_5	1867/94	1867/97	P2/n	**580**	**1.84**	**0.17**
6554: P,T-brackets						
6554_1	1867/133	1867/132	C2/c	*<678*	*2.1**	
6554_1		*Ibid.*		*<700*	*2.7**	
6554_4	1867/99	1867/97	C2/c	*<671*	*2.1**	
6554_4		*Ibid.*		*<694*	*2.7**	
6554_6	1867/111	1867/110	P2/n	*<800*	*2.1**	
6554_6		*Ibid.*		*<829*	*2.7**	
6554_7	1867/118	1867/119	C2/c	*<708*	*2.1**	
6554_7		*Ibid.*		*<731*	*2.7**	
6554_8	1867/129	1867/131	C2/c	*645<*	*2.1**	
6554_8		*Ibid.*		*667<*	*2.7**	
17432: P,T-fields						
17432_2	1865/11	1864/34	C2/c	**750-780**	**2.5-2.7**	
17432_3	1865/11	1864/12	C2/c	**750-780**	**2.7-2.9**	
17432_5	1864/39	1864/38	C2/c	**762-773**	**2.5-2.8**	
17432_6	1864/39	1865/15	P2/n	**650-700**	**2.6±1**	
17432_7	1865/1	1865/2	C2/c	**775±4**	**2.7±.2**	
17432: P,T-brackets						
17432_1	1864/51	1864/50	C2/c-P2/n	*667<T<788*	*2.3**	
17432_1		*Ibid.*		*684<T<800*	*2.8**	
17432_2	1865/11	1864/34	C2/c-P2/n	*655<T<772*	*2.3**	
17432_2		*Ibid.*		*671<T<790*	*2.8**	
17432_3	1865/11	1864/12	C2/c	*730<*	*2.3**	
17432_3		*Ibid.*		*750<*	*2.8**	
17432_4	1865/13	1865/14	C2/c-P2/n	*639<T<750*	*2.3**	
17432_4		*Ibid.*		*653<T<767*	*2.8**	
17432_5	1864/39	1864/38	C2/c	*765<*	*2.3**	
17432_5		*Ibid.*		*780<*	*2.8**	
17432_6	1864/39	1865/15	P2/n	*745<*	*2.3**	
17432_6		*Ibid.*		*760<*	*2.8**	
16809: P,T-fields						
16809_1	1867/47	1867/44	C2/c	**755±5**	**2.1±.2**	
16809_2	1867/46	1867/87-93	P2/n	**649±.5**	**2.37**	
16809: P,T-brackets						
16809_3	1867/69	1867/68	C2/c	*<815*	*2**	
16809_3		*Ibid.*		*<836*	*2.5**	
16809_4	1867/85	1867/83	C2/c	*<816*	*2**	
16809_4		*Ibid.*		*<836*	*2.5**	

* input values

Institutul Geologic al României

Plate III
Near-peak p-T paths of the eclogites in the "Topolog Formation"

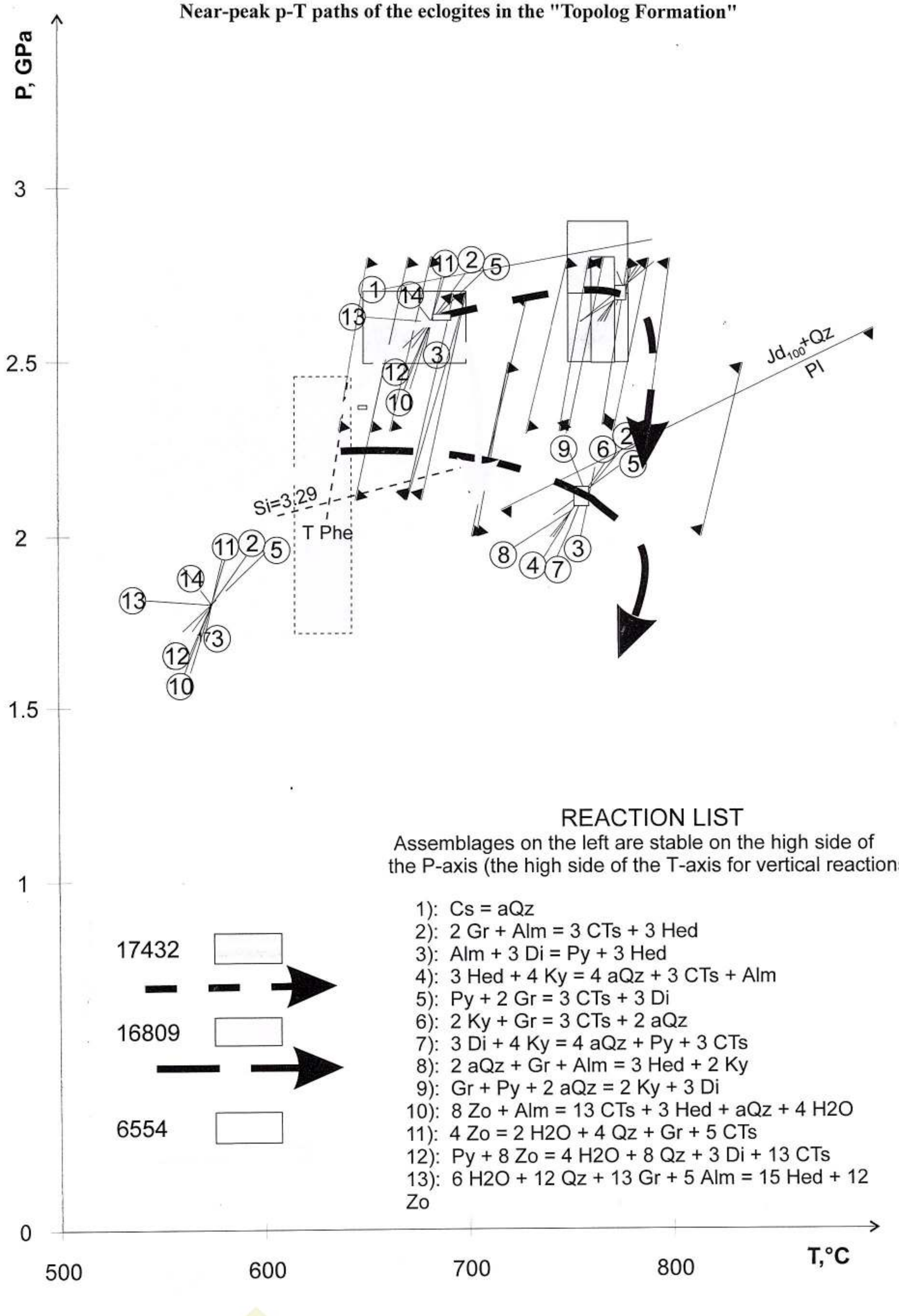

Institutul Geologic al României

culated invariant points. For the equilibria involving the most jadeite-rich pyroxene, calculations with primitive omphacite yielded 650-700^0 C and 26.1± .1 GPa. Pyroxenes with lower jadeite contents indicated consistent equilibrium conditions for disordered omphacite around 775^0 C and 2.7 GPa. Temperature brackets at 2.3-2.8 GPa for poorly equilibrated mineral pairs are consistent with these values. The pT values thus derived imply near-isobaric heating of around 100^0 C at peak conditions. Once again, the consistency with omphacite phase relations asserted by Carpenter & Smith (1981) is maintained, but the fit with alternative models is proorer. High-pressure isobaric heating is also consistent with the fact that practically all quartz inclusions in external shells of garnet are surrounded by radial cracks, most probably originating from important differential volume increase of quartz as compared with the host garnet. An alternative explanation for the presence of radial cracks would be volume expansion of silica by the coesite-quartz inversion during uplift. However, the rock contains evidence rather for the absence of coesite at all stages, according to the calculated equilibrium conditions and also to the presence of plagioclase inclusions preserved in the voids of the garnet aggregates. The limiting conditions for the persistence of plagioclase in armoured inclusion is given by two reactions: spontaneous breakdown of the Ca-richer plagioclase, forming pure jadeite and quartz, represent the upper pressure limit, while the lower temperature limit is given by the breakdown of the same to kyanite + grossular. These equilibria imply plagioclase forming before cessation of garnet growth, by isothermal decompression /heating + decompression around 800^0 C and 2.1 GPa.

For sample 16809 garnet-clinopyroxene thermobarometry yielded also near isothermal path at the highest pressure (Tab. 2), going from 650^0 C, 2.37 GPa for disordered high-jadeite omphacite to ca. 755^0 C for ordered lower-jadeite omphacite. The results are in good agreement with all three clinopyroxene phase relationships mentioned above. Equilibria involving phengite were also studied for this sample. An averaged Si=3.29 isopleth for the Fe- and Mg-phengites coexisting with garnet and kyanite, as well as equilibria involving phengites in the system KCFMASH poorly constrain a large pT-field around 625-650^0 C, 1.7-2.4 GPa for the early phengite-bearing eclogitic assemblages in the sample. The pT array of all samples is also consistent with a unique clockwise path: nevertheless persistence of zoisite and absence of kyanite in sample 16809 rules out the heating of this sample beyond 700^0 C even at unitary water activities. Therefore the evolution of the studied sample points to an intricate burial-uplift history of eclogites belonging to the same belt and implies important differential movement.

3. Evolution of retrograde assemblages

The nature and extent of retrograde imprints differs from sample to sample. Samples 17432, 17433 are strongly oriented and at the same time show only minor symplectites around pyroxene and kyanite, making evidence of high strain under near-peak conditions, followed by rapid uplift at low water activities. Another possibility would be significant cooling during upflit, along a path approximately paralleling the jadeite+quartz=plagioclase reaction curve. Sample 16809 contains abundant symplectites with external coarse-grained intergrowths which abruptly become finer-grained towards inside, showing a relatively slower two-stage upflit. Sample 6554 contains abundant symplectites with constant grain-size, intermediate in dimension as compared with those in the previous sample. Although a straighforward correlation between forming temperature and symplectite wavelenght seems hardly probable, it is nevertheless likely that plagioclase breakdown in this sample started at lower temperatures than that in sample 16809, in agreement with the calculated pT-paths. Thermobaric estimates like that attempted by Joanny et al. (1991) can only be of very limited reliability, since the basic assumptions therein are strongly questionable: omphacite breakdown to simplectite is by no means an isochemical discontinuous precipitation, the assumed reaction temperatures are poorly constrained, and at the same time the absence of quartz in textural equilibrium casts serious doubts on the pyroxene-plagioclase barometry. It seems more reasonable to assume a mechanism mostly driven by intracrystalline diffusion, as it is apparent in the corundum/spinel+plagioclase symplectites around kyanite.

Overprinting by an amphibole-bearing assemblage implies important hydration, which can occur during emplacement in the host mica-rich rocks or may be caused due to percolation by ascending fluids.

4. Concluding remarks

The mineralogy of the studied eclogites clearly proves eclogitization of oceanic mafic rocks during burial along a subduction zone. The preservation of the final part of the prograde path indicates quartz-producing eclogitization accompanied by dehydration of amphibole bearing assemblages. This process results in continuous increase of water activity along the prograde path, also identified by Massonne (1992), who alternatively explained it by an external water influx.

Institutul Geologic al României

The thermal regime of the Topolog Complex eclogites is characterized by unusually high peak temperatures, consistent with the presence of disordered omphacite containing less than ca. 35-40 % jadeite. More unusual is the near-isobaric heating at peak pressured, supported, apart from thermobarometric estimations, by well-developed radial cracks around quartz inclusions and garnet zonation.

Mineral assemblages in the rock types adjacent to the eclogites in the metamorphic pile not only preclude the possibility of a coherent eclogitic terrane, but also imply tectonic juxtaposition of at least three lithologies with contrasting metamorphic history. Therefore, at least a part of the Topolog Complex represents a major crustal discontinuity in the Cumpăna Suite of the Făgăraş Mountains, most presumably a suture. This is a view shared by Costin & Menot (in press), who assume upflit of the eclogitic rocks along a deep-seated transpressive dislocation.

However, the mechanism invoked would imply a more coherent regional metamorphic pattern, and is not fully consistent with the relatively rapid uplift required to preserve the eclogitic assemblages. It is therefore more probable that the differential upflit of the eclogites might be due to buoyant ascent of the felsic rocks in which they resided after reaching peak pressures. Isobaric heating represents a process of shifting-away from the thermal gradient typical of a subduction zone. Most probably it results from detachment of the downgoing slab followed by deep-seated incorporation and a period of storage in the overriding plate, prior to upflit. The close field association with felsic gneisses favours this interpretation, especially when these felsic rocks inherit relics that indicate higher metamorphic grade than the middle grade background made up of pelitic and semipelitic lithologies. In this respect, the Topolog Complex contains two feldspar-, biotite- linear gneisses with large garnet porphyroblasts. Despite pervasive retrogression in these rocks, the fabric indicates flowing under high differential stress and the mineral assemblages retains high-grade relics, strongly ressembling the Vătafu Gneiss in the Lotru Suite of the Getic Nappe basement, that also associate with high-temperature eclogites (Săbău, 1995).

Derived pT-paths illustrate the lack of coherence among different eclogite bodies belonging to the same belt and among these and host rocks in eclogite belts associated to regional metamorphic terrains, and highlight complicated mechanisms of sampling and uplift of parts of the downgoing plate in compressional plate boundaries evolving from subduction to collision.

Acknowledgements

Microprobe analyses were perfomed during the tenure of an Alexander von Humboldt Fellowship by the first author. The support of Prof. Werner Schreyer in providing the facilities at the Ruhr University in Bochum is gratefully acknowledged. I. Gheuca kindly contributed by providing some of the eclogite samples and thin sections.

References

Berman, R. G. (1988) Internally-consistent thermodynamic data for minerals in the system Na_2O- K_2O-CaO-MgO-FeO-Fe_2O_3-Al_2O_3-TiO_2-SiO_2-H_2O-CO_2, *J. Petrology 29*, p. 445-522.

— **(1990)** Mixing properties of Ca-Mg-Fe-Mn garnets, *The American Mineralogist, 75*, p. 328-344.

— **(1991)** Thermobarometry using multiequilibrium calculations: a new technique with petrologic applications, *Canadian Mineralogist 29*, p. 833-855.

Brown, T. H., Berman, R. G., Perkins, E. H. (1988) Ge0-Calc: Software package for calculation and display of pressure-temperature- composition phase diagrams using an IBM or compatible personal computer, *Computer and Geosci. 14*, p. 279-289.

Carpenter, M. A. (1978) Solid solution and cation ordering limits in high-temperature sodic pyroxene from the Nybö eclogite pod, Norway, *Mineral. Magazine, 44*, p. 37-44.

— **, Smith, D. C. (1981)** Kynetic control of ordering and exsolution in omphacites, *Contr. Mineral. Petrol. 67*, p. 17-24.

Costin, G., Menot, R-P. (in press) Some mineralogical, chemical and thermobarometrical data on the Făgăraş and Leaota eclogites (South Carpathians, Romania), *Compte Rendu des Académie des Sciences, Paris.*

Gheuca, I. et al. (1987) *Report, Archives I.G.R.*, Bucureşti.

— **(1988)** Versantul sudic al Munţilor Făgăraş, litostratigrafie şi tectonică, *D.S. Inst. Geol. Geofiz., 72-73/5*, p. 93-117, Bucureşti.

Massone, H.-J. (1991) Druck-Temperatur-Entwicklung phengitführender Eklogite, em Mitt. Österr. Miner. Ges., 136, 55-77.

— **(1990)** Thermochemical determination of water activities relevant to eclogitic rocks: in Kharaka, Y.K. & Maest, A.S. (eds.) Water - rock interaction: proc. 7th intern symp on water-rock interaction, Park City, Utah, USA; 1523-1526, A.A. Balkema, Rotterdam, Brookfield.

— **(1995)** Thermodynamic properties of micas on the basis of high-pressure experiments in the systems K_2O-MgO-Al_2O_3-SiO_2-H_2O and K_2O-FeO-Al_2O_3-SiO_2-H_2O *Bochumer geol. u. geotech. Arb. 44*, p. 109-113.

Joanny, V., van Roermund, H., Lardeaux, J. M. (1991) The clinopyroxene/plagioclase symplectite in retrograde eclogites: a potential geothermobarometer, *Geologische Rundschau, 80/2*, p. 303-320.

Săbău, G. (1995) Evidence for eclogite emplacement via crust doubling in the Lotru Crystalline Series, South Carpathians, *Europrobe Workshops - PANCARDI, Stara Lesna 1995, Abstracts*, p. 18-19.

Ştefănescu, M. et al. (1982) *Report, I.G.R. Archives, Bucharest.*

Received: February 25, 1998
Accepted: March 25, 1998

Institutul Geologic al României

THE GREENSTONES FROM THE ANCHIMETAMORPHIC GROŞI FORMATION OF NE BANAT, ROMANIA

H. SAVU, I. TIEPAC, C. UDRESCU

Institutul Geologic al României, str. Caransebeş nr. 1, 79678 Bucureşti 32.

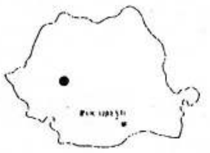

Key words: Greenstones. Petrography. Trace elements. Tectonic setting. Origin. Banat. Romania.

Abstract: The greenstones associated with the anchimetamorphic rock from the Groşi Formation are mostly represented by basic metatuffs. Their age is Lower Carboniferous. The initial tuffs originated in a basaltic magma, resulting from the partial melting of a mantle source. Most rocks - excluding the tuffs contaminated with sedimentary materials - inherited the main characteristics of their parental magma. This magma underwent a weak differentiation process by fractional crystallization. During the basic tuffs sedimentation and their anchimetamorphism, the major and trace element composition was altered, some elements being partially lost. Consequently, on different tectonic setting diagrams the greenstones plot in various fields, depending on the trace elements used and on the alteration degree of their composition. But most rock characteristics show a tholeiitic parental magma of within-plate type.

Introduction

The presence of some very low-metamorphosed crystalline schists in the basement of the Groşi-Tisa region, in the NE of Banat, was pointed out by Papiu (1949, unpubl. rep.) and Savu (1957, unpubl. rep.). In 1965 S. Peltz and M. Peltz described such schists between the Tisa and Ioneasca Valley. Later on, Peltz et al. (1970) reported similar rock from the Groşi-Bulza area. In both cases they also remarked the presence of some low-metamorphosed basic rocks. Savu et al. (1992 a) showed that these metamorphic rocks thrust over the Mesozoic unmetamorphosed formations of the Mureş Zone (Mureş Ophiolitic Suture) and named the resulting nappe the "Tisa Unit". They also mentioned strong mylonitizations along the thrust plane. In 1996 Savu et al. considered these crystalline schists as an anchimetamorphic volcano-sedimentary formation. In contrast with them, Dinică et al. (1996) supposed these crystalline schists as resulting from the Barremian-Aptian sedimentary deposits of the Mureş Zone, mylonitized along a shear zone.

Occurrences, Tectonics and Rocks Age

According to Savu et al. (1996), within the Groşi-Tisa region and its extension toward ENE, the following structural levels have been separated: (1) an Austrian infra-structure and (2) a post-Austrian super-structure (Fig. 1).

The infra-structure includes two tectonic units, the thrust relations of which were achieved during the Austrian movements: the Tisa Unit and its 'autochthon' - represented by the Căpalnaş-Techereu Unit, the latter being formed of the Alpine ophiolites and sedimentary deposits (Liassic-Cretaceous) of the Mureş Zone. Most part of the thrust plane is covered by formations belonging to the post-Austrian super-structure, represented by Laramian volcanics (K_2-Pg_1) and Upper Cretaceous and Neogene sedimentary deposits. After the Austrian movements, this area underwent a tectonic uplift and an intense erosion. Therefore, the Laramian volcanics unconformably lie over different stratigraphic terms of the two mentioned tectonic units.

The Tisa Unit extends south of the north-facing thrust plane, between Groşi, Bulza and Tisa (Fig. 1). It consists mainly of the anchimetamorphic rocks of the Groşi Formation which, at Coştei, support the products - especially pillow basalts - of a Triassic bimodal volcanism of within-plate type, associated with unmetamorphosed quartz-sandstones (Savu et al., 1992b). These anchimetamorphic rocks occur from under the super-structure formations in a few

Institutul Geologic al României

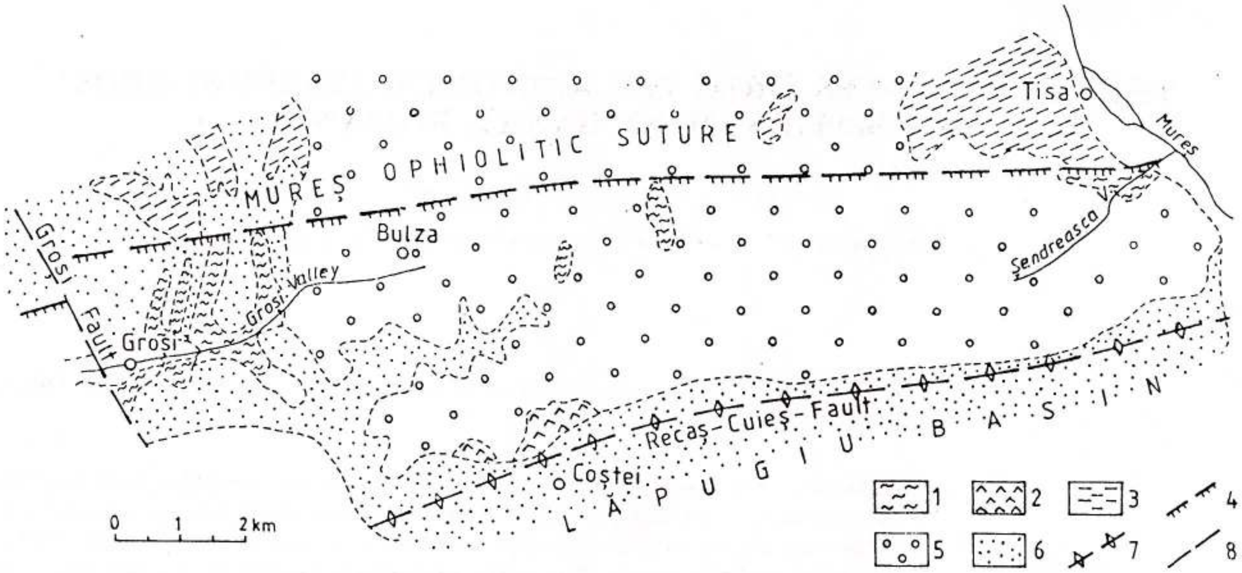

Fig. 1 – Map of the Groşi - Coştei - Tisa region. Infra-structure: 1, Groşi Formation; 2, Coştei Triassic basalts and sandstones; 3, Barremian-Aptian; 4, thrust; super-structure: 5, Laramian (banatitic) continental arc volcanics; 6, Neogene-Quaternary deposits; 7, crustal fault; 8, normal fault.

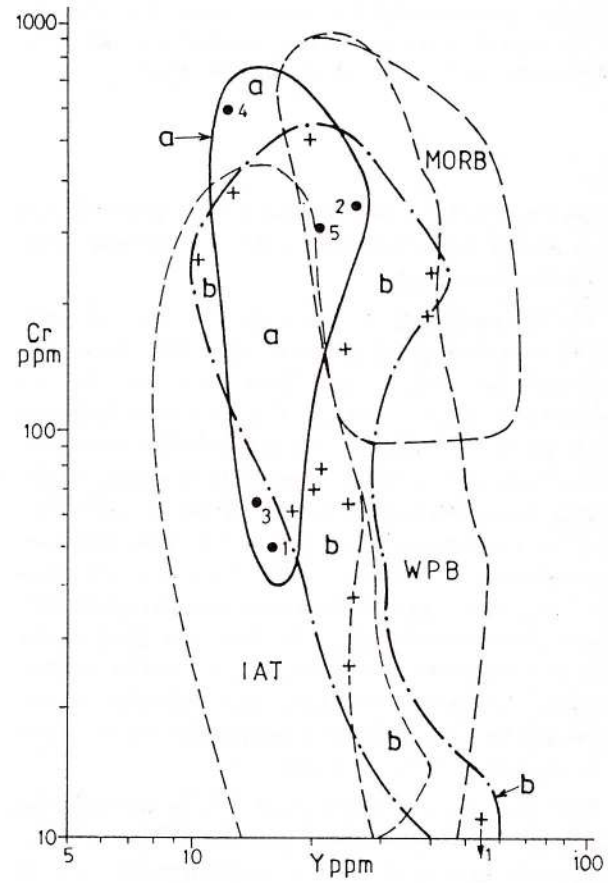

Fig. 2 - Plot of the Groşi greenstones (1-5) and of the Coştei basalts (+) on the Cr-Y diagram. Fields according to Pearce (1980): IAT, volcanic arc basalts; WPB, within-plate basalts; MORB, mid-ocean ridge basalts; a, Groşi greenstones field; b, Coştei basalts field.

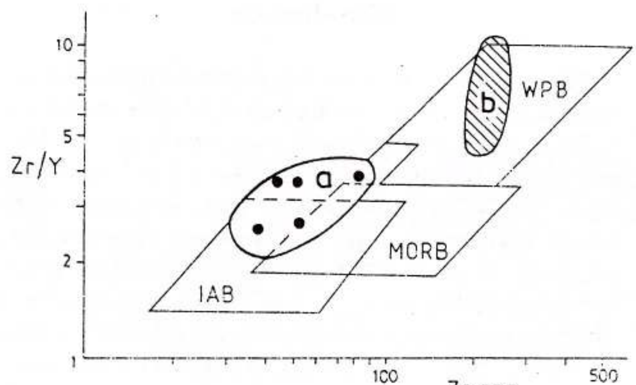

Fig. 3 - Plot of the Groşi greenstones and of the Coştei basalts on the Zr/Y - Zr diagram. Fields according to Pearce and Norry (1979): WPB, within-plate basalts; MORB, mid-ocean ridge basalts; IAB, island arc basalts; a, Groşi greenstones field; b, Coştei basalts field.

inliers, like those of Groşi, Coştei, Bulza, Ioneasca Valley and on the Şendreasca and Moşelu brooks at Tisa (Fig. 1). The rocks, mostly represented by phyllites, are striking N 65^{0}E with a SE dipping of ca 46^0. West of Groşi the phyllites were sectioned and deformed by the NW-SE Groşi fault (Savu, 1995), getting a sheared rock aspect.

Institutul Geologic al României

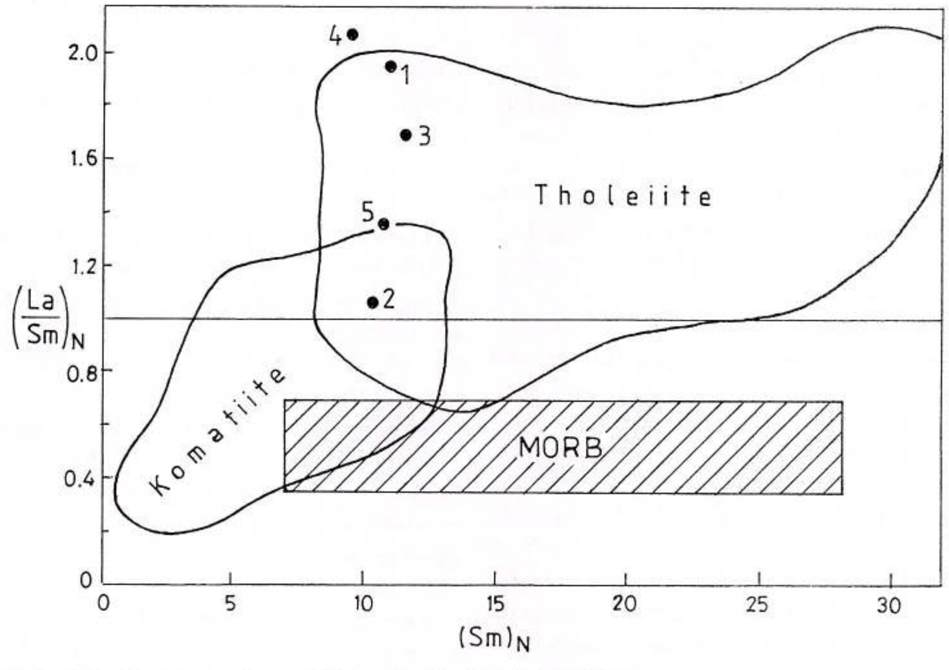

Fig. 4 - Plot of the Groşi greenstones (1-5) on the (La/Sm)N -(Sm)N diagram. Fields according to Jahn et al. (1980).

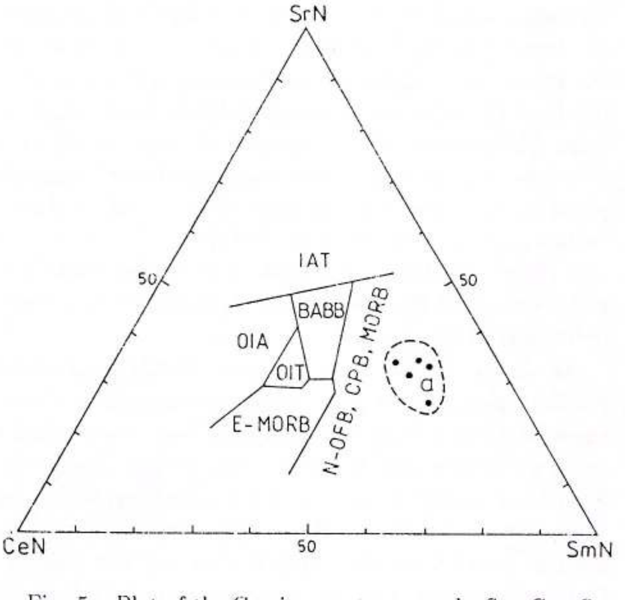

Fig. 5 - Plot of the Groşi greenstones on the Sr - Ce - Sm diagram. Fields according to Ikeda (1990): IAT, island arc tholeiites; OIA, ocean island alkali basalts; OIT, ocean island tholeiites; BABB, back arc basin basalts; N-OFB, 'normal' ocean floor basalts; OPB, ocean plate basalts; MORB, mid-ocean ridge basalts; a, Groşi greenstones field.

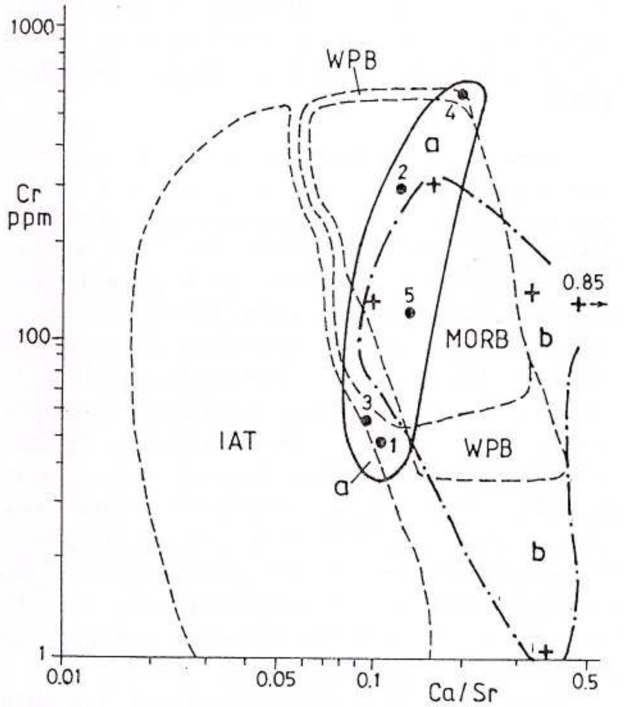

Fig. 6 - Plot of the Groşi greenstones (1-5) and of the Coştei basalts (+) on the Cr - Ce/Sr diagram. Fields according to Pearce (1980): MORB, mid-ocean ridge basalts; WPB, within-plate basalts; IAT, island arc tholeiites; a, Groşi greenstones field; b, Coştei basalts field.

Referring to the age of the Groşi Formation, Papiu (1949) and Savu (1957) considered it as Paleozoic. Peltz and Peltz (1965) attributed these formations even to the Baikalian (Assynthic) cycle. According to Dinică et al. (1996), these anchimetamorphic rocks have resulted from the Barremian-Aptian sedimentary deposits of the Mureş Zone. This cannot

Institutul Geologic al României

be accepted because of the following field evidences: 1. at Coştei the anchimetamorphic rocks support Triassic unmetamorphosed quartz-sandstones and pillowed basalts (Savu et al., 1992b); 2. the Barremian-Aptian deposits from the Mureş Zone, located north of the thrust plane (Fig. 1), are not metamorphosed; 3. the Barremian-Aptian deposits are made up mainly of psamitic rocks, whereas the Groşi Formation consists predominantly of phyllites of pelitic nature; 4. the Barremian-Aptian deposits are never associated with eruptive rocks, neither within the Mureş Zone nor in the Southern Carpathians and Eastern Carpathians, because when they have been sedimented, the island arc volcanism from the Alpine oceans had ended long ago (J_3 -Lower Neocomian), and the Laramian (banatitic) continental arc magmatism (K_2-Pg_1) had not started yet. The igneous rocks, rarely occurring in the Barremian-Aptian from the east part of the Mureş Zone (Trascău Mts), represent in fact exotic blocks of Upper Jurassic island arc volcanics, which are associated with Stramberg limestone olistoliths (Savu, 1990); 5. the anchimetamorphic rocks of Groşi Formation occur as exotic blocks in the Barremian-Aptian deposits, especially within their lower horizon, where they are associated with pebbles of Paleozoic microcline granites (Savu et al., 1996); 6. moreover, olistoliths of the same rocks are to be found in the mélange with pyroclastic matrix of Upper Jurrasic age from the Mureş Zone (Savu, 1994).

According to our opinion, as the Groşi Formation is pre-Triassic in age, it must represent the uppermost sequence of the epimetamorphic crystalline schists pile of the Poiana Ruscă Mts. They are connected with this massif under the Neogene deposits and the Laramian volcanics from the Lăpugiu Basin. (Fig. 2). The radiometric datings of the Poiana Ruscă crystalline schists at 300-340 Ma (Pb/Pb and of 217 ± 5 to 363 ± 23 Ma (K/Ar), which are consistent with the spore-pollen associations, indicate a Devonian-Lower Carboniferous age (Kräutner et al., 1972). It means that their metamorphism took place during the Sudetian movements and they were accidentally resetted by the Alpine orogeny. Towards east the Groşi Formation correlates with the low-metamorphosed schists of the Paleozoic Vărmaga Formation described by Berbeleac (1964).

According to Savu (1983), the Groşi Formation and the Poiana Ruscă crystalline schists belong to the Transylvanian microplate. The Groşi Formation is located on the northwestern margin of the sialic part of this plate, which was partly subducted under the ophiolites and the sedimentary formations of Mureş Zone. During the Austrian movements the Groşi Formation thrust over the Mureş Zone Alpine formation. As shown by the geophysical data (Savu, Andrei, 1993), along the northern margin of the Lăpugiu Basin the Groşi Formation was cut by the Recaş-Cuieş crustal fault (Andrei et al., 1975).

Petrography

The Groşi anchimetamorphic rocks belong to two petrotypes: (1) pelitic phyllites and (2) greenstones. As much as the Groşi Formation outcrops in the mentioned inliers, it occurs like a bedded series, in which the phyllites are prevalent, the greenstones occuring only as interbedded layers. The clastic sequence consists of metapelitic or meta-aleuritic bands, represented by sericite-chlorite phyllites and chlorite quartzites, in which thin bands or lenses of metapsamitic rocks are observed, among which graphitic quartzites or carbonatic rocks occur, locally beside carbonatic quartzites.

The greenstones resulted from basic tuffs. The rocks occuring in more important inliers, like those located east of Groşi, and on the Şendresca Valley at Tisa, are usually formed of clondy albite crystalloblasts, included in a mass of chlorite of pennine or clinochlore type, resulting from volcanic glass. In the groundmass knots of lenticular aspect represent a result of the clinopyroxene crystalloclast transformation. They consist of an aggregate of very fine chlorite lamellae and uralite fibres, associated with minute pistacite granulae. A fine dust of iron and titanium oxides is present in these greenstones. The structure and the mineralogical composition of these rocks are consistent with Ramberg's (1952) and Barth's (1952) definition of greenstones.

As shown by the thin sections, the normal rocks exhibit primary and undeformed metamorphic structures, determined by the prograde very low regional metamorphism (see Winkler, 1967). But along the Tisa Unit thrust plane, the anchimetamorphic rocks have been mylonitized. Because the thrust plane was almost parallel to the phyllites strike, but disconformable to their primary stratification and foliation, these rocks have been refolded and a S_2 plane was supperposed over their initial structure. Such examples are to be observed on the Moşelu and Ioneasca valleys. Similar structures were formed along the Groşi transversal fault, upon which Dinică et al. (1996) insisted.

Geochemical Data and Tentatives to Determine the Rocks Tectonic Setting by Trace Element Analysis

As the major element analyses were missing, the greenstones geochemistry relied only on the trace ele-

Institutul Geologic al României

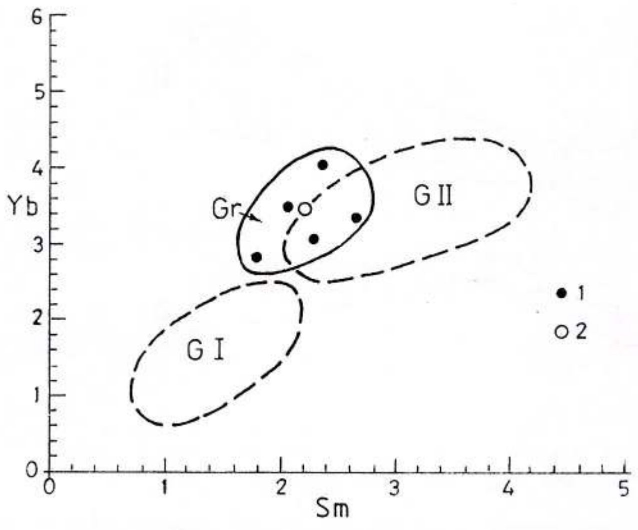

Fig. 7 – Plot of the Groşi greenstones (1) and of their average content (2) on the Yb-Sm diagram. Fields according to Kim and Iacobi (1996): GI and GII are the two basic rock groups from the Hawley Formation. Gr, Groşi greenstones field.

ment data (Tabs. 1 and 2), the averages of which were compared with the averages from the Triassic Coştei basalts and with those from the continental crust.

The high enough Ni and Cr average contents in the Groşi greenstones indicate rather basic rocks, resulting from a primitive and less fractionated magma. These contents, as well as the Ni/Co average value (Tab. 3), are close to those from the Coştei basalts. The Ni average is lower than that in continental crust. The Cr average content is more than two times higher than that in the Coştei basalts, but the Co average content is a little lower than that in the other two petrological units in Table 1. Likewise, the V average content is lower than that in the Coştei basalts, while the Sc average content is almost equal to it and very close to that in the continental crust. It is to note that the V/Zr average value in the Groşi greenstones (Tab. 3) is lower than the value of this ratio in the Finland greenstones (Jahn et al., 1980). A small difference was noticed between the Y average content (17.4 ppm) in the Groşi greenstones and that of 25 ppm in the Groşi basalts. In fact, both values are a little lower than the Y average content in within-plate basalts (Pearce, Cann, 1973).

The Zr average content in the Groşi greenstones is more than three times lower than that in the Coştei basalts and almost two times lower than that in the continental crust (Tab. 1). But it has almost the same value as its average content in continental basalts (Pearce, Cann, 1973). The Zr/Y average value (Tab. 3) is close to that in the Finland tholeiitic greenstones (Jahn et al., 1980). According to the Cr and Y values the Groşi greenstones plot within the island arc basalts (Fig. 2). It is worth noting that a part of the Coştei basalts plot in the same area. On the Zr/Y - Zr diagram (Fig. 3) the Groşi greenstones lie in an intermediate position between the WPB, MORB and IAB fields, while the Coştei basalts occupy their normal place.

The Sr average content of 232 ppm in the Groşi greenstones is higher than that in the Coştei basalts (137.5 ppm) and close to that of 260 ppm in the continental crust. In comparison with other continental basalts, this content is generally lower, excepting that of 187 ppm from the Indian within-plate basalts (Pearce, Cann, 1973).

Cu is lower in the Groşi greenstones than in the Coştei basalts. The Pb and Ga average contents are in the first rocks roughly higher than in the second. In comparison with the Pb and Cu average contents from the continental crust (Tab. 1), the value of 18 ppm Pb in the Groşi greenstones is more than two times higher and that of 33.3 ppm Cu is more than two times lower.

The average $\sum$ REE of 47.35 ppm, (Tab. 3) in the Groşi greenstones is a little higher than that of 35.90 ppm from the Coştei basalts. The LREE/HREE average value of 7.75 in the first rocks is also higher than the average value (4.35) of this ratio in the second rocks (Savu et al., 1992 a).

The La average content of 5.74 ppm in the Groşi greenstones (Tab. 2) is lower than that of 9.33 ppm in the Coştei basalts and than that of 16 ppm La in the continental crust. The $(La/Yb)_N$ average value (Tab. 3) is close enough to that from the Coştei basalts, but the $(La/Ce)_N$ average value is three times lower than that in these basalts. The $(La/Sm)_N$ average value is close to that in the Coştei basalts.

The Sm average content of 2.26 ppm in the Groşi greenstones is lower than that of 3.17 ppm from the Coştei basalts and than that of 3.5 ppm in the continental crust. The Eu/Sm average value of 0.47 (Tab. 3) lies between the values of the continental tholeiites (0.16-0.55) established by Cullers and Graf (1984), which indicates the affiliation of the Groşi greenstones to this petrographic type. It is to note that, the La/Ta average value of 4.23 (Tab. 3) is lower than those of different basic rock types from ocean basins presented by Saunders (1984). The $(La/Sm)_N$ - $(Sm)_N$ diagram (Fig. 4) shows the tholeiitic character of the Groşi greenstones, that correlates quite well with their general composition. Consequently, on the Sr-Ce-Sm diagram (Fig. 5) these rocks plot within a restricted field located in the OPB domain.

Institutul Geologic al României

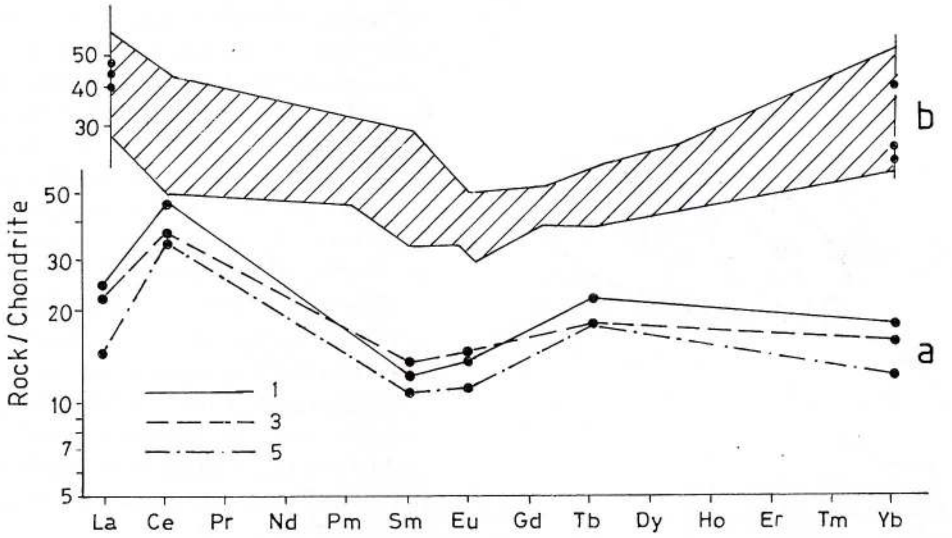

Fig. 8 – Chondrite-normalized patterns of the Groşi greenstones (a) and of the Coştei basalts (b); 1 - 5 represent the samples in the Table 1.

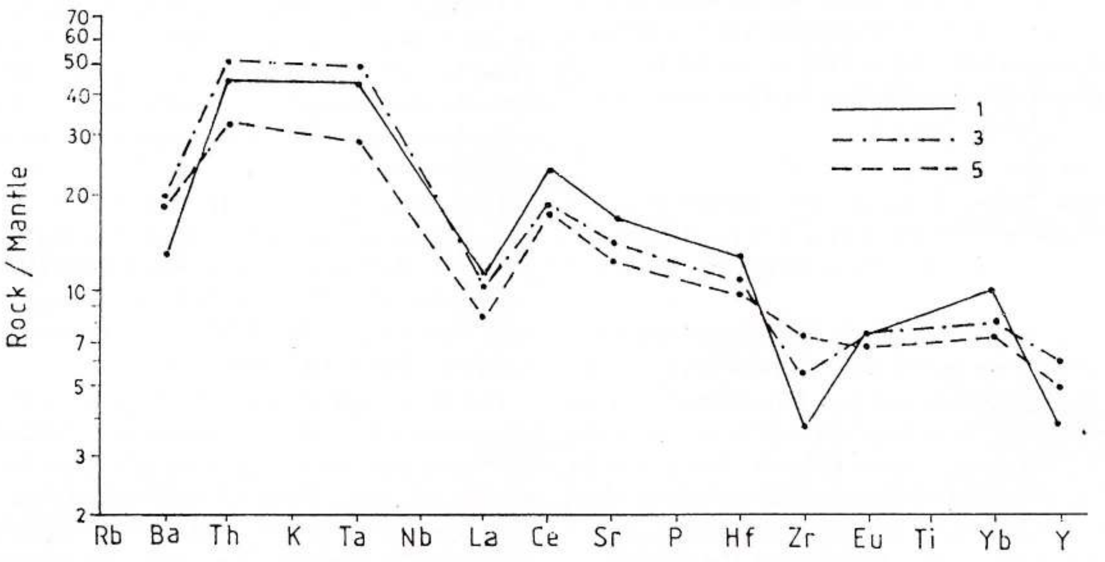

Fig. 9 – Spinder diagram for the Groşi greenstones; 1 - 5 represent the samples in Table 1.

The Ce average content of 33.2 ppm in the Groşi greenstones is almost two times higher than that from the Coştei basalts and is tantamount to the Ce average content of 33 ppm in the continental crust. The (Ce/Sm)N and (Ce/Yb)N average values are higher than those in the Coştei basalts (Tab. 3). The last value shows an enrichment of greenstones in LREE, especially in Ce and a depletion in HREE. It is interesting that the (Ce/Yb)N average value of 2.5 in the Groşi greenstones lies between the values of 0.3 and 3.4 of the same ratio established by Hart et al. (1973) and O'Nions et al. (1976) in volcanic basic rocks from Iceland. On the Cr-Ce/Sr diagram in Figure 6, both Groşi greenstones and Coştei basalts plot in the WPB (+ MORB) field.

The Eu average content in the Groşi greenstones is close to that from the Coştei basalts (Tab. 2) as well as to that in the continental crust. In comparison with the Tb average content of 0.60 ppm in the continental crust and of 0.70 ppm in the Coştei basalts, that of 0.95 ppm in the Groşi greenstones is higher. On the contrary, the Yb average content of 3.42 ppm in the Groşi greenstones is lower than that in the Coştei basalts, but a little higher than that of 2.2 ppm from the continental crust. On the Yb-Sm diagram (Fig. 7) the Groşi rocks are close to the Group II amphibolites from the Paleozoic Hawley Formation in Massachusetts, investigated by Kim and Iacobi (1996).

Institutul Geologic al României

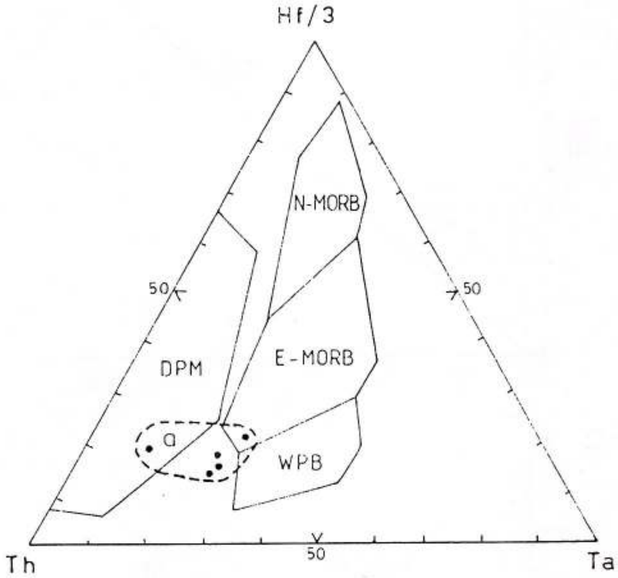

Fig. 10 - Plot of Groşi greenstones on the Hf/3 - Th - Ta diagram. Fields according to Wood et al. (1979): DPM, destructive plate margin; WPB, within-plate basalts; N-MORB, 'normal' mid-ocean ridge basalts; E-MORB, 'anomalous' mid-ocean ridge basalts; a, Groşi greenstones field.

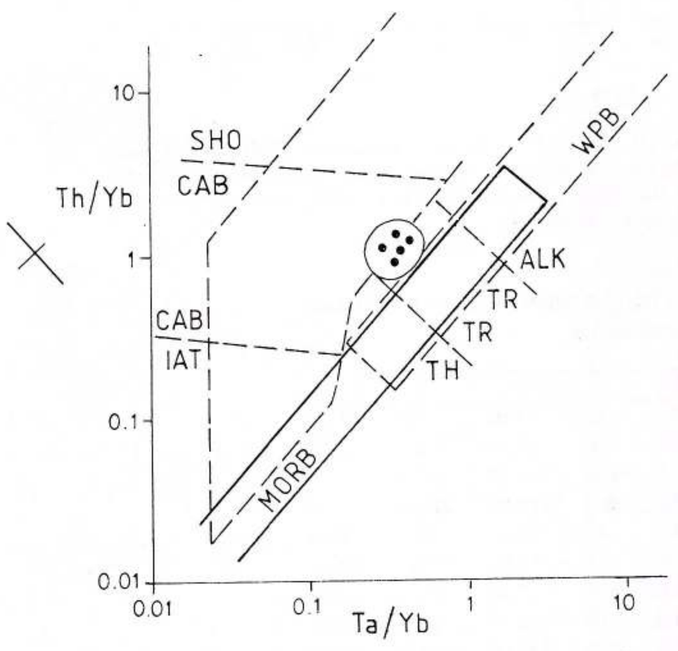

Fig. 11 - Plot of the Groşi greenstones on the Th/Yb - Ta/Yb diagram. Fields according to Pearce (1982): SHO, shoshonites; CAB, calc-alkaline basalts; IAT, island arc tholeiites; WPB. within-plate basalts; ALK, alkaline; TR, transitional; TH, tholeiitic; MORB, mid-ocean ridge basalts; a, Groşi greenstones field.

The REE chondrite-normalized patterns (Fig. 8) of the Groşi greenstones, showing strong negative Sm and Eu anomalies, are almost similar to the pattern depleted in LREE presented by Cullers and Graf (1984) for continental basalts. These anomalies seem to indicate both an inheritance from the partial melting of basic parental magma and a process of a certain fractional crystallization of this magma (Philpotts, Schnetzler, 1968). The diagram in Figure 9 shows, according to Cullers and Graf (1984), that this differentiation led to an enrichment of magma in Th, K and Ta as well as in Ce, and to a depletion in La and heavy elements, with a strong Zr and Y decrease. The pattern set reminds us of the models presented by Condie (1976) for the Archean greenstones.

The Hf and Ta average contents (Tab. 2) in the Groşi greenstones are almost similar to those from the Coştei basalts and from the continental crust. On the Hf-Th-Ta diagram (Fig. 10) the Groşi greenstones plot in a field placed between the WPB, DPM and MORB fields. The Th average content of 3.34 ppm in the Groşi greenstones is very close to that of 3.5 ppm from the continental crust. On the Th/Yb - Ta/Yb diagram (Fig. 11) the Groşi greenstones occur in a restricted field situated within the transition zone between the WPB and MORB array and the field of calc-alkaline basalts.

Behaviour of Trace Elements during the Greenstones Genesis

As shown in the previous chapter, on the numerous tectonic setting diagrams, the Groşi greenstones plot in different fields, depending on the trace elements taken into consideration, as follows: within the IAV field or nearby it when Y, Cr and Zr were used (Figs. 2 and 3), in an intermediate position between DPM (CAB), WPB and MORB (E-MORB) fields when Hf, Th, Ta and Yb were used (Figs. 10 and 11), and within the WPB (+MORB) field when Cr, Ce Sr and Sm were used (Figs. 5 and 6). It is in contrast with the behaviour of the trace elements in igneous rocks - other than tuffs (meta-tuffs) - which usually plot in the same field on various tectonic setting diagrams.

For the same purpose, the very mobile Sr and the imobile Hf, Sm and Y reported to Zr fromt he Groşi greenstones were compared (Fig. 12) with the same elements determined in the meta-basic rocks from the Hawley Formation (see Kim and Iacobi, 1996). It resulted that, in both basic rock series Sr presented an aleatory distribution (Fig. 12 A), indicating the influence of the post-emplacement processes on its behaviour.

On other diagrams (Fig. 12 B, C, D), while the Hawley Formation rocks plot along linear trends, showing a direct correlation with Zr - a character inherited from the basic parental magma - the Groşi greenstones plot in fields placed either on these linear trends or nearby them, marking again an alteration

Institutul Geologic al României

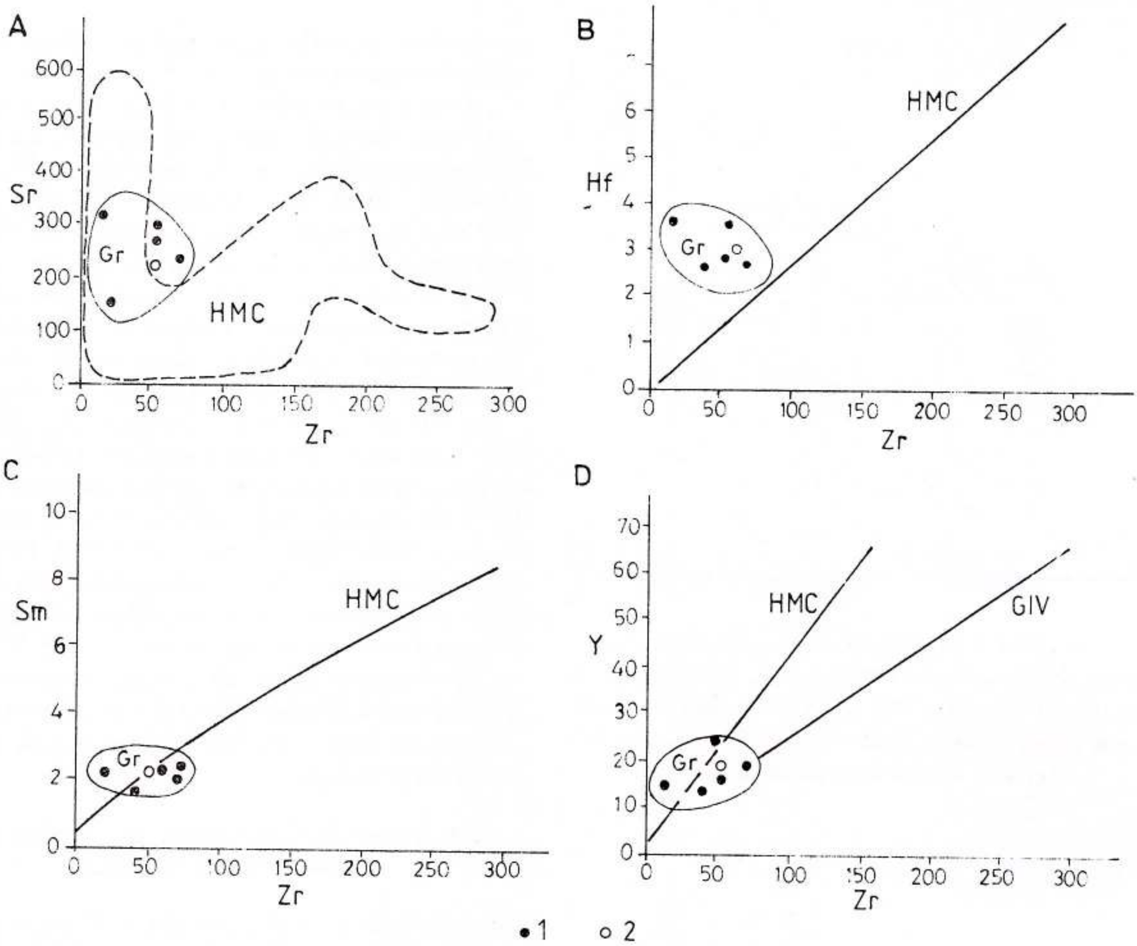

Fig. 12 – Plot of the Groşi greenstones (Gr) on the Sr, Hf, Sm and Y versus Zr diagrams. HMC indicate the aleatory distribution of Sr and the linear correlation of the other elements in the meta-basic rocks from the Hawley Formation, according to Kim and Iacobi (1996); GIV are the CMIS (Group IV) rocks from the same formation; 1, Groşi greenstones; 2, Groşi greenstones average.

Table 1
Distribution of trace elements in the basic rocks and in the continental crust

	1	2	3	4	5	6	7	8
Nippm	20.0	82	21	100.0	42	53.00	68.0	105.0
Co	16.0	34	20	24.0	30	24.80	32.0	29.0
Cr	50.0	320	60	600.0	130	232.00	97.5	–
V	170.0	210	230	180.0	300	218.00	278.3	–
Sc	30.0	36	29	30.0	40	33.00	32.5	30.0
Zr	38.0	57	54	44.0	72	53.00	174.4	100.0
Y	15.0	24	16	13.0	19	17.40	25.0	20.0
Ba	80.0	82	115	95.0	110	96.40	29.5	250.0
Sr	320.0	290	270	150.0	230	232.00	137.5	260.0
Pb	29.0	20	16	7.0	18	18.00	2.8	8.0
Cu	110.0	9	21	8.5	18	33.30	55.0	75.0
Ga	15.0	19	20	14.0	14	16.40	11.5	–
Sn	6.5	<2	<2	<2.0	<2	-	-	2.5

1-5, Groşi greenstones contents determined by emission spectrography; 6, Groşi greenstones average; 7, Coştei basalts average (according to Savu et al., 1992 b); 8, Continental crust average (according to Taylor and McLennan, 1985; Hofmann, 1988). Nb <10 ppm.

Institutul Geologic al României

Table 2
Distribution of REE, Hf, Ta and Th in the basic rocks and in the continental crust

	1	2	3	4	5	6	7	8
La ppm.	7.30	3.10	7.20	6.20	4.90	5.74	9.33	16.00
Ce	39.00	38.00	31.00	27.00	31.00	33.20	16.67	33.00
Sm	2.40	2.10	2.70	1.80	2.30	2.26	3.17	3.50
Eu	1.04	1.01	1.05	0.75	0.84	0.94	0.73	1.10
Tb	1.05	1.02	0.93	0.77	0.97	0.95	0.70	0.60
Yb	4.10	3.60	3.40	2.90	3.10	3.42	5.30	2.20
Hf	3.50	3.60	2.90	2.60	2.80	3.00	2.93	3.00
Ta	1.60	1.50	1.60	1.20	1.00	1.38	1.33	1.00
Th	3.90	2.90	4.10	3.00	2.80	3.34		3.50

1-5, Groşi greenstones contents determined by the neutron activation analysis; 6, Groşi greenstones average; 7: Coştei basalts average (according to Savu et al., 1992 b); 8, Continental crust average (according to Taylor and McLennan, 1985; Hofmann, 1988).

Table 3
The values of some trace element ratios from the Groşi greenstones and the Coştei basalts

	1	2	3	4	5	6	7
Ni/Co	1.25	2.41	1.05	4.16	1.40	2.05	2.14
V/Zr	4.47	3.68	4.26	4.09	4.16	4.13	–
Zr/Y	2.53	2.37	3.37	3.38	3.78	3.08	8.11
La/Ba	0.09	0.03	0.06	0.06	0.04	0.06	0.31
Eu/Sm	0.43	0.48	0.38	0.69	0.36	0.47	0.61
La/Ta	4.56	2.06	4.50	5.16	4.90	4.23	
(La/Yb)N	1.20	0.58	1.42	1.41	1.06	1.14	1.18
(La/Ce)N	0.48	0.21	0.60	0.59	0.41	0.46	1.45
(La/Sm)N	1.91	0.92	1.67	2.16	1.34	1.60	1.85
(Ce/Sm)N	3.92	4.36	2.77	3.62	3.25	3.58	1.27
(Ce/Yb)N	2.46	2.72	2.35	2.40	2.58	2.50	0.81
Σ REE	54.89	48.83	46.28	39.42	47.35	47.35	35.90
LREE/HREE	7.86	7.67	7.60	8.49	7.90	7.75	4.33

1-5, Groşi greenstones; 6, Groşi greenstones average; 7, Coştei basalts average.

of the initial (magmatic) proportion, even between the imobile elements. This alteration of the Groşi rocks, with some major and trace element-loss, could have been favoured by the ash structure of the volcanic tuffs, from which the greenstones resulted, because it is very permeable to the alteration agents.

The rocks alteration occurred in two circumstances: (1) during the tuffs sedimentation in the sea water and (2) during the rocks metamorphism. In the first case the volcanic ash reactioned with the salted sea water, getting more or less altered and losing some chemical elements. In the second case, the change in the trace element composition was determined by the transformation of volcanic ash and of the rare crystalloclasts (plagioclase, clinopyroxene) into metamorphic minerals. During this process, from the magmatic high-temperature minerals network and from the volcanic glass Ca, Mg, Fe and their covalent trace elements have been released. A part of them entered the low-temperature mineral network and another part was transported out by metamorphic solutions, depending especially on the CO_2 concentration.

Conclusions

The Groşi greenstones are basic volcanic rocks interbedded with the clastic anchimetamorphic schists of the Groşi Formation, the age of which is Lower Carboniferous. They resulted predominantly from basic tuffs. These rocks that inherited most of the parental tholeiitic magma characteristics, were formed by partial melting of a mantle source and underwent a weak differentiation process by fractional crystallization. The basic rocks, together with their host rocks, have been influenced by a very low regional metamorphism (anchimetamorphism), under chlorite isograde conditions. During the sedimentation and metamorphism of these tuffs the major

Institutul Geologic al României

and trace element composition was altered, so that on various tectonic setting diagrams the greenstones plot in different fields. The Groşi greenstones are coeval with the basic component of the Devonian-Lower Carboniferous bimodal volcanics associated with the epimetamorphic crystalline schists from the Poiana Ruscă Mts and with the Sillurian-Lower Carboniferous greenstones ('metabasalts') from the Highiş-Drocea Mts, which are mostly within-plate basic metatuffs, too.

References

Andrei, J., Calotă C., Scurtu F. (1975) Considérations structurales sur le sillon ophiolitique des Monts Métalifères à l'aide des données géophysiques et des certains éléments quantitatifs obtyenues grâce au modelage. *Rev. roum. géol., géophys., géogr.*, 19, p. 101-111, Bucureşti.

Barth, T.F.W (1952) *Theoretical Petrology*, 378 p., New York.

Berbeleac, I. (1964) Cercetări geologice şi petrografice în cristalinul insulei Rapolt (Boi-Rapolt-Raporţel). *D. S. Inst. Geol.*, XLIX/1, p. 3-14, Bucureşti.

Condie, K. C. (1976) Trace-element geochemistry of Archean greenstone belts. *Earth Science Rev.*, 12, p. 393-417, Amsterdam.

Cullers, R. L., Graf, J. L. (1984) Rare earth elements in igneous rocks of the continental crust: predominantly basic and ultrabasic. In P. Henderson (Edit.). Rare Earth Element Geochemistry, Elsevier, p. 237-274, Amsterdam.

Dinică, I., Pană, D., Conovici, M., Roşu, E. (1996) Metamorfism dinamic alpin în Zona Mureş. *An. Inst. Geol. Rom.*, 69, p. 207-210, Bucureşti.

Hart, S. R., Schilling, J. G., Powell, J. L. (1973) Basalts from Iceland and along the Reykjanes Ridge: Sr isotope geochemistry. *Nature Phys. Sci.*, 246, p. 104-107.

Hofmann, A. W. (1988) Chemical differentiation of the Earth: the relationship between mantle, continental crust and ocean crust. *Earth Planet. Sci. Lett.*, 90, p. 297-314, Amsterdam.

Jahn, B., Auvray, B., Blais, S., Capdevila, R., Cornichet, J., Vidal, R., Hameurt, J. (1980) Trace element geochemistry and petrogenesis of Finish greenstone belts. *J. Petrol.*, 21, p. 201-244, Oxford.

Kim, J., Iacobi, R. D. (1996) Geochemistry and tectonic implications of Hawley Formation meta-igneous units: Northwestern Massachusetts. *Am. J. Sci.*, 296, p. 1126-1174, New Haven, Conn.

Kräutner, H. G., Mureşan, M., Iliescu, V., Mânzatu, S., Vâjdea, E., Tănăsescu, A., Ioncică, M., Andăr, A., Anastase, Ş. (1972) Devonian-Carboniferul inferior epimetamorfic din Poiana Ruscă. *D. S. Inst. Geol., LIX/4*, p. 5-62, Bucureşti.

Pearce, J. A. (1980) Geochemical evidence for the genesis and eruptive setting of lavas from Tethyan ophiolites. In A. Panayiotou (Edit.). *Proc. Intern. Ophiolite Symp.*, Cyprus, 1979, p. 261-272, Nicosia.

— **(1982)** Trace element characteristics of lavas from destructive plate boundaries. In R.S. Thorpe (Edit.) Andesites, John Wiley , p. 525-517, London.

— **, Cann, J. R. (1973)** Tectonic setting of basic volcanic rocks determined using trace element analysis. *Earth Planet. Sci. Lett.*, 19, p. 290-300, Amsterdam.

— **, Norry, M. J. (1979)** Petrogenetic implications of Ti, Zr, Y and Nb variation in volcanic rocks. *Contrib. Mineral. Petrol.*, 69, p. 33-47, Berlin.

Peltz, S., Peltz, M. (1965) Notă asupra unor iviri de şisturi cristaline în regiunea Tisa-Ioneasca. *D.S. Com. Geol.*, LI/1, p. 109-116, Bucureşti.

— **, Peltz, M., Urcan, T. (1970)** Contribuţii la cunoaşterea vulcanismului neogen din regiunea Groşi-Bulza-Fintoag. *D.S. Inst. Geol.*, LV/1, p. 109-134, Bucureşti.

Philpotts, J. A., Schnetzler, C. C. (1968) Europium anomalies and the genesis of basalts. *Chem. Geol.*, 3, p. 5-13, Amsterdam.

Ramberg, H. (1952) The Origin of Metamorphic and Metasomatic Rocks. Univ. Chicago Press, 317 p., Chicago.

Saunders, A. D. (1984) The rare earth element characteristics of igneous rocks from the ocean basins. In P. Henderson (Edit.) Rare Earth Element Geochemistry. Elsevier, p. 205-236, Amsterdam.

Savu, H. (1983) Geotectonic and magmatic evolution of the Mureş Zona (Apuseni Mountains) - Romania. *An Inst. Geol. Geofiz.*, LXI, p. 253-262, Bucureşti.

— **(1984)** Mélangeul cu matrice piroclastică asociat arcului insular sudic al Zonei Mureş. *St. cerc. geol., geofiz., geogr. (Geol.)*, 29, p. 36-43, Bucureşti.

— **(1990)** Remarks on the Mesozoic magmatic activity in the Trascău Mountains (Mureş Zone). *Rev. roum. Géol., Géophys., Géogr. (Géol.)*, 34, p. 13-24, Bucureşti.

— **(1995)** An attempt to correlate the geological phenomena with the connected South Transylvanian System of Crustal Fractures. Studia Univ. Babeş-Bolyai, *Geologia*, Cluj, XL, 1, p. 127-136.

— **(1996)** Genesis and structure of the Mureş Zone. *An. Inst Geol. Rom.*, 69, p. 179-180 (abstract), Bucureşti.

— **, Andrei, J. (1993)** Source of the Căzăneşti-Ciuiaş gravity anomaly in the Drocea Mountains ophiolites (Mureş Zone) and its metallogenic implications. *Rom. J. Geophysics*, 16, p. 59-66, Bucureşti.

— **, Udrescu, C., Neacşu, V. (1992 a)** Petrology, geochemistry and origin of the Laramian volcanics of the Mureş Couloir, between Zam and Gurasada. *Rom. J. Petrol.*, 75, p. 117-130, Bucureşti.

— **, Udrescu, C., Neacşu, V., Stoian, M. (1992 b)** The Coştei basalts: Products of a pre-Mureş Ocean continental intra-plate volcanism. *Rev. Roum. Géol.*, 36, p. 35-34, Bucureşti.

— **, Udrescu, C., Neacşu, V. (1996)** The ophiolites of the Mureş Couloir between Căpâlnaş and Tisa (Mureş Zone). *Rom. J. Petrol.*, 77, p. 61-70, Bucureşti.

Taylor, S. R., McLennan, S. M. (1985) The continental crust: its composition and evolution. Blackwell, Oxford, 312 p.

Winkler, H. S. F. (1967) Petrogenesis of Metamorphic Rocks. Spring. Verl., 237 p., Berlin.

Institutul Geologic al României

Wood, D. A., Joron, J. L., Treuil, M. (1979) A re-appraisal of the use of trace elements to classify and discriminate between magma series erupted in different tectonic setting. *Earth Planet. Sci Lett.*, 45, p. 326-336, Amsterdam.

Ykeda, Y. (1990) CeN/SrN/SmN: A trace element discriminant for basaltic rocks from different tectonomagmatic environments. *N. Jb. Miner. Mh, H 4*, p. 145-158, Stuttgart.

Received: February 1, 1998
Accepted: February 24, 1998

Institutul Geologic al României

Institutul Geologic al României

PETROGENESIS OF THE CERNA GRANITOIDS (BANAT – SOUTH CARPATHIANS)

N. STAN, I. TIEPAC, C. UDRESCU

Institutul Geologic al României, str. Caransebeş nr. 1, 79678 Bucureşti 32.

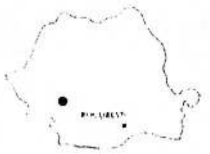

Key words: Peraluminous monzogranites. S-I type. Mantle. Crustal anatexis. Hybrid magmas. Volcanic arc (VAG). Collision (COLG).

Abstract: The Cerna granitoids, weakly peraluminous, with biotite and hornblende, originate, according to the mineralogical, chemical, minor and REE parameters, both in basic melts coming from the mantle or charnokite-granulitic rocks (type I) and in crustal continental melts (type S). The metaluminous basic melts become weakly peraluminous when they are mixed with hydroxilate crustal anatectic magmas and when the fractional crystallization of hornblende and clinopyroxene begins. From the tectonic point of view, the basic melts appeared under conditions of external volcanic arc of plate margin (VAG). Later on the hybrid magmas (mantle + crust) occurred as the granitic volcanic arc was gradually involved in the continent-continent collision process (VAG - COLG). Finally, the Cerna granitoids, weakly peraluminous, were emplaced under late- and post-collision conditions (COLG).

Introduction

The Cerna granitoids, represented by monzogranites, are cropping out in the right slope of the Cerna Valley, north of the Băile Herculane, on a lenght of about 10 km. They are overlain by Mesozoic deposits and are likely to penetrate a pre-Silurian crystalline basement (Fig. 1).

Mineralogical and chemical parameters

Monzogranites are constituted of quartz (15-20 %), oligoclase-andesine, locally zoned (30-40 %), microcline, microcline-perthite (10-15 %), biotite (3-7 %), and hornblende (0-5 %). The femic minerals are frequently opacitized and chloritized. Sphene occurs at the expense of hornblende. Apatite and zircon are rarely found. Muscovite is observed accidentally as a secondary mineral.

The granitoids are locally penetrated by quartziferous diorite-porphyry veins and very rarely by aplites.

The monzogranites are weakly peraluminous: Mol $Al_2O_3/CaO + K_2O + Na_2O$ (ASI) = 1.01 - 1.11 (mean X = 1.08), with normative corundum: 1.13 - 3.34; X=2.16. The colour index is low: 8.62 - 15.53; X=11.50. The SiO_2 values are high, with a narrow variation range: 68.09 - 71.27 %; X=70.10 % (Tables 1 and 2). On the Q-A-P (Fig. 2) and R_1-R_2 (Fig. 3) diagrams the granitoids are situated in the crustal anatexis zone, the "continent-continent collision" field. These parameters are characteristic of the type Sgranites. Other parameters assign the Cerna granites to type I: $Fe^{3+}/Fe^{3+} + Fe^{2+}$ =0.20 - 0.80, X=0.40; Na_2O = 3.78 - 4.17 %; X=4.01 %. The S-I classification is mainly based on the criteria proposed by Chappell and White (1974), Hine et al. (1978), White and Chappell (1983), Pitcher (1982, 1987, 1993).

REE and minor elements

The low values of REE and of the LREE/HREE ratios for the Cerna monzogranites (Table 4) are compatible with the values presented by Cullers and Graf (1984). The REE fractionation is moderate: La/Lu(cn)=6.91-19.82, X=10.38; La/Yb(cn)=8.42-10.24, X=10.71 (Tab. 4). The Eu anomaly, weakly negative, is noticed at four samples; two samples do not have Eu anomalies (Fig. 4). This situation is compatible with the values of the ratios Eu/Sm=0.26-0.40, X=0.32. The reduced REE fractionation is explained by the poorness of the accessory minerals and by the presence of hornblende which can retain HREE to a certain extent. The Eu negative anomaly signifies the involvment of plagioclase in the magmas genesis, either in partial melt processes or in fractional crystallization processes.

Institutul Geologic al României

Table 1
Chemical composition: major elements (%) for the Cerna granitoids (Banat)

Oxides	C_1	C_2	C_4	C_6	C_9	C_{10}	C_{14}	C_{12}
SiO_2	70.70	70.80	70.00	68.09	69.77	71.27	71.20	76.38
TiO_2	0.24	0.36	0.29	0.39	0.48	0.34	0.34	0.00
Al_2O_3	14.30	14.59	14.91	15.77	14.46	14.24	14.37	12.76
Fe_2O_3	0.39	0.96	0.83	2.22	0.85	0.96	1.08	0.77
FeO	1.73	1.39	1.73	0.56	1.58	1.13	1.24	0.00
MnO	0.05	0.07	0.08	0.09	0.07	0.05	0.05	0.03
MgO	0.88	1.14	1.20	0.87	1.37	1.12	1.14	1.17
CaO	2.20	1.14	2.53	1.85	1.65	1.28	1.04	0.74
K_2O	3.15	3.27	3.10	4.40	3.23	3.60	2.32	4.66
Na_2O	4.04	3.95	3.78	4.17	4.08	4.04	5.46	3.70
P_2O_5	0.08	0.13	0.10	0.12	0.09	0.07	0.07	0.00
H_2O^+	1.04	1.55	0.88	1.25	1.23	1.56	1.52	0.56
CO_2	0.80	0.00	0.47	0.00	0.79	0.00	0.00	0.00
Total	99.62	99.62	99.90	99.78	99.65	99.66	99.83	99.77

C_1 ... C_{10}: monzogranites C_{14}; granodiorite porphyry C_{12}; aplites
Analyst: Erna Călinescu

Table 2
Chemical parameters; (m=minimum; M=maximum; X=average)

	m M	X
SiO_2 %	68.09–71.27	70.10
Na_2 %	3.78–4.17	4.01
K_2O %	3.10–4.40	3.45
$Fe^{3+}/(Fe^{3+} + Fe^{2+})$	0.20–0.80	0.40
Mol.$Al_2O_3/CaO+K_2O+Na_2O$	1.014–1.110	1.08
Colour index	8.62–15.53	11.50
corundum norm.	1.13–3.34	2.16

Institutul Geologic al României

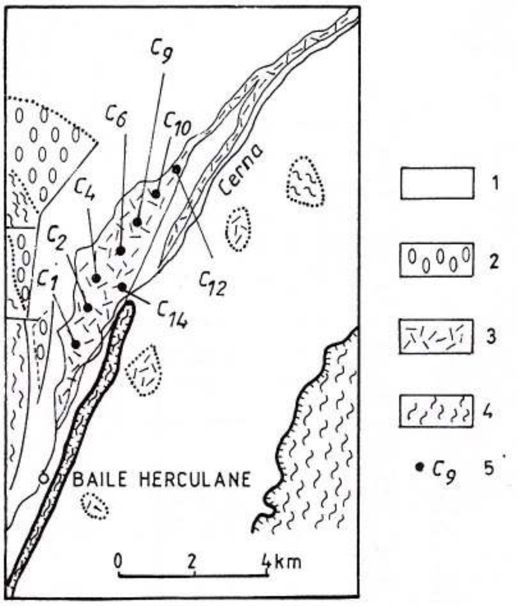

Fig. 1 – Geological sketch with the location of the Cerna granitoid: 1, Mesozoic; 2, Permian; 3, Cerna granitoids; 4, crystalline schists; 5, sample location.

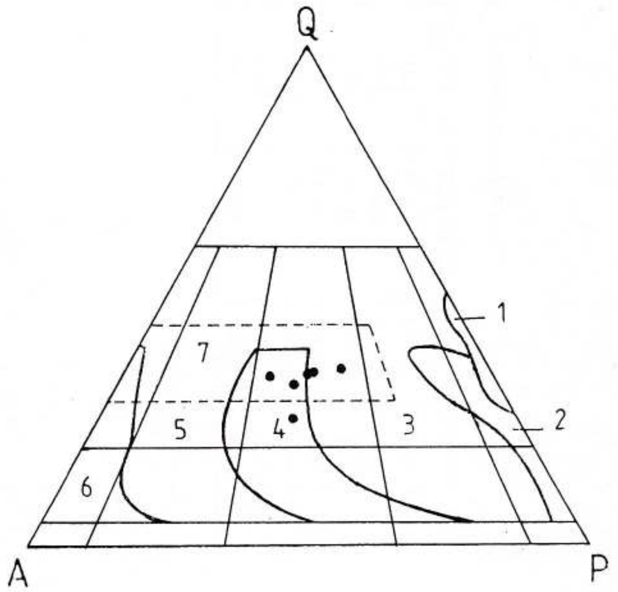

Fig. 2 – Q-A-P diagram (Rittman norm); variation fields of the granitoid series after Lameyre and Bowden (1982); 1, tholeiitic series; 2, trondhjemitic calc-alkaline series (low K): 3, granodioritic calk-alkaline series (medium K); 4, monzo-granitic calc-alkaline series(high K); 5, aluminous granitoids from alkaline provinces; 6, alkaline and peralkaline granitoids; 7, granitoids formed as a result of crustal fusion.

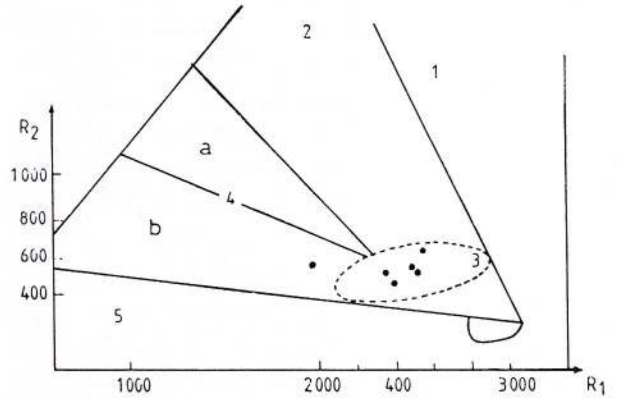

Fig. 3 – R_1-R_2 diagram (de la Roche et al., 1982); field delimited by Batchelor and Bowden (1985) for the tectonic discrimination of the granitoids: 1, ocean ridge granites, fractioned from the mantle (ORG); 2, Andine-type granites, ocean/continent subduction; 3, Hercynian-type granites, continent/continent syncollision; 4, Caledonian-type granites, late orogenic (a) and post-collision (b); 5, anorogenic granites; 6, post-orogenic granites.

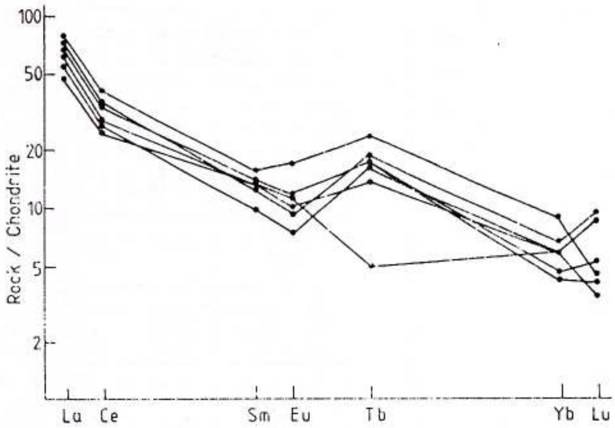

Fig. 4 – Patterns of the chondrite normalized REE from Cerna granitoid.

As compared to the values mentioned by Eby and Kochhar (1990) and Eby et al. (1992) the following ratios of the minor elements in the Cerna granitoids indicate sources from the mantle: Zr/Hf=29.76, Nb/Ta=16.54, Y/Nb=0.85 (average values, Tab. 4). Harker diagrams (Fig. 5) also suggest the origin of the granitoids in the mantle or in basaltic melts because most of the elements taken into account, namely: $Na_2O + K_2O$, Y, Ga, Sc, Sr, partially MgO, show unsignificant variations versus SiO_2. However, TiO_2 and Zr present in comparison with SiO_2 unlinear variations, which indicate crustal-continental

Institutul Geologic al României

Table 3

REE and minor elements contents (ppm) in the Cerna granitoids (Banat)

	La	Ce	Sm	Eu	Tb	Y	Yb	Lu	Zr	Hf	Ta	Nb	Cs	Sc	Rb	Sr	Ba	Cu	Ga	Ni	Co	Cr	V	Th
C1	17.1	22.1	1.9	0.54	0.82	14.0	0.95	0.17	120	2.6	1.2	18.0	6.2	3.3	106	180	860	6.5	15.0	4.5	2.3	10.2	29.0	16.8
C2	15.0	19.6	2.1	0.83	0.77	10.0	0.93	ned.	105	3.1	0.4	11.0	5.2	3.7	82	240	1592	10.0	13.0	5.5	2.7	18.2	32.8	10.6
C4	21.0	22.9	2.7	0.74	0.58	10.0	1.30	0.11	76	3.2	1.0	15.0	4.2	4.5	106	240	693	9.5	19.0	4.5	3.7	23.5	28.0	16.3
C6	23.5	33.0	3.1	1.25	1.18	13.0	1.90	0.14	145	3.6	0.8	20.0	8.6	4.2	144	280	2770	18.0	12.0	3.5	2.1	15.6	50.0	16.9
C9	19.6	26.9	2.6	0.81	0.22	10.0	1.20	0.28	50	3.8	1.1	10.0	5.7	5.6	146	170	640	16.0	11.5	5.0	4.3	19.6	26.0	17.1
C10	20.6	28.7	2.7	0.69	0.92	11.0	1.30	0.31	75	3.5	1.3	10.0	5.5	4.7	175	160	634	14.0	15.0	4.0	3.3	16.6	23.0	21.3
C14	16.6	29.3	1.9	0.78	0.89	10.0	1.10	0.14	85	3.5	1.2	10.0	4.8	0.5	104	10	562	7.0	16.0	4.0	3.9	21.1	26.0	19.6
C12	9.7	15.8	2.2	0.34	1.04	10.0	1.40	0.21	32	2.8	1.2	10.0	4.3	1.0	220	40	236	11.0	11.0	3.0	0.8	18.0	3.0	42.6

Analysts: I. Tiepac and C. Udrescu

Table 4

Characteristic ratios of same REE and minor elements (ppm)

	La/Lu(cn	La/Yb(cn)	Ce/Yb(cn)	Eu/Sm	$\sum$REE	LREE/HREE	Zr/Hf	Nb/Ta	Y/Nb
C1	10.59	12.24	6.0	0.28	43.67	21.24	46.15	15.00	0.77
C2	0.00	10.97	5.50	0.40	39.23	21.58	33.87	27.50	0.91
C4	19.82	10.87	4.56	0.27	49.33	23.30	23.75	15.00	0.67
C6	17.62	8.42	4.53	0.40	64.07	18.51	40.27	25.00	0.65
C9	7.34	11.09	5.82	0.31	51.61	28.88	13.15	9.09	1.00
C10	6.91	10.71	5.73	0.26	55.22	21.83	21.42	7.69	1.10
X	10.38	10.71	5.36	0.32	50.52	22.56	29.76	16.54	0.85

X: mean values

Institutul Geologic al României

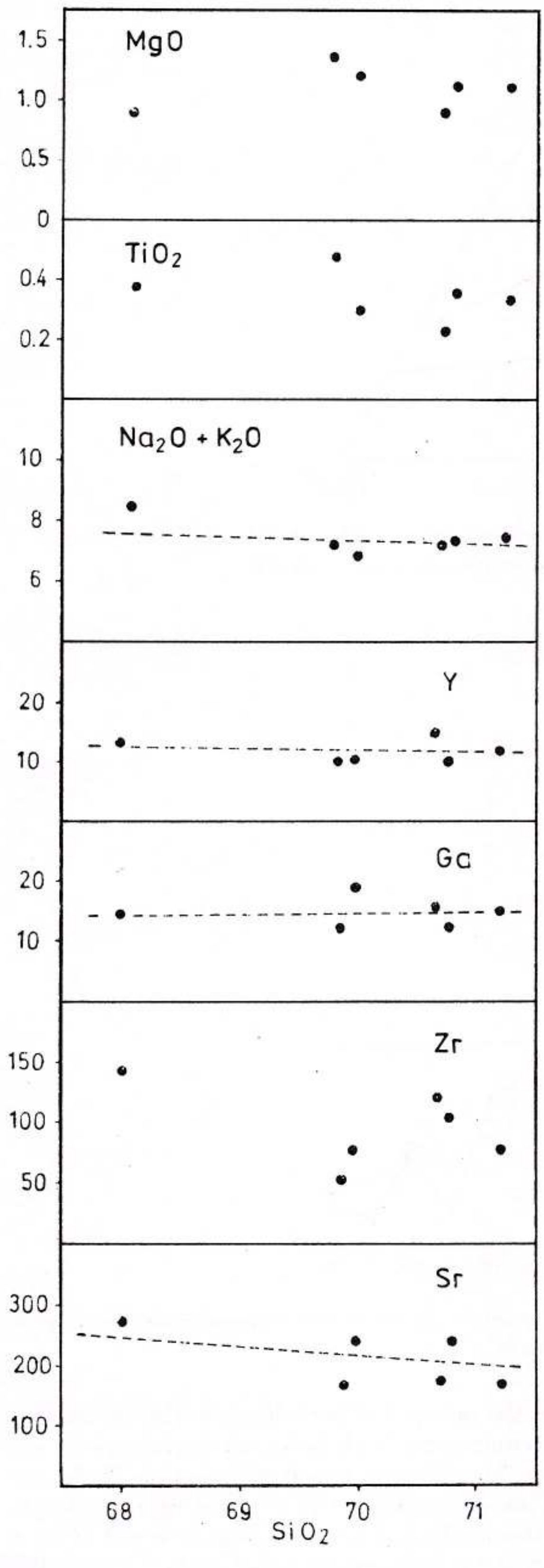

Fig. 5 - SiO_2-MgO, TiO_2, Na_2O+K_2O (%) and Y, Ga, Zr, Sr (ppm) diagram.

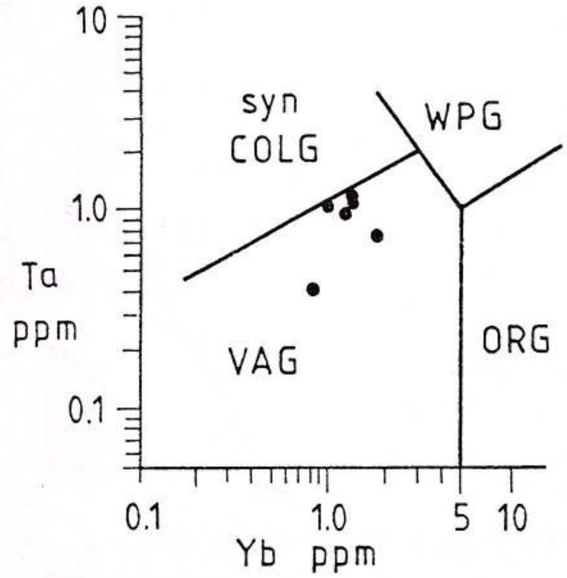

Fig. 6 - Ta-Yb diagram (Pearce et al., 1984): Syn-COLG: collision granites; WPG: within plate granites; VAG: volcanic arc granites; ORG: ocean ridge granites.

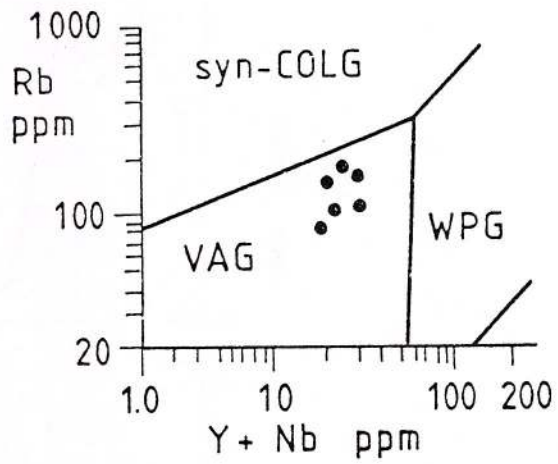

Fig. 7 - Rb-(Y+Nb) diagram (Pearce et al., 1984). See legend to Fig. 6.

sources.

On the Ta-Yb and Rb-(Y+Nb) diagrams, for the tectonic discrimination of the granitoids (Figs. 6, 7), the analyses plot in the VAG field and on the Rb/30-Hf-Ta x 3 diagram (Fig. 8) four samples plot in the field of late or post-collision rocks and two samples in the VAG field. The contour of the diagram "ORG normalized geochemical patterns" (Fig. 9) for the Cerna granitoids is quite similar to the contour of the diagram of the post-collision gra-

Institutul Geologic al României

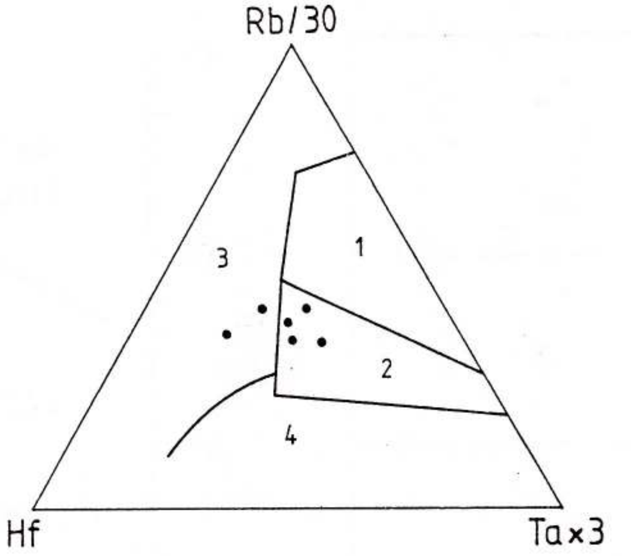

Fig. 8 – Rb/30–Hf–Ta x 3 diagram (Harris et al., 1986); 1, syncollision granites (COLG); 2, late and post-collision granites; 3, volcanic arc granites (VAG); 4, within plate granites (WPG).

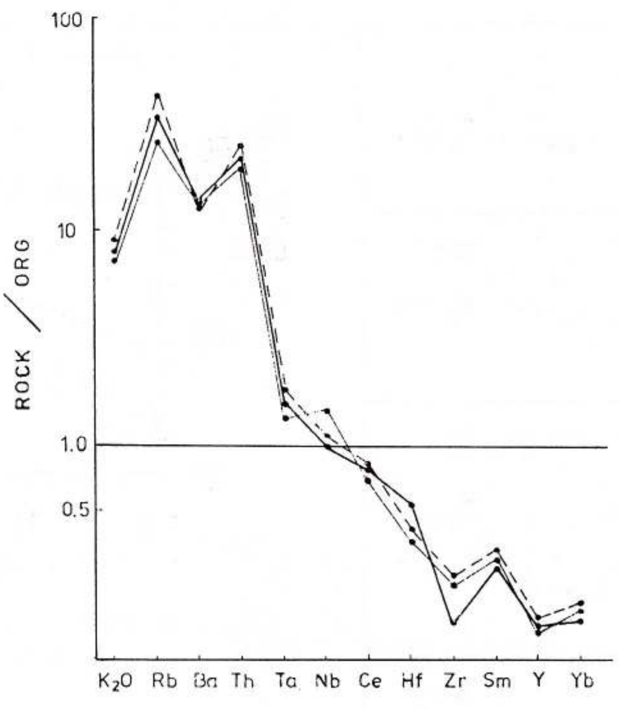

Fig. 9 – ORG normalized geochemical patterns diagram in Cerna granitoid (A), versus post-colisional granitoids (B, after Pearce et al., 1984).

nitoids drawn up by Pearce et al. (1984).

Data interpretation; discussions

The geochemical, mineralogical and tectonic parameters show that the Cerna granitoids belong partly to type I and partly to type S. A petrogenetic modelling in a tectonic setting is starting from the weakly peraluminous character of the granitoids and from the presence of hornblende in the mineralogical composition. Such rocks can originate, in a first phase, from the partial melt of the mantle (Balakrishnan and Rajamani, 1987) or of the charnockite-granulite-amphibolite (lower lithosphere at a P of about 5 Kb and a temperature below 1,000 ^{0}C, Sarvathaman and Leelanandam, 1992). The fractionation of hornblende and of clinopyroxene under almost anhydrous conditions from the basic protomagma leads

Institutul Geologic al României

to the alumina saturation of the extracted liquid which becomes tonalitic-metaluminous (Balakrishnan and Rajamani, 1987). Such magmas frequently occur within a tectonic setting of plate margin volcanic arc (Pitcher, 1982, 1987, 1993). The ascent of the tonalitic magmas concomitantly with the thickening, sinking and melting of the continental crust leads to the formation of the hybrid magmas. The water extracted from the crust by the dissociation of the hydroxilate minerals plays a decisive part in the evolution of the melts. In the hybrid magmas (basic melts + continental crust) the fractional crystallization (involving of plagioclase in the process, biotite and hornblende crystallization) begins to work. This process of fractional crystallization is supported by the Eu negative anomaly from the Cerna granitoids.

ASI units of the magmas are changed both by the presence of water (Ellis and Thompson, 1986) and by the fractional crystallization (Abbot, 1981). The higher the water quantity is, the greater the contribution of the crust, and consequently ASI>1 and the liquid becomes peraluminous. If the water quantity is small the mantle influence is higher, that is ASI<1, therefore the liquid remains metaluminous. On the other hand the fractional crystallization of hornblende and clinopyroxene from metaluminous magmas determines its evolution toward peraluminous melts. Metaluminous sources for weakly peraluminous granites have been mentioned by Anderson (1983) and Sarvathaman and Leelanandam (1992) for some granitoids from America and India, respectively.

From the tectonic point of view, the external volcanic arc of plate margin is gradually involved in time in a continent-continent collision process (VAG–COLG). The subsequent continent-continent collision determines the appearances of major faults in the upper crust, already regionally metamorphosed. On these major dislocations the magmas, mostly crystallized and defined from the petrochemical point of view, are collected and settled under late or post-collisional tectonic conditions (COLG).

Finally, the Cerna granitoids display type S characters with geochemical features specific to type I, the latter inherited from the mantle protomagmas. The zircon crystals from the Cerna granitoids also come from two sources, mantle and crust (Robu, Robu, 1992).

In the last phase of the granitoid magma, solidification took place in a weakly hydrated environment (lack of pegmatites) and at the same time oxidating (the femic minerals are strongly opacitized, impregnated with iron oxides, and pink-coloured potassic feldspars are frequently found).

This petrogenetic model (MASH - proposed by Hildreth and Moorbath in 1988) is also supported by the metaluminous-peraluminous characters of the Culmea Cernei granitoids represented by tonalites, granodiorites and monzogranites (Iancu et al., 1994), situated to the north, within the same geo-tectonic setting as the Cerna monzogranites. The metaluminous granitoids (tonalites and granodiorites) could represent the source of the weakly peraluminous monzogranites.

References

Abbot, R. N. Jr. (1981) AFM liquidus projections for granitic magmas, with special reference to hornblende, biotite and garnet. *Can. Mineral.* 19, p. 103-110.

Anderson, J. L. (1983) Proterozoic anorogenic granite plutonism of America. *Geol. Soc. Amer. Mem.* 161, p. 133-154.

Balakrishnan, S. and Rajamani, V. (1987) Geochemistry and petrogenesis of granitoids around the Kolar Schist Belt, South India: Constraints for the evolution of the crust in the Kolar area. *Jour. Geol.* 95, p. 219-240.

Batchelor, R. A., Bowden, P. (1985) Petrogenetic interpretation of granitoid rock series using multicationic parameters. *Chem. Geol.*, 48, p. 43-55.

Chappell, B. W., White, A. J. R. (1974) Two contrasting granite types. *Pac. Geol.*, 8, p. 173-174.

Cullers, R. L. and Graf, J. L. (1984) Rare Earth Elements in Igneous Rocks of the Continental Crust: Intermediate and silicic rocks-ore petrogenesis. In Handerson (editor) Rare Earth Geochemistry. *Development on Geochemistry*, 2, p. 275-308.

Eby, G. N., Kochhar, N. (1990) Geochemistry and Petrogenesis of the Malani Igneous Suite, North Peninsular India. *Jour. Geol. Soc. India*, 36, p. 109-130.

—, Krueger, H. W., Creasy, J. W. (1992) Geology, geochronology and geochemistry of the White Mountains batholith, New-Hamphire, in Puffer J. H. and Ragland P. G. eds., Eastern North American Mesozoic Magmatism: *Geological Society of America Special Paper*, 268, p. 379-397.

Ellis, J. D., Thompson, A. B. (1986) Subsolidus and partial melting reactions in the quartz-excess CaO + MgO + Al_2O_3 + SiO_2 + H_2O. System under water excess and water-deficient conditions for the origin of peraluminous melts from mafic rocks. *Jour. Petrol.* 27, p. 91-121.

Harris, N. B. W., Pearce, J. A. and Tindle, A. G. (1986) Geochemical characteristics of collision - zone magmatism. In Coward M. P. and Reis A. C. (editor). *Collision tectonics.* Spec. Publ., Geol. Soc., 19, p. 67-81.

Hine, R., Williams, I. S., Chapell, B. W., White, A. J. R. (1978) Contrasts between I and S type granitoids of the Kosciusko batholith. *J. geol. Soc. Aust.*, 25, p. 219-234.

Iancu, V., Andăr, A., Udrescu, C. (1994) Culmea Cernei granitoids structural setting and petrochemical data. *Rom. J. Petrol.*, 76, p. 19-31.

Lamèyre, J., Bowden, P. (1982) Plutonic rock types series: discrimination of various granitoid series and related rocks. *Jour. Vulc. Geoth. Res.*, 14, p. 169-186.

Institutul Geologic al României

La Roche, H. de, Leterrier, J., Grandelaude, P., Marchal, M. (1980) A classification of volcanic and plutonic rocks using R_1-R_2 diagram and major-element analyses. Its relationships with current nomenclature. *Chem-Geol*, 29, p. 183-210, Amsterdam.

Pearce, G. A., Harris, N. B., Tindle, A. G. (1984) Trace element discrimination diagrams for the tectonic interpretation of granitic rocks. *Jour. Petrol.*, 25, p. 956-983.

Pitcher, W. S. (1987) Granites and yet more granites forty years on. *Geol. Rund.* 76/1, p. 51-79., Stuttgart.

— **(1982)** Granite Type and Tectonic Environment in Mountain Building Procesess. Hsu, K. J. editor New-York Academic Press, p. 9-40, London.

— **(1993)** The Nature and Origin of Granite. 321 p. Blackie Acad. Prof.

Robu, N., Robu, L. (1992) Etude de cristaux de zircon de quelques granitoides de Banat (Ogradena, Cherbelezu, Sfârdin, Cerna). *Rom. J. Mineral.*, 75, p. 91-99, Bucureşti.

Sarvothaman, H. and Leelanandam, C. (1992) Peraluminous, Metaluminous and Alkaline Granites from Parts of Andhara Pradesh and Karnataka in the Dharwar Craton: A Critical Reappraisal of Existing Data. *Jour. Geol. Soc. India*, 39, p. 279-291.

Streckeisen, A. L. (1967) Classification and nomenclature of igneous rocks. *New Yahrb. Mineral. Abh.*, 107 (2/3), p. 144-240, Stuttgart.

White, A. J. R., Chappell, B. W. (1983) Granitoid types and their distribution in the Lachlan Fold Belt, southeastern Australia. *Mem. Geol. Soc. Amer.*, 159, p. 21-34.

Received: July 1, 1996
Accepted: December 4, 1998

Institutul Geologic al României

INSTRUCTIONS TO AUTHORS

ROMANIAN JOURNAL OF PALEONTOLOGY publishes original scientific contributions dealing with any subject of this field.

Only papers presenting concisely and clearly new information will be accepted. The manuscript will be submitted for critical lecture to one or several advisers. Papers will be definitely rejected after a second unsatisfactory revision by the authors. The manuscripts will not be returned to the authors even if rejected.

Manuscripts are prefered in English or French. Manuscripts submitted in Romanian will be accompanied by an abstract in English or French (maximum 10 per cent of the manuscript volume).

Papers should be submitted on diskette and typed text in duplicate to the secretary of the Editorial Board, including the reproduction ready original figures. The manuscript should comprise: text (with a title page which is the first page of it), references, key words, abstract, illustrations, captions and a summary for technical purposes.

Author(s) should add a separate sheet with a short title (colontitle) of maximum 60 strokes and a summary indicating the hierarchy of headings from the text listed in decimal classification (1; 1.1; 1.1.1) but not exceeding four categories.

Text should be on diskette, format ASCII and 2 copies, holding an empty place of 3 cm on the left side of the page. The text cannot exceed 10 typewritten pages (including references and figures).

Front page (first page of the text) should comprise: a) title of the paper (concise but informative) with an empty space of 8 cm above it; b) full name(s) of the author(s); c) institution(s) and address(es) for each author or group of authors; d) text.

Footnotes should be numbered consequtively.

Citations in the text should include the name of the author and the publication year. Example: Ionescu (1970) or (Ionescu, 1970). For two authors: Ionescu, Popescu (1969) or (Ionescu, Popescu, 1969). For more than two authors: Ionescu et al. (1980) or (Ionescu et al., 1980). For papers which are in course of print the publication year will be replaced by "in press". Unpublished papers or reports will be cited in the text like the published ones.

Abstract, of maximum 20 lines (on separate sheet), must be in English, summarizing the main results and conclusions (not a simple listing of topics).

Key words (max. 10 items), in English or French, following the language used in the text (or the Resumé if the text is in Romanian), given in succession from general to specific, should be typed on the abstract page.

References should be typed in double-line spacing, listed in alphabetical order and chronological order for authors with more than one reference. Abbreviations of journals or publishing houses should be in accordance with the recommendations of the respective publications or with the international practice.

Examples:

a) journals:

Giuşcă, D. (1952) Contributions à l'étude cristallochimique des niobates. *An. Com. Geol.*, XXIII, p. 259–268, Bucureşti.

– , Pavelescu, L. (1954) Contribuţii la studiul mineralogic al zăcămîntului de la Muşca. *Comm. Acad. Rom.*, IV, 11–12, p. 658–991, Bucureşti.

b) special issues:

Strand, T. (1972) The Norwegian Caledonides. p. 1–20. In: Kulling, O., Strand, T. (eds.) Scandinavian Caledonides, 560 p., Interscience Publishers.

c) books:

Bălan, M. (1976) Zăcămintele manganifere de la Iacobeni. Ed. Acad. Rom., 132 p., Bucureşti.

d) maps:

Ionescu, I., Popescu, P., Georgescu, G. (1990) Geological Map of Romania, scale 1:50,000, sheet Cîmpulung. Inst. Geol. Geofiz., Bucureşti.

e) unpublished papers or reports:

Dumitrescu, D., Ionescu, I., Moldoveanu, M. (1987) Report. Arch. Inst. Geol. Geofiz., Bucureşti.

Papers or books published in Russian, Bulgarian or Serbian etc. should be mentioned in the references transliterating the name and titles. Example:

Krasheninnikov, V. A., Basov, I. A. (1968) Stratigrafiya kainozoia. Trudy GIN, 410, 208 p., Nauka, Moskow.

Illustrations (figures and plates) must be numbered and submitted as originals on separate sheets (tracing papers), ready for reproduction. The thickness of the lines, lettering and symbols on figures should be large enough to be easily read after size-reduction. The original size should not extend beyond the print area of the page: column width 8 cm, page width 16.5 cm, page length 23 cm for figures; the width of line drawings should not extend over a single (16.5/23) or double (23/33 cm) page area and must be selfexplanatory (including title, authors, legend etc.). The graphic scale is obligatory.

Photographic illustrations (black-and-white only) must be of high quality and should be grouped into plates 16/23 cm in size. Each plate should have the photos numbered, i.e. Pl. I, Fig. 1; Pl. II, Fig. 1.

Tables should be numbered and entitled. Original size of the tables should correspond to the above mentioned (8/16.5 or 16.5/23) dimensions of the printing area.

Author(s) will receive only one set of preprint proofs which must be returned, with corrections, 10 days after receiving them. Only printing errors should be corrected, no changes in the text can be accepted.

Thirty offprints of each paper are supplied to the author(s) free of charge.

Editorial Board

Institutul Geologic al României

INSTRUCŢIUNI PENTRU AUTORI

ROMANIAN JOURNAL OF PALEONTOLOGY publică contribuţii ştiinţifice originale referitoare la acest domeniu.

Vor fi acceptate numai lucrările care prezintă concis şi clar informaţii noi. Manuscrisul va fi supus lecturii critice a unuia sau mai multor specialişti; după a doua revizie nesatisfăcătoare din partea autorilor va fi respins definitiv şi nu va fi înapoiat.

Manuscrisele trebuie prezentate, de regulă, în engleză sau franceză; cele prezentate în limba română trebuie să fie însoţite de un rezumat, în engleză sau franceză, de maximum 10 % din volumul manuscrisului.

Lucrările trebuie depuse, pe dischetă şi text pe hârtie în două exemplare, la secretariatul Comitetului de redacţie, inclusiv ilustraţiile în original. Manuscrisul trebuie să cuprindă:. textul (cu o pagină de titlu, care este şi prima pagină a lucrării), bibliografie, cuvinte cheie, abstract, ilustraţii, explicaţii ale figurilor şi planşelor, şi un sumar cu scop tehnic.

Se va adăuga o filă separată cu un colontitlu de maximum 60 semne şi un sumar, în care se va indica ierarhia titlurilor din text în clasificarea zecimală (1; 1.1; 1.1.1), care nu trebuie să depăşească patru categorii.

Textul va fi predat pe dischetă, format ASCII şi două copii pe hârtie, cu un spaţiu liber de 3 cm în partea stîngă a paginii şi nu trebuie să depăşească 10 pagini (inclusiv bibliografia şi figurile).

Prima pagină a textului va cuprinde: a) titlul lucrării (concis, dar informativ), cu un spaţiu de 8 cm deasupra; b) numele întreg al autorului (autorilor); c) instituţia (instituţiile) şi adresa (adresele) pentru fiecare autor sau grup de autori; d) text.

Notele de subsol se vor numerota consecutiv.

Citările din text trebuie să includă numele autorului şi anul publicării. Exemplu: Ionescu (1970) sau (Ionescu, 1970). Pentru doi autori: Ionescu, Popescu (1969) sau (Ionescu, Popescu, 1969). Pentru mai mult de doi autori: Ionescu et al. (1980) sau (Ionescu et al., 1980). Pentru lucrările care se află sub tipar, anul publicării va fi înlocuit cu "in press". Lucrările nepublicate şi rapoartele vor fi citate în text ca şi cele publicate.

Abstractul, maximum 20 rînduri (pe filă separată), trebuie să fie în limba engleză şi să prezinte pe scurt principalele rezultate şi concluzii (nu o simplă listă cu subiecte abordate).

Cuvintele cheie (maximum 10) trebuie să fie în limba engleză sau franceză, corespunzător limbii în care este lucrarea (sau abstractul, dacă textul este în română), prezentate în succesiune de la general la specific şi dactilografiate pe pagina cu abstractul.

Bibliografia se prezintă în ordine alfabetică şi cronologică pentru autorii cu mai mult de o lucrare. Abrevierile titlului jurnalului sau ale editurii trebuie să fie conforme cu recomandările respectivelor publicaţii sau cu standardele internaţionale.

Exemple:

a) jurnale:

Giuşcă, D. (1952) Contributions à l'étude cristallochimique des niobates. *An. Com. Geol.*, XXIII, p. 259–268, Bucureşti.

– , Pavelescu, L. (1954) Contribuţii la studiul mineralogic al zăcămîntului de la Muşca. *Comm. Acad. Rom.*, IV, 11–12, p. 658–991, Bucureşti.

b) publicaţii speciale:

Strand, T. (1972) The Norwegian Caledonides. p. 1–20. In: Kulling, O., Strand, T. (eds.) Scandinavian Caledonides, 560 p., Interscience Publishers.

c) cărţi:

Bălan, M. (1976) Zăcămintele manganifere de la Iacobeni. Ed. Acad. Rom., 132 p., Bucureşti.

d) hărţi:

Ionescu, I., Popescu, P., Georgescu, G. (1990) Geological Map of Romania, scale 1:50,000, sheet Cîmpulung. Inst. Geol. Geofiz., Bucureşti.

e) lucrări nepublicate sau rapoarte:

Dumitrescu, D., Ionescu, I., Moldoveanu, M. (1987) Report. Arch. I.G.R., Bucureşti.

Lucrările sau cărţile publicate în rusă, bulgară, sârbă etc. trebuie menţionate în bibliografie transliterînd numele şi titlurile. Exemplu:

Krasheninnikov, V. A., Basov, I. A. (1968) Stratigrafiya kainozoia. Trudy GIN, 410, 208 p., Nauka, Moskow.

Ilustraţiile (figuri şi planşe) trebuie numerotate şi prezentate în original, pe coli separate (hîrtie de calc), bune pentru reprodus. Dimensiunea liniilor, a literelor şi a simbolurilor pe figuri trebuie să fie suficient de mare pentru a putea fi citite cu uşurinţă după ce au fost reduse. Dimensiunea originalului nu trebuie să depăşească suprafaţa tipografică a paginii: lăţimea coloanei 8 cm, lăţimea paginii 16,5 cm, lungimea paginii 23 cm, pentru figuri, iar pentru planşele liniare nu trebuie să depăşească dimensiunile unei pagini simple (16,5/23 cm) sau duble (23/33 cm) şi trebuie să fie autoexplicativă (să includă titlul, autori, explicaţie etc.). Scară grafică obligatorie.

Ilustraţiile fotografice (numai alb-negru) trebuie să fie clare, cu contrast bun şi grupate pe planşe de 16/23 cm. In cadrul fiecărei planşe numărătoarea fotografiilor se repetă (de. ex. Pl. I, fig. 1, Pl. II, fig. 1).

Tabelele vor fi numerotate şi vor avea un titlu. Dimensiunea originală a tabelelor trebuie să corespundă dimensiunilor tipografice menţionate mai sus (8/16,5 sau 16,5/23).

Autorii vor primi un singur set de corectură, pe care trebuie să-l înapoieze, cu corecturile corespunzătoare, după 10 zile de la primire. Numai greşelile de tipar trebuie corectate; nu sînt acceptate modificări.

Autorii vor primi gratuit 30 de extrase pentru fiecare lucrare.

Comitetul de redacţie

166990

Institutul Geologic al României

Toate drepturile rezervate editurii Institutului Geologic al României
All rights reserved to the Geological Institute of Romania

Translation and language review by:
Adriana Năstase, Mariana Borcoş

Editorial Staff:
Natalia Conovici, Cristian Toth

Illustration:
Paraschiv Toader, Veronica Sdrula

Printing:
N. Păleanu, E. Ştefan, P. Jurjea, F. Dumitru

Institutul Geologic al României

Institutul Geologic al României